

J-PARC

ANNUAL REPORT 2012

JAPAN PROTON ACCELERATOR RESEARCH COMPLEX

J-PARC Annual Report 2012

Contents

Preface	1
Accelerators	3
Overview	4
LINAC	5
RCS	7
MR	9
Materials and Life Science Experimental Facility	13
Overview	14
Neutron Source	16
Neutron Science	18
Muon Science	22
Neutron Device	24
Particle and Nuclear Physics	25
Hadron and Nuclear Physics	26
Kaon Physics	27
Muon Physics	28
Neutrino Experimental Facility	28
Cryogenics Section	31
Overview	32
Superconducting Magnet System for the T2K Beamline	32
Superconducting Kaon Spectrometer (SKS)	32
The Superconducting Magnet System for the Muon Beam Line at MLF	33
Cryogen Supply and Technical Support	33
R&D for the J-PARC Project: COMET	34
R&D for the Future J-PARC Project: New Muon g-2/EDM and Muonium HFS	34
Information System	35
J-PARC Network (JLAN) Upgrade	36
Statistics of Network Utilization	36
Statistics of Computer Resource Utilization	38
Transmutation Studies	41
Activities	42
Safety	45
Radiation Safety	46
Users Office	49
User Program	53

Organization and Committees	61
Organization Structure	62
Members of the Committees Organized for J-PARC	63
Main Parameters	67
Events	69
Events	70
Publications	77
Publications in Periodical Journals	78
Conference Reports and Books	82
JAEA Reports	86
KEK Reports	86



Preface

In this report, we are summarizing primarily the activities and outcomes from July 2012, after the restoration from the 2011 Earthquake, to May 2013 before the radioactive material leak accident at the Hadron Experimental Facility occurred, whereas all the statistics are given based on the numbers of FY2012 (April 2012 to March 2013). In this period, the critical part of the restoration work from the damage caused by the earthquake was completed, and eight cycle operations were reserved for users in FY2012 and two cycles in April and May 2013, following the original schedule.

The most remarkable achievement is that the proton beam power increased smoothly as planned, like as 310 kW from the 3 GeV synchrotron (RCS) to the Materials and Life Experimental Facility (hereafter MLF), and 50-300 kW at the fast extraction mode from the 50 GeV synchrotron (the main ring) to the Neutrino Experimental Facility (hereafter Neutrino), and also at the slow extraction mode about 15 kW to the Hadron Experimental Facility (hereafter Hadron). Users conducted many experiments with appreciably stable as well as high intensity beams at all J-PARC facilities. Consequently, year 2012 was a time of remarkable progress.

Regarding the MLF progress, two new neutron beamlines of SPICA and PLANET were added into the instrumental suit, and the commissioning was carried out almost on schedule and became available for users from the beginning of April 2013. At long last the construction of the new high-intensity ultra-slow muon beamline began in the MUSE for the muon users. It also should be noted that the world's highest intensity muon beam was successfully obtained at the D-line. A significant increase in the number of proposals for general use at the MLF also indicated the sound recovery from the earthquake's aftermath.

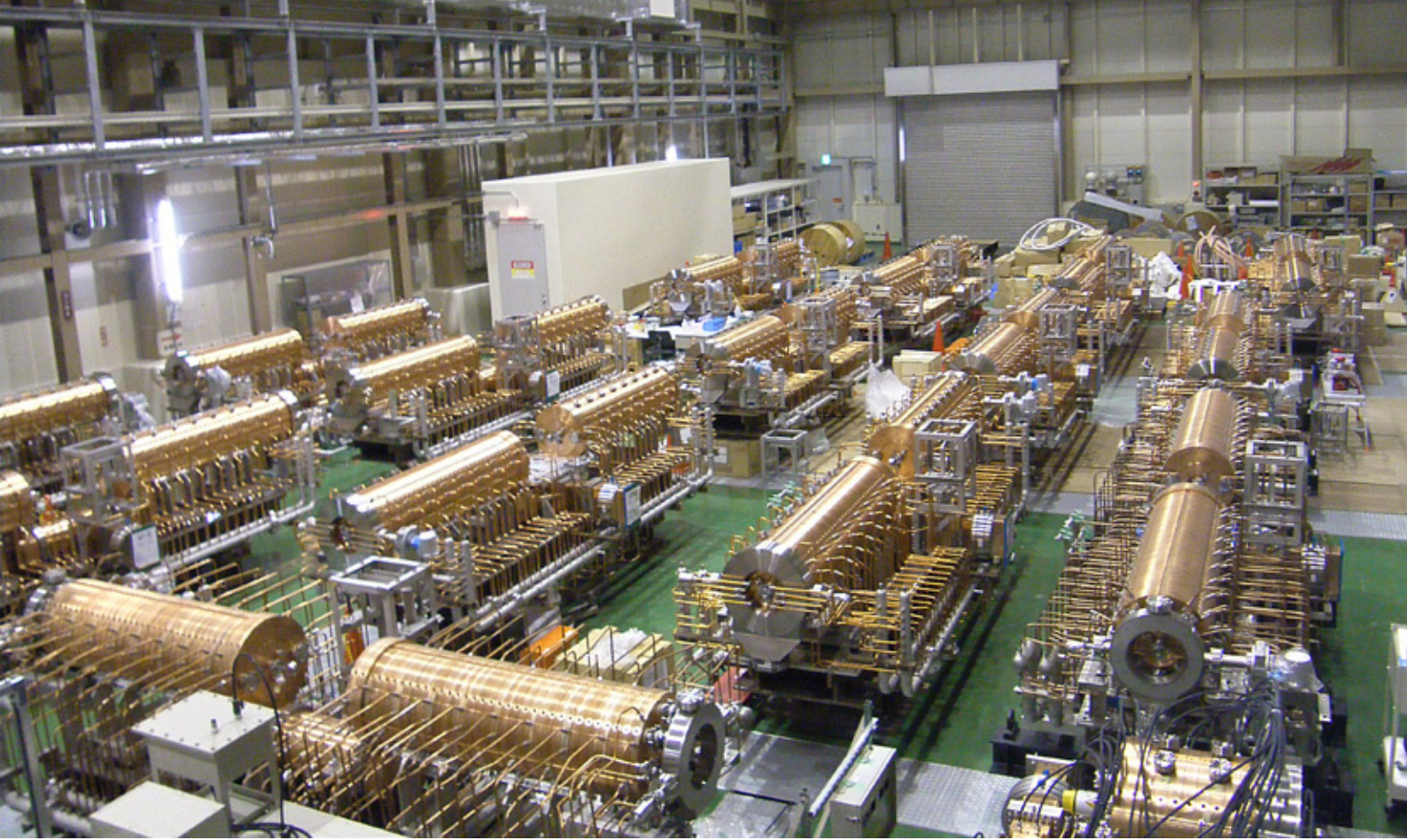
As of the neutrino T2K experiment, event data for the electron neutrino appearance at the detector, Super Kamiokande, had accumulated steadily with increasing the number of POT (protons on target) at J-PARC. The T2K collaboration presented the first experimental indication for oscillations from muon neutrinos to electron neutrinos at an international conference in the fall of 2012.

One of the most important achievements in this period was that we finally could start a user operation for the kaon experiments at the Hadron with using up to 15 kW power at the slow extraction mode of the MR.

Over all, we demonstrated that in this period J-PARC was the world-class forefront multi-purpose experimental facility in terms of high beam performance.

Yujiro Ikeda

Director of the J-PARC Center



Accelerators

Overview

J-PARC was extensively damaged by the earthquake on March 11, 2011, but it was successfully restored. We started the beam tuning in December 2011 and the user programs in January 2012.

The accelerator’s status in FY 2012 (from April 2012 to March 2013) and partially in FY 2013 is summarized in Figure 1. The main topics related to the beam operation are as follows:

- (1) The user operation was planned about 190 days in total and we had delivered beam to the users almost as scheduled in FY 2012.
- (2) In the beginning of April 2012, the beam power from the 3-GeV RCS (Rapid Cycling Synchrotron) for MLF users was 200 kW. We demonstrated 275 kW delivery for about 3 days at the end of June, which was a preparatory operation for further power up. In November we achieved a power jump from the 200 kW level to 270 kW for the users’ beam. Beams with power of 300 kW have been constantly delivered to MLF since January 2013.
- (3) We demonstrated new record power levels of over 500 kW (equivalent beam) for MLF and the beam loss data were compared with those of simulations and measured before the earthquake.
- (4) The user run of MR-FX (Main Ring-Fast eXtraction) started at 160 kW, and the power was increased to 220–230 kW.
- (5) The user run of MR-SX (Main Ring-Slow eXtraction) started at 3.5 kW, and the power was increased to 24 kW. An extraction efficiency of 99.5% has been maintained for the Hadron users. We also demonstrated 30 kW extraction in the accelerator study.

The operation statistics and the trip time by system in FY 2012 are shown in Figures 2 and 3, respectively. The total operation time was 6,328 hours (including startup and conditioning) and the user operation hours and the

beam availability rate of each experimental facility are as follows: 4,664 hours (93%) for MLF; 3,323 hours (89%) for NU (Neutrino); and 907 hours (88%) for HD (Hadron). These statistics indicate that there were no significant problems in FY 2012.

At the beginning of the J-PARC operation in 2008, we encountered troubles in the RFQ (Radio Frequency Quadrupole linac). Recently, however, the number of trips caused by the RFQ was reduced to several per day, and the main reason of the downtime was a problem with the high voltage power supply system (HVDC) of the linac.

Some of the work done to repair the earthquake damage to the linac building was not compatible with the beam operation. The repair work resumed in the summer shutdown period from July 2012. The fixing of the cranes in the klystron gallery and in the accelerator tunnel was completed. In addition, the walls and the pillars were also repaired, and grout was poured into the hollow spaces under the floor before the beam operation was resumed in September.

A full energy (400 MeV) and higher peak beam current (50 mA) linac is required to reach the nominal performance of 1 MW at RCS and 0.75 MW at MR. For the energy upgrade, we plan to install a new accelerating structure ACS (Annular-ring Coupled Structure) and a 400 MeV RCS injection system. And we also need to increase the peak beam current by replacing the ion source and the RFQ. The MR fast extraction aims at the designing power by shortening the repetition cycle. To implement this, the development of a main electromagnetic power supply with a high repetition rate and an acceleration system with high gradient is the key. The R&D and construction for power upgrade components are proceeding.

Month	FY2012												FY2013						
	4	5	6	7	8	9	10	11	12	1	2	3	4	5	6	7			
Operation (Run#)	← #42 →		← #43 →		Summer Maintenance			← #44 →		← #45 →		← #46 →		← #47 →		← #48 →		← #49 →	
MLF (3 GeV)	200-220kW		275kW					534kWeq. 210kW 270-290kW		300kW		556kWeq.							
MR-Slow Ext. (30 GeV)			14kWeq. 3.5→6kW							20kWeq. 11kW 10-15kW		14kW		30kWeq. 15-24kW					
MR-Fast Ext. (30 GeV)	220kWeq. 160-190kW							160-200kW		200-220kW		200-230kW						Hadron Accident	

eq.:Equivalent beam power (Single shot or short period demonstration)

Fig. 1. Run summary of FY 2012.

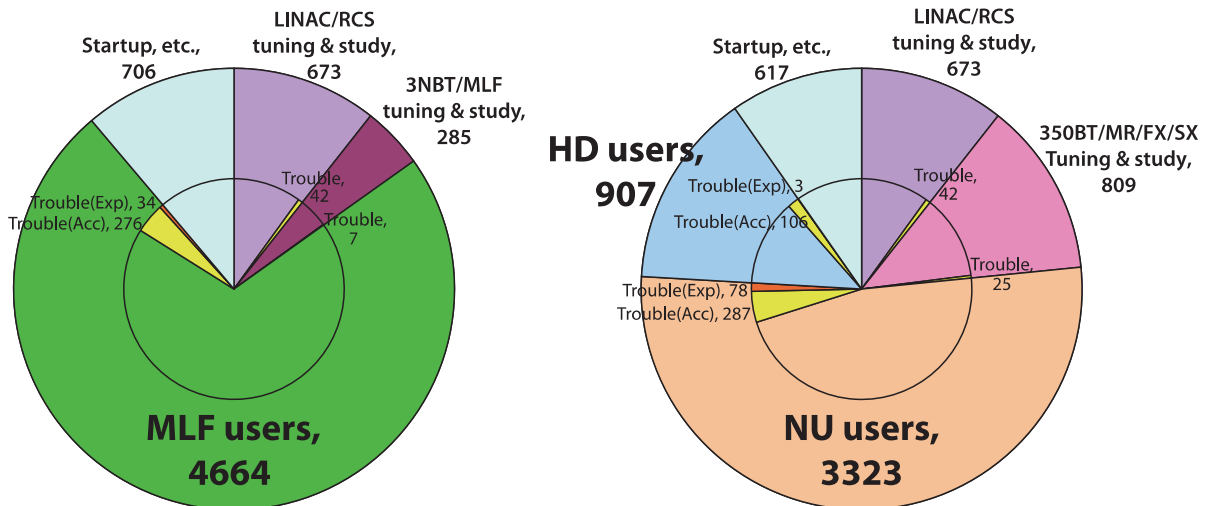


Fig. 2. Operation statistics of MLF and NU+HD in FY 2012. The total operation time was 6,328 hours.

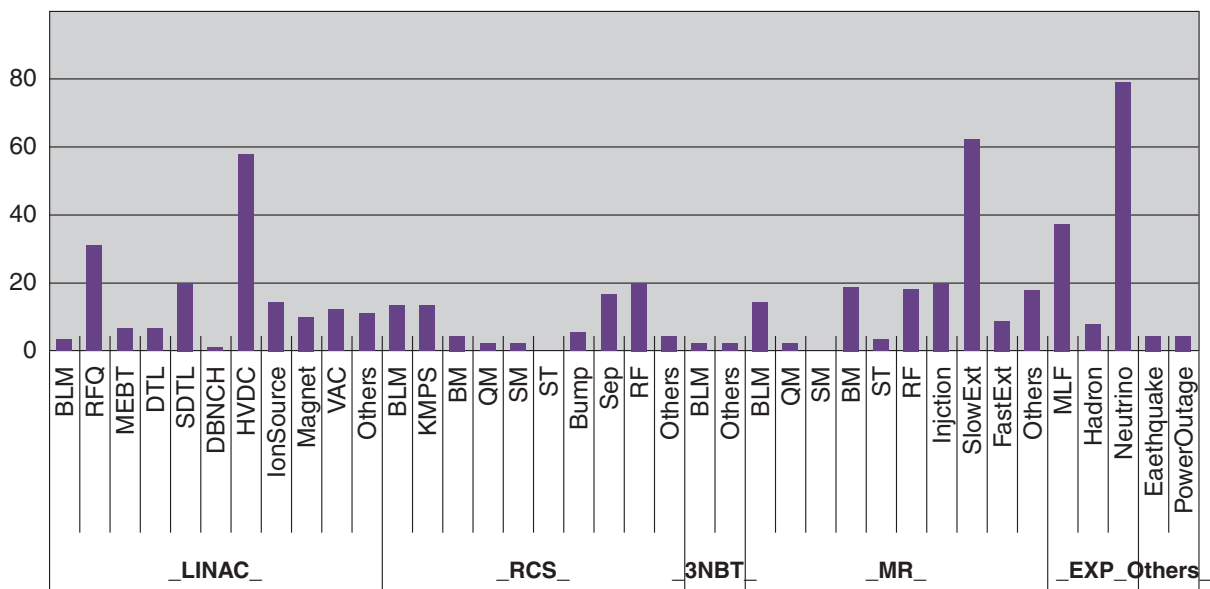


Fig. 3. Downtime statistics in hours by components in FY 2012 (April 2012 – March 2013).

LINAC

After the summer shutdown in 2012, we increased the beam power for the MLF user operation from 220 kW to 300 kW, which corresponds to a linac beam power of 18 kW. In November 2012, we conducted a beam study to demonstrate our highest beam power from RCS. In this study, the linac peak current was increased from the nominal 15 mA to 25 mA. The RCS beam power reached 540 kW, which corresponds to a linac beam power of 33 kW. The beam loss measurement in the demonstration operation indicated that we can increase the linac beam power to 30 kW with reasonable increase of beam loss.

The bunch shape monitor has been developed under collaboration with the INR (Institute for Nuclear

Research: Russia) for the measurement of the longitudinal beam distribution. In order to perform the test measurement, three monitors were installed during the summer shutdown in 2012, and the commissioning was performed. In that commissioning, we successfully obtained the bunch profile of the H⁻ beam at the end of the SDTL (Figure 4).

An RFQ had been a component with the highest trip rate since the discharge problem in 2008, but the trip rate decreases to comparable to other linac components by performing the conditioning at the interval of the beam operation continuously. Other linac components such as the klystron and SDTL are keys to improv-

ing the total linac availability. In February 2013, the trip rate of the klystron for DTL2 increased significantly. Because we suspected that the trip was caused mainly by an electron gun in the klystron, we replaced the klystron with a spare one.

At SDTL5, there is an unstable power region where the VSWR increases sharply. Moreover, the region widened during the operation and forced us to increase the operating amplitude to 116% just before the summer shutdown in 2012. To solve this problem, we improved the vacuum condition of the cavity, and performed careful conditioning of the cavity during the shutdown period. As a result of the countermeasures, the upper limit of the unstable power region successfully decreased.

The filament-driven ion source is supplying the beam without any serious troubles. The results of recent beam runs show that the ion source is capable of continuous operation for 1,100 hours with a beam current of approximately 20 mA.

The linac power upgrade program is now in progress. The program includes an upgrade of the intensity and the energy of the linac. For the intensity upgrade, we plan to replace the ion source and the RFQ to deliver a peak current of 50 mA. For the energy upgrade, the energy will be increased to 400 MeV by adding ACS after the SDTL.

A cesiated RF-driven H^- ion source has been developed for the program. The ion source extracts a beam of more than 60 mA with a duty factor of 2.5%, which satisfies the requirements of the program. From the experimental results of a continuous operation that lasted a hundred hours, the total cesium consumption for 50 days was estimated to be 0.74 g. A spark rate of less than once a day was observed at this consumption rate. The value seems to be acceptable because it is the same level as that of the current cesium-free ion source.

The fabrication of a new RFQ for 50 mA acceleration

was completed in March 2013. All the mechanical and low power RF measurements and checks were finished. The results showed that the alignment precision, the field distribution and the vacuum characteristics were within the desired goals. An RFQ test stand was newly constructed to perform the beam acceleration test of the new RFQ before the installation to the linac (Figure 5). The RF-driven H^- ion source will be tested simultaneously to check the stability and reliability through the long term continuous operation.

The mass production of the ACS modules was completed, and the modules are now stored in the J-PARC linac building until the installation onto the beam line starts in August, 2013 (Figure 6). Currently, pumps and vacuum components are being installed on the cavities for testing the vacuum conditions. We started the high power test of the ACS modules in 2010, however, the test was suspended because the test area was damaged due to the earthquake in 2011. The test area was restored in March 2013, and we are now preparing to resume the test. Before the installation it will be possible to test only five modules at most, because of time constraints. The remaining modules, therefore, have to be conditioned after the installation.

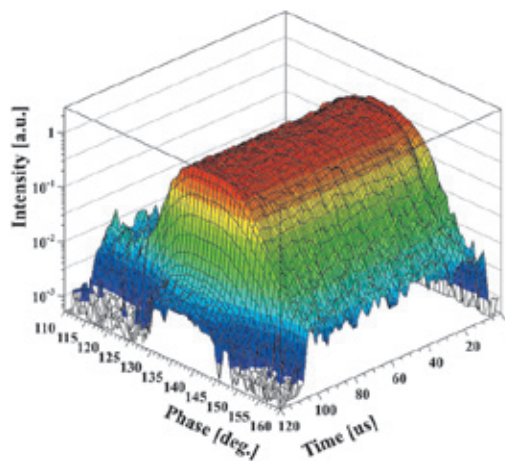


Fig. 4. Example of a bunch shape monitor measurement.

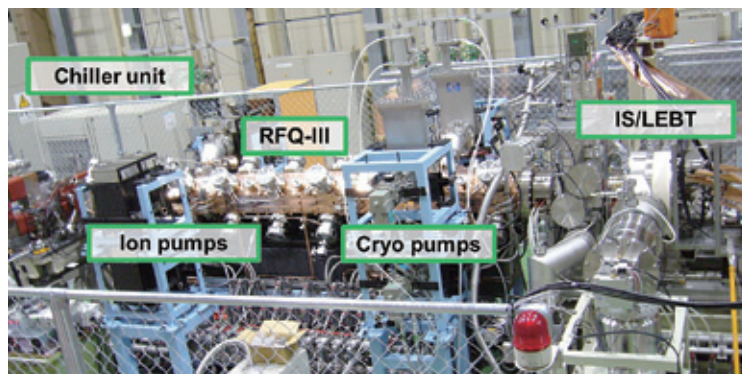


Fig. 5. RFQ test stand for the beam acceleration test of the new RFQ.



Fig. 6. ACS modules waiting to be installed.

RCS

The user operation resumed from mid-January 2012 with a 120 kW beam for the MLF and a 300 kW equivalent beam for the MR, respectively, after the earthquake. The beam power gradually increased, and then, on 13th January 2013, it reached 300 kW for the MLF users. There were no significant problems and the average availability was about 95% for this specific year. The activation of the RCS components was measured after 24 days of continuous user operation with a beam power of 300 kW. The activation was measured on the surface of the beam pipe and the point at one foot distance 4 hours after the beam stopped. The measurement didn't show very high activation area because the highest value was about 1.2 mSv/h on the surface of the beam pipe close to the beam collimator. When we need to work close to this location, we should take care to reduce the exposure, that is why we already prepared an additional radiation shield to be used during maintenance.

During this year we made mainly five progresses for stable and high intensity operation of the RCS. To reduce the beam loss in the RCS and for the users, it would be necessary to work on a treatment for leakage field and a new painting scheme operation. We performed a high-intensity beam trial of up to 540 kW and also improved the beam simulation code. The preparation for the 400 MeV beam injection has continued and new power supplies for painting the bump magnet have already been in-service for the user operation. The details of several advancements are described as follows:

1) Treatment for leakage field at the extraction area.

One source of beam loss in the RCS is the leakage magnetic field from the beam transport line (called the 3NBT line) at the extraction area. To reduce this leakage magnetic field, new vacuum chambers and bellows made from permeability alloy (called permalloy) were installed in the straight section of the extraction area. Since these chambers were installed close to steering magnets, the magnetic field strength of the steering magnet-decreased by about 30%, caused by the permalloy bellows. However, it was no problem to do COD correction because the power supplies of the steering magnets had sufficient margin to do it. The leakage magnetic field from the 3NBT line could be reduced by more than 50% for the dipole, skew dipole and quadrupole components and by more than 25% for the skew quadrupole component. These values are sufficiently small to realize much lower beam loss in the case of a 300 kW beam power user operation.

2) Difference in the beam shape for the MLF and the MR.

There are two difference requirements for the beam of the RCS from the MLF and the MR, because the RCS is a power source for the MLF and the injector for the MR. The MLF requires wide and uniform transverse beam distribution on the neutron production target to reduce the damage to the target, on the other hand, the MR requires narrow one because the apertures of the beam transport line and the ring are limited. Since difference phase space painting at injection for each beam

can meet the requirements, two pulse steering magnets were installed in the transport line from the linac to the RCS. In order to obtain relatively smaller transverse emittance at extraction, those magnets were designed to perform a smaller injection painting for the MR beam as compared to the MLF one. These two magnets worked well and are already in operation for switching to a painting area of 100π mm mrad for the MR as compared to that of 150π mm mrad for the MLF beam [1].

3) High intensity beam trial.

We have performed a high intensity beam trial of up to 540 kW. Figure 7 shows the signal of the beam current monitor (DCCT) and the total beam loss rate in the case of beam power ranging from 105 kW-equivalent to 539 kW-equivalent. The beam power was controlled by the pulse length of the injection beam from the Linac. The pulse length was changed from 100 μ s to 500 μ s. The beam was extracted from the RCS to the beam dump located at the beam transport line to the neutron production target.

Almost no beam loss was observed from injection to extraction in the case of less than 300 kW-equivalent beam power, but obvious beam loss occurred when the beam power was more than 400 kW-equivalent[2].

Figure 8 shows the beam loss monitor signal for the entire RCS in the case of 212 kW user operations and the case of the beam power ranging from 105 kW-equivalent to 539 kW-equivalent in the high intensity beam test. In the user operation the extracted beam from the RCS is transported to the neutron production target, and the beam is transported to the beam dump (called 3NBT

dump) located at the beam transport line to the neutron production target in the case of beam test. Almost all beam loss was localized at the ring collimator and the loss rate was about 2%; this was acceptable because the design value of the beam loss was 3%.

The beam loss source in the injection area is the foil hitting by the circulating beam in the ring because the beam loss increases linearly according to the beam power.

It was found that non-linear beam loss occurred in the collimation area. One of the causes of this beam loss is misalignment of the main components due to the earthquake damage because beam loss did not occur in the case of 400 kW equivalent beam power before the earthquake. Since the other cause of the loss is not clear, we should continue to study the beams and develop a beam simulation code to find the source of the beam loss.

We estimated the activation in the case of the 540 kW beam power user operation from data of 200 kW operation and summarized it in Table 1. The activation is estimated to be 1.5 mSv/h in the collimator and the injection area, which is an acceptable value to perform the user operation. This 540 kW beam power corresponds to 1.6 MW for 400 MeV injection in terms of the Lasslett tune shift. This high-intensity trial showed the significant progress we reached in designing an output beam power of 1 MW.

References

- [1] P. Saha et al., Proceedings of IPAC13, MOPME022.
- [2] H. Hotchi, Proceedings of IPAC13, THPWO033.

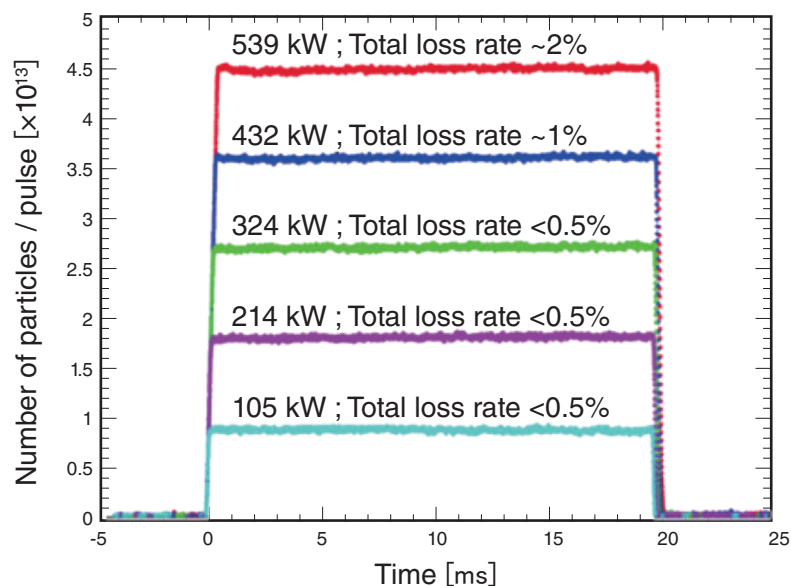


Fig. 7. Signal of the beam current monitor (DCCT) in the case of increasing the beam power from 105 kW equivalent to 539 kW equivalent.

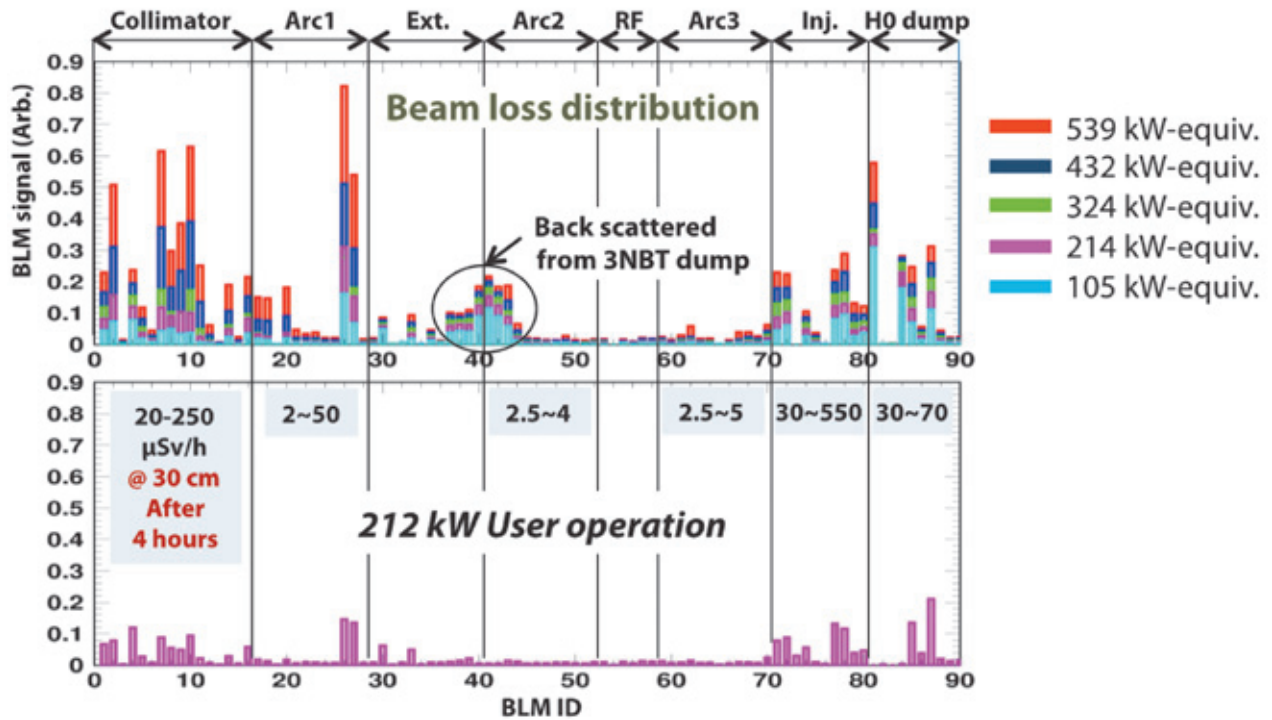


Fig. 8. Beam loss monitor signal for the entire RCS in the case of 212 kW user operations and for the case of increasing the beam power from 105 kW-equivalent to 539 kW-equivalent in the high intensity beam test.

Table 1. Measurement values of activation on the surface of the beam pipe 4 hours after the beam stop in the case of a 3-week long 212 kW user operation, and the estimated activation in the case of a 540 kW operation.

Power [kW]	Activation [$\mu\text{Sv/h}$]					
	Colli.	Arc1	Arc2	Arc3	Inj.	dump
212	<250	<50	<4	<5	<550	<70
	(measurement)					
540	<1500	<125	<10	<12.5	<1375	<175
	(estimation form 212 kW operation)					

MR

Figure 9 shows the operation history of the MR from April 2010 to March 2013, the end of FY 2012. For the FX mode, beam delivery to the T2K experiment, the beam power was increased by shortening the acceleration cycle time and by increasing the number of extracted particles per pulse. The shortening of the cycle time was achieved by improvements to the main magnet power supplies and installation of additional rf systems to attain a higher accelerating power. The number of the rf systems was five until June 2010. A 6th system was installed during the 2010 shutdown, the 7th and 8th during the 2011 shutdown and finally the 9th during the 2012 shutdown. For the SX mode, the beam delivery to

the hadron experimental hall, the cycle time is fixed at 6 s. The beam power was gradually increased by performing accelerator study to achieve a high extraction efficiency and good time structure of the extracted beam intensity.

The beam power delivered to the T2K experiment was limited in the operation between March and June 2012 for the following reasons:

(1) A large beam loss in the injection timing was observed. The loss was caused by deterioration of the injection kicker performance due to a discharge problem of the impedance matching resistors. A new injection

kicker system was installed in the shutdown period after the earthquake. The discharge problem was found after a two-month routine operation. The cause of the discharge in the matched resistors was poor electric contact between the aluminum electrode and the ceramic resistor. It was indicated by a gradual increase of the resistance during operation. An improved resistor—a Cu ring inserted between the ceramics and the electrode—has a longer lifetime of more than 4 months. These improved resistors have been adopted in the operation since June 2012 and damaged resistors are replaced on scheduled maintenance days before performance deterioration.

(2) From the end of May 2012, the beam intensity was limited to lower than 160 kW in order to keep the radioactive level lower than the critical value for the exhaust gas at machine building No. 3. In the MR, there are three machine buildings. Each of them has air conditioning system for the tunnels, chiller, and pumping system for water cooling of the magnet. The amount of radioactivity in the exhaust gas is strictly regulated. In the operation with beam power of 180 kW, the instantaneous radioactive level in the exhaust gas of machine building No. 3 increased and closed at the legally accepted value of 0.5 mBq/cc, it is defined as the averaged value of three months. It meant that radioactive air from the accelerator tunnel was leaked into the machine building. For this reason, the beam power was kept below 160 kW. A close examination of the machine building revealed that the dampers of the air circulating system were not sufficiently airtight. During the summer shutdown period, the dampers were replaced by new ones with a better seal. As a result of this change, the radioactive level in the exhaust gas under 200 kW beam operation decreased from approximately 1.0 mBq/cc to 0.1 mBq/cc.

Several scheduled improvements of the MR were performed during the 2012 summer shutdown period as follows:

(1) The capacity of the ring collimator was increased from 0.45 kW to 2 kW by installing an additional set of collimators and local shields.

(2) The 9th RF cavity was installed in the ring. It can be operated also as a second harmonic system to reduce the space charge effect of the beam bunch.

(3) A transverse 100-MHz rf system was installed to improve the duty factor of the SX mode. Figure 10 shows the newly installed strip-line kickers for the rf system. In order to suppress the vacuum pressure rise due to the multipactoring effect in the strip-line kicker, 12

sets of solenoid coils were installed on the beam duct of the strip-line kicker.

After the summer shutdown period, the delivered beam power to the T2K experiment was gradually increased as shown in Fig. 9. The maximum beam power reached 240 kW in March 2013.

For the SX mode, the operation with 15-kW delivered beam power started from December 2012. The extraction efficiency for the 15 kW operation is kept at ~95%, the same as the efficiency for the 6 kW beam operation, using the dynamic bump scheme.

The most serious issue to be solved in the SX operation is a spike-like time structure in the extracted beam. The structure is brought by fluctuation of the betatron tune, which is caused by current ripples of $\Delta I/I \approx 10^{-4}$ for the main magnet power supplies. In order to improve the time structure, a transverse 50-MHz rf system has been adopted since February 2012. The transverse rf system improves the duty factor, an index to evaluate the quality of the time structure of the extracted beam, from ~17% to 30% as reported in the last annual report. In the SX operation after the summer shutdown, the additionally installed new transverse rf system, which can cover the higher frequency of up to 100 MHz was switched on. Figure 11 shows a typical time structure of the extracted beam intensity (beam spill) and the circulating beam current for beam intensity of 15 kW with the new transverse rf system. The extracted beam intensity was measured by a photomultiplier with a plastic scintillator placed in the beam transport line to the hadron experimental hall. The duty factor with the new transverse rf system was improved by up to ~44% in the user operation.

The challenge to be met soon is improving the manner of the beam loss handling in the MR.

The following are potential corrections for the beam loss issue:

(1) The loss power capacity will be increased from 2 kW to 3.5 kW by installing additional sets of collimators and iron shields.

(2) Parts of the beam ducts made of stainless steel will be replaced with titanium ducts to reduce the residual radiation dose. Similarly, both of the two electrostatic septa will be replaced with new ones, which have vacuum chambers made of titanium.

(3) The injection kicker system will be improved to make the rise time shorter. Moreover, a small kicker system will be installed to compensate for the extra kicks

made by the injection kicker system (the extra kicks bend the orbit of the previously injected beam bunches).

(4) In order to increase the beam power, the increment of the repetition cycle of the main magnet was

continuously examined. A voltage control scheme of the deceleration period will be installed into the control system of the magnet power supplies in order to reduce the period from 2.48 s to 2.40 s.

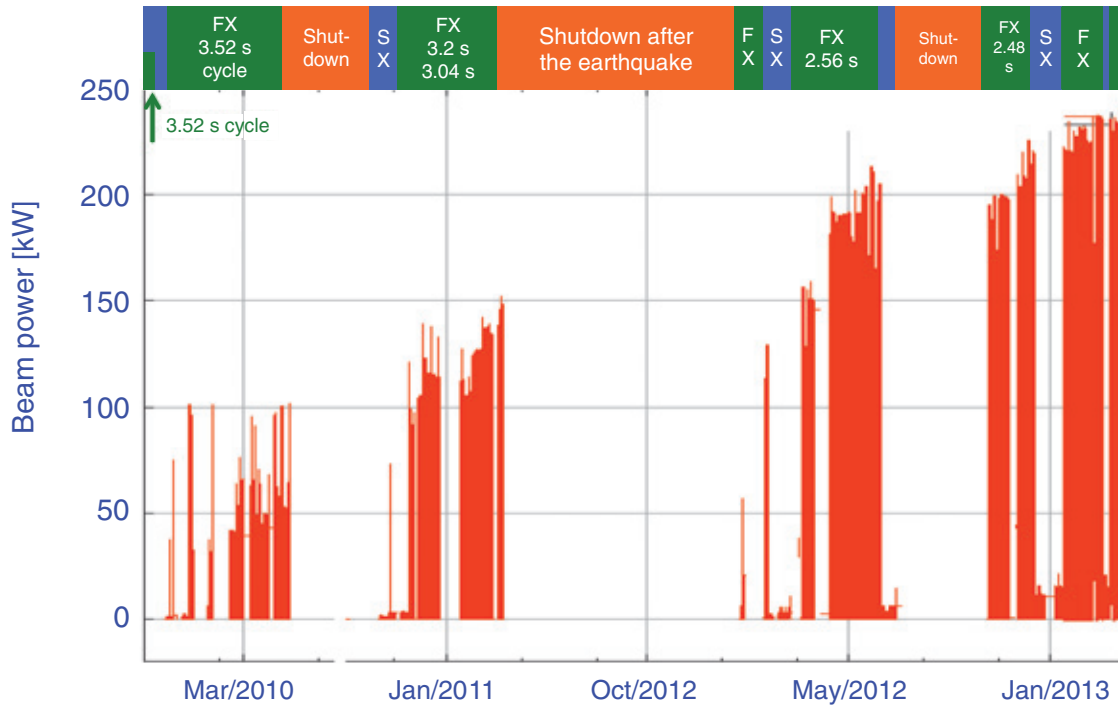


Fig. 9. History of delivered beam power as of the end of March 2013.

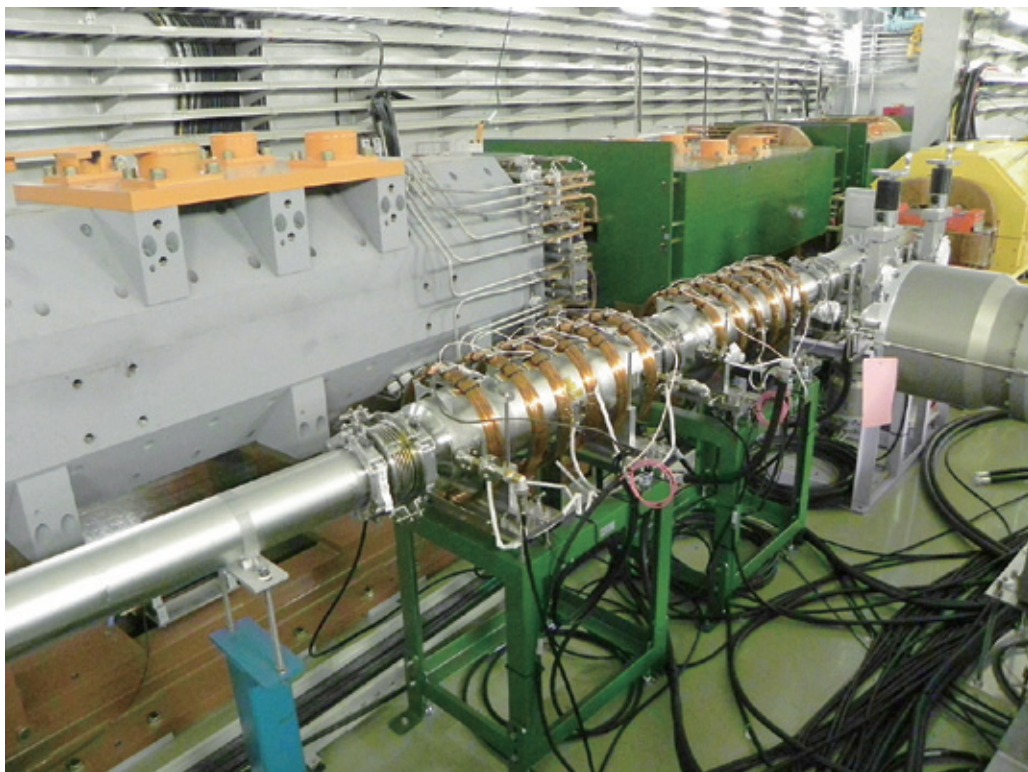


Fig. 10. Strip-line kickers of the new 100-MHz transverse rf system.

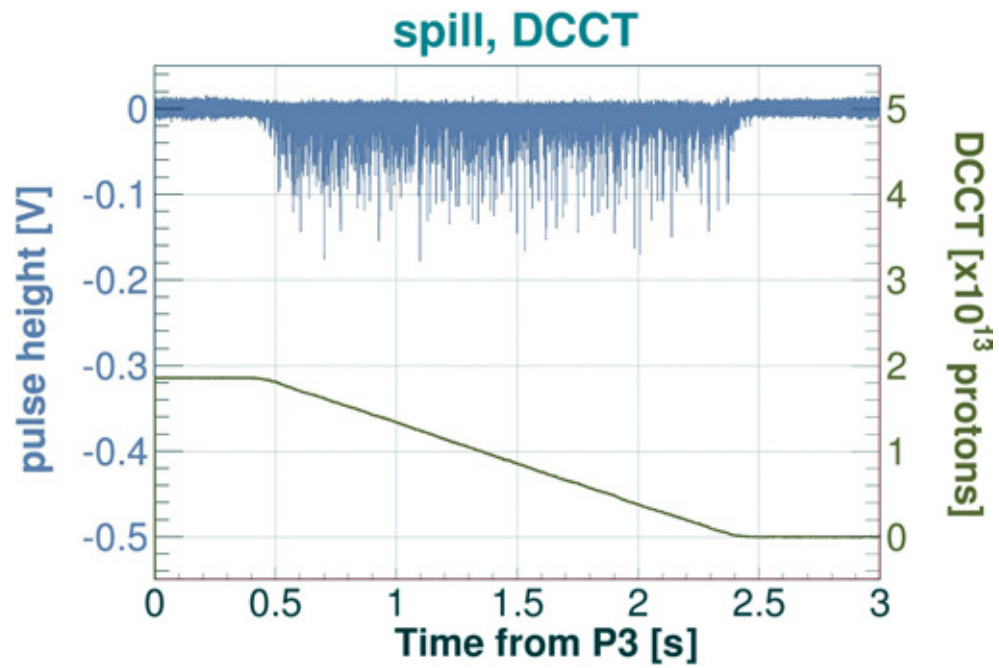


Fig. 11. Extracted beam spill signal (blue) and circulating beam current (green) for the SX operation with 15 kW beam power.



Materials and Life Science Experimental Facility

Overview

After recovering from the damage of the Great East Japan Earthquake of March 2011, the user program of Material and Life Science Experimental Facility (MLF) was restarted in January 2012. The very stable operation with 200 kW proton beam power continued until the summer shutdown. In October, the operation resumed and we achieved 534 kW as the maximum beam power in the commissioning, although just for a short time due to the license regulation. After this test, the 350 kW operation (nominal beam power: 300 kW) successfully continued until May 2013, when an accident occurred at the Hadron Facility.

Although the delivery of the bubbling system to mitigate pitting damages in the target container was delayed for half a year, we were able to install it in the Hg loop and started operation in November, which enabled us to ramp up the accelerator power to 350 kW. The mitigation effect was clearly observed by a laser Doppler vibrometer. However, we had a trouble due to unexpected intrusion of Hg into the branching He pipes. This problem will be solved by improving the

pipng system.

Four new beam lines joined the user program. Those are BL02 (DNA), BL15 (TAIKAN), BL17 (SHARAKU) and BL18 (SENJU). All of them are constructed and operated under the legislation regulating the user promotion program. BL06 (VIN ROSE), BL22 (ERNIS) and BL23 (POLANO) are under construction. A new beam port of muon, U-line, was also funded by a grant and its construction started.

The numbers of users at MLF in fiscal year 2012 hit a record high (735 for neutron and 72 for muon).

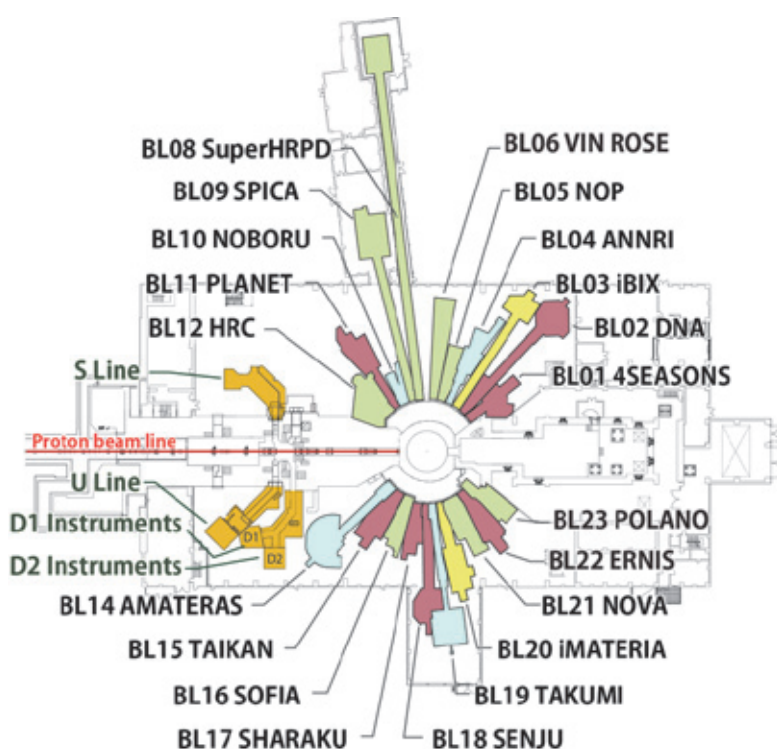
The numbers of submitted/ approved proposals gradually increased and those for the 2012A and 2012B rounds were 253/225 and 349/235, respectively.

Although the start of the direct user support activities of CROSS-Tokai was delayed by about 10 months due to the earthquake, the CROSS-Tokai engaged in its core business of managing the proposal selection process for the Public Beamlines (5 instruments in 2012), delivering high-quality user support and promoting utilization.

Table 1. Beam statistics for the MLF user program in Japan fiscal year 2012.

No. of run cycle	Nominal beam power (kw)	Duration	Scheduled time(*) (h)	Availability
#42	210	00am on 04/01/2012 – 07am on 05/25/2012	1147	81.6%
#43	210	09am on 05/29/2012 - 09am on 07/02/2012	777	96.4%
#44	210	09pm on 10/18/2012 - 09am on 11/12/2012	516	94.1%
#45	210, 280	09pm on 11/21/2012 - 06am on 12/27/2012	801	92.8%
#46	300	09am on 01/13/2013 - 07am on 02/22/2013	886	93.8%
#47	300	09pm on 02/25/2013 - 09pm on 03/26/2013	636	94.5%

(*) Note: The scheduled time excludes the duration allocated for the purpose of beam study for the 3-GeV proton beam transport line and/or the mercury target in MLF.



Neutron Instruments

BL	Name of Instruments	Moderator	Status
BL01	4SEASONS: 4D-Space Access Neutron Spectrometer	Coupled	in use
BL02	DNA: Biomolecular Dynamics Spectrometer	Coupled	In use
BL03	iBIX: IBARAKI Biological Crystal Diffractometer	Coupled	in use
BL04	ANNRI: Accurate Neutron-Nucleus Reaction measurement Instrument	Coupled	in use
BL05	NOP: Neutron Optics and Fundamental Physics	Coupled	in use
BL06	VIN ROSE: Village of Neutron ResONance Spin Echo spectrometers	Coupled	under construction
BL08	S-HRPD: Super High Resolution Powder Diffractometer	Poisoned	in use
BL09	SPICA: Special Environment Neutron Powder Diffractometer	Poisoned	commissioning
BL10	NOBORU: NeutrOn Beam-line for Observation & Research Use	Decoupled	in use
BL11	PLANET: High Pressure Neutron Diffractometer	Decoupled	in use
BL12	HRC: High Resolution Chopper Spectrometer	Decoupled	in use
BL14	AMATERAS: Cold-Neutron Disk-Chopper Spectrometer	Coupled	in use
BL15	TAIKAN: Small and Wide Angle Neutron Scattering Instrument	Coupled	in use
BL16	SOFIA: Soft Interface Analyzer	Coupled	in use
BL17	SHARAKU: Polarized Neutron Reflectometer	Coupled	in use
BL18	SENJU: Extreme Environment Single Crystal Neutron Diffractometer	Poisoned	in use
BL19	TAKUMI: Engineering Materials Diffractometer	Poisoned	in use
BL20	iMATERIA: IBARAKI Materials Design Diffractometer	Poisoned	in use
BL21	NOVA: High Intensity Total Diffractometer	Decoupled	in use
BL22	ERNIS: Energy Resolved Neutron Imaging System	Decoupled	under construction
BL23	POLANO: Polarization Analysis Neutron Spectrometer	Decoupled	under construction

Muon Instruments

BL	Name of Instruments	Status
D1	D1 Instrument	in use
D2	D2 Instrument	in use
U Line		under construction
S Line		under construction

Fig. 1. Status of the neutron and muon instruments at the MLF as of March, 2013.

Neutron Source

Progress of the 3-GeV proton beam transport facility

The fabrication of two octapole magnets was completed and they were delivered to MLF (Fig.2). Those magnets will reduce the current peak density of the incident proton beam with Gaussian distribution profile by about 30% and make the profile flatter. This 'beam-flattering' system will be installed in the summer of 2013 to ease the pitting damage on the mercury target vessel. We developed an automatic beam collection system which is useful for fine beam tuning to prevent serious damage to the beam line components caused by beam loss. We also developed an automatically controlled beam position compensation system based on the EPICS to correct the beam position in vertical direction at the mercury target, because the position was changed by the magnetic field leak from the solenoid magnet installed at a new secondary muon beam line. Thanks to the present system, the beam position at the mercury target became more stable. In April 2013, we succeeded to deliver a high power beam of 0.5 MW to the neutron production mercury target for a demonstration of the accelerator performance. The intensity

of the proton beam per pulse was 20 kJ/pulse, which exceeded the intensity of the beam provided with a power of 1 MW at SNS of ORNL.

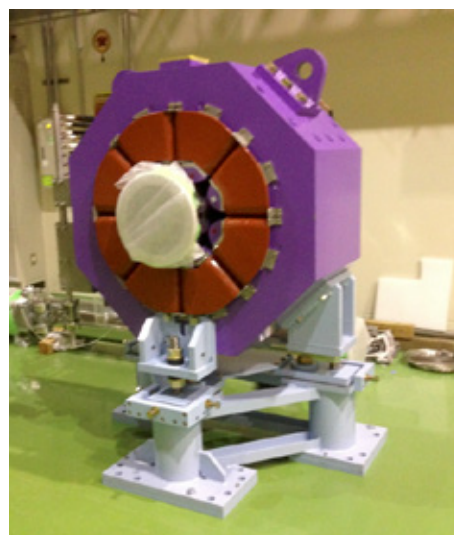


Fig. 2. Octapole magnet for beam flattening at the mercury target.

Success in mitigating pressure wave in the mercury target by injecting gas micro-bubbles

The injection of helium-gas micro-bubbles into the mercury target vessel started in November 2012; in this process helium gas flows from the upper space of the surge tank towards the swirl type bubbler in the target vessel through a compressor of a gas supplying device, as shown in Fig. 3. The vibration of the target vessel induced by the pressure wave was monitored by a novel in-situ diagnostic system using laser Doppler vibrometer (LDV) from the top of the shielding plug above the mercury target. As shown in Fig. 4, it was confirmed that the displacement velocity was certainly mitigated to about one-third by the micro-bubble injection for the 310 kW proton incidence. This is the first result in the world proving the mitigation effect of gas micro-bubbles on running mercury target. This suc-

cess enabled us to increase the power of the incident proton beam up to 300 kW for the MLF user program.

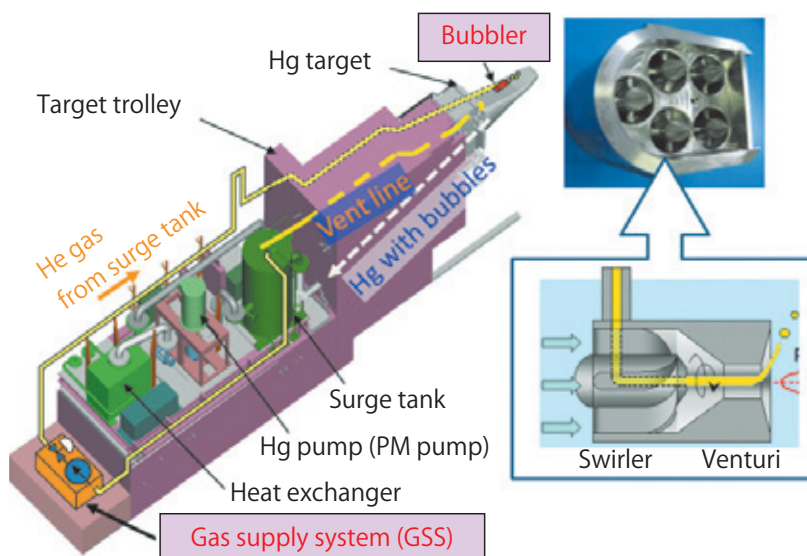


Fig. 3. Illustration of the mercury circulation system. Pictures of the swirl bubbler are also depicted.

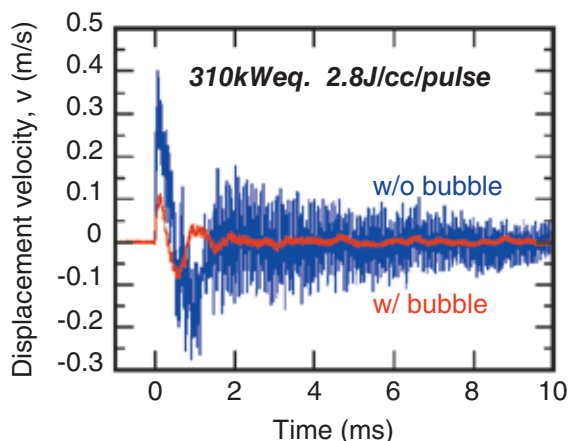


Fig. 4. Displacement velocity of the mercury target vessel measured with Laser Doppler Vibrometer for the 310 kW proton beam injection with a power density of 2.8 J/cc/pulse. Blue and red lines represent the data without and with micro-bubbles injection, respectively.

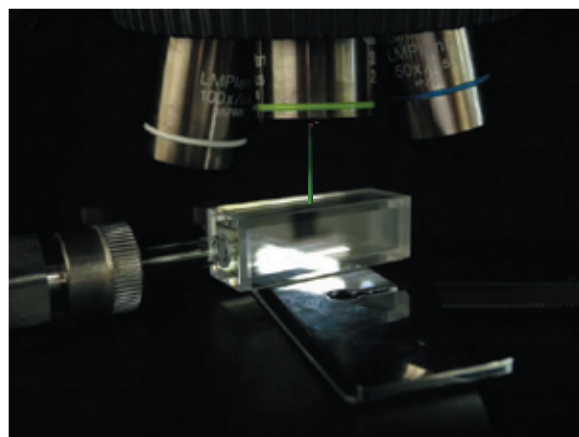


Fig. 5. Analysis of hydrogen gas collected in a glass-cell with a laser Raman spectroscopy.

Verification of 100% para-hydrogen concentration in the moderator system during the operating period

The supercritical hydrogen moderators of J-PARC were optimized to provide a high-intensity neutron beam, good pulse shape with narrow width, and fast decay (short tail) by using 100% para-hydrogen. The intensity and the pulse tail of neutrons emitted from a moderator are very sensitive to the fraction of para-hydrogen. It is of interest to measure the para-hydrogen fraction in the cryogenic hydrogen loop because such measurement has never been done at large scale spallation neutron source yet. We added a sampling line to

the hydrogen loop after a moderator and sampled gaseous hydrogen through two buffers connected to the sampling line in series to reduce the pressure from 1.5 MPa down to ca. 0.03 MPa. We collected hydrogen into quartz-glass-cells at the end of the buffer line during an operations period with a proton beam power of 300 kW and after the operations ended, respectively. As a result of analyses with a laser Raman spectroscopy (see Fig. 5), it was confirmed that the para-hydrogen fraction was kept 100% as designed.

Progress of the cryogenic hydrogen system

When a 1-MW proton beam is injected onto the target, a huge heat load of 3.75 kW is imposed stepwise upon the hydrogen loop. A heater and an accumulator are equipped in the cryogenic hydrogen loop to mitigate a pressure fluctuation below 0.1 MPa caused by this stepwise heat load and keep the feed hydrogen temperature constant. In 2012, we confirmed that this function was definitely activated at beam power of 300 kW and 532 kW. For the 532 kW case, a temperature rise of 1.3 K occurred at the outlet of the moderators. The pressure fluctuation was mitigated to the predicted level of 44 kPa, with controlling the feed hydrogen temperature constant, although it temporarily increased by 0.08 K. The present result indicates that the cryogenic hydrogen system would be operated stably for the 1 MW proton beam operation.

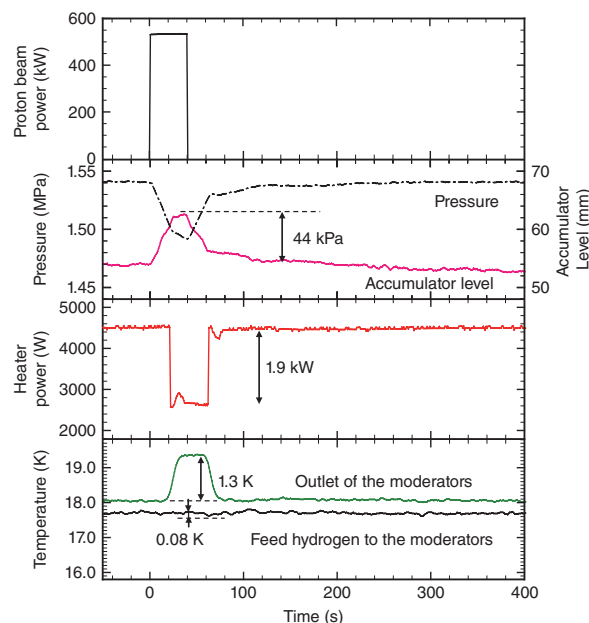


Fig. 6. Dynamic behaviors of cryogenic hydrogen loop for the 532-kW proton beam incidence.

Neutron Science

Switching of intra-orbital spin excitations in electron-doped iron pnictide superconductors *(S. Iimura et al.)*

The iron pnictide superconductor $\text{LaFeAsO}_{1-x}\text{H}_x$ shows a unique phase diagram in Fig. 7. In addition to the first superconducting dome with the optimal critical temperature (T_c) of 29 K adjacent to the AFM phase, the second dome with an optimal T_c of 36 K is broadly spread around $x \sim 0.35$; a T -linear resistivity, often referred to as the non-Fermi-liquid state, is observed above the T_c . According to previous theoretical calculations, the development of the spin density wave (SDW)-type spin fluctuations is unlikely in such heavy electron-doping conditions $x > 0.3$ due to the change of the Fermi surface (FS), whereas the observed T -linear resistivity implies the crucial relation between the spin fluctuations and the second dome.

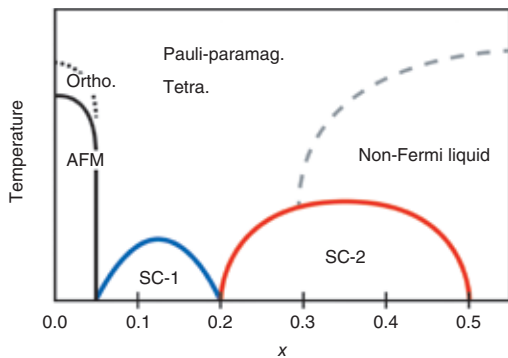


Fig. 7. Schematic phase diagram of $\text{LaFeAsO}_{1-x}\text{H}_x$.

Thus, we performed inelastic-neutron-scattering (INS) measurements to investigate the dynamic spin states of $\text{LaFeAsO}_{1-x}\text{D}_x$ with $x = 0.1, 0.2,$ and 0.4 corresponding to the top of the first dome, the T_c valley, and the top of the second dome, respectively. For the sample compositions $x = 0.1, 0.2,$ and 0.4 , the T_c 's were 27, 14, and 34 K, respectively. Several INS measurements were performed using the Fermi chopper spectrometer 4SEASONS in J-PARC. All data presented here were obtained at incident energy of 45.1 meV.

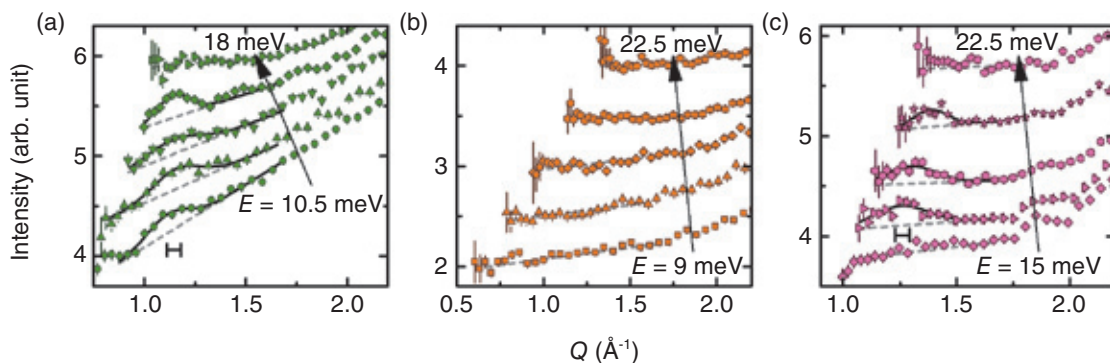


Fig. 8. Constant E -scans of $\text{LaFeAsO}_{1-x}\text{D}_x$ with (a) $x = 0.1$, (b) 0.2 , and (c) 0.4 at $T = 7$ K.

Figures 8 (a), (b) and (c) show the doping dependency of the INS intensity from $\text{LaFeAsO}_{1-x}\text{D}_x$ with $x = 0.1, 0.2,$ and 0.4 at 7 K as a function of momentum transfer (Q) at several fixed energy transfers (E). For composition $x = 0.1$ [Fig. 8(a)], a peak is observed at $Q = 1.14 \text{ \AA}^{-1}$ and in $10 < E < 17$ meV. The Q value is very close to the wave vector for the two-dimensional stripe-type AFM order in the parent phase $Q_{\text{AFM}}^{2\text{D}} = (1 \ 0 \ 0) \sim 1.1 \text{ \AA}^{-1}$ in orthorhombic notation, indicating fluctuations of the SDW. For $x = 0.2$, the magnetic peak completely disappears [Fig. 8(b)]. As x increased to 0.4 [Fig. 8(c)], a peak appears again at $Q = 1.25\text{--}1.38 \text{ \AA}^{-1}$ in $16 < E < 22$ meV.

Figure 9 shows the calculated spin susceptibility based on the RPA applied to a five-orbital model of $\text{LaFeAsO}_{1-x}\text{H}_x$ that was derived from the band calculation using VCA for the doping effect. The calculated χ_s at $x = 0.08$ and 0.40 have a peak at $Q = (\pi, 0) \sim 1.1 \text{ \AA}^{-1}$ and $(\pi, 0.35\pi) \sim 1.2 \text{ \AA}^{-1}$, respectively, which agree well with the experimental values. The FS analysis shows that the origins of the two χ_s peaks are different; the former is derived from the nesting within $\text{Fe-}3d_{yz, zx}$ whereas the latter is due to the nesting within $\text{Fe-}3d_{x^2-y^2}$, indicating the switching of the two intra-orbital nestings within the $3d_{yz, zx}$ and $3d_{x^2-y^2}$ by electron doping. These experimental findings and calculations imply that the orbital multiplicity plays an important role in the doping and/or material dependence of the T_c of the iron pnictides.

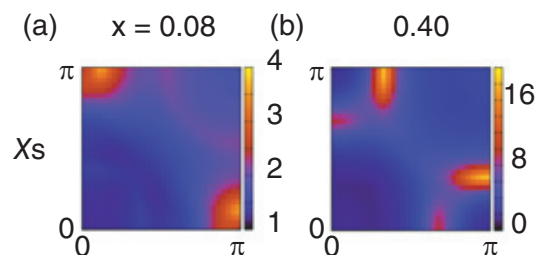


Fig. 9. Contour plot of the spin susceptibility for (a) $x = 0.08$ and (b) 0.40 .

Neutron Brillouin Scattering Experiments on HRC (S. Itoh et al.)

On the High Resolution Chopper Spectrometer (HRC at BL12), the neutron Brillouin scattering (NBS) experiments became feasible by reducing the background noise at low angles down to $\phi = 0.5^\circ$. NBS is the most promising way to observe excitations in the forward direction from powders, polycrystals, or liquids. Owing to the kinematical constraints of neutron spectroscopy, incident neutron energy (E_i) in sub-eV region with high resolution ($\Delta E/E_i$) at low scattering angles (ϕ) is necessary for measuring scattering in the meV transferred energy (E) range near (000).

First, NBS experiment was performed to observe spin waves in a polycrystalline sample of a nearly-cubic perovskite, $\text{La}_{0.8}\text{Sr}_{0.2}\text{MnO}_3$, (Curie temperature: $T_C = 316$ K), whose magnetic properties are well elucidated. Figure 10 shows the dispersion relation of spin waves in $\text{La}_{0.8}\text{Sr}_{0.2}\text{MnO}_3$ measured with $E_i = 102$ meV and $\Delta E = 2$ meV. The observed dispersion relations at 6 and 245 K were well fitted to $E = DQ^2$, where Q is the scattering vector. The obtained D values were 130 ± 13 and 88 ± 2 $\text{meV}\text{\AA}^2$ at 6 and 245 K, respectively. These values are in good agreement with the results ($D = 131$ and 89 $\text{meV}\text{\AA}^2$ at 14 and 250 K, respectively) obtained by the previous experiments using a single crystal. That demonstrated the feasibility of NBS experiments on the HRC.

Next, the spin waves in a polycrystalline ferromagnet, SrRuO_3 ($T_C = 165$ K), were similarly measured. This material also has a nearly-cubic perovskite structure showing an anomalous Hall effect, but a large single crystal suitable for inelastic neutron scattering experiments has not yet been synthesized. The measurement was performed at 7 K with $E_i = 102$ meV, and well-defined spin wave peaks were observed. As shown in Fig. 10, the dispersion relation of spin waves in SrRuO_3 was well fitted to $E = E_0 + DQ^2$ with an apparent energy gap E_0 .

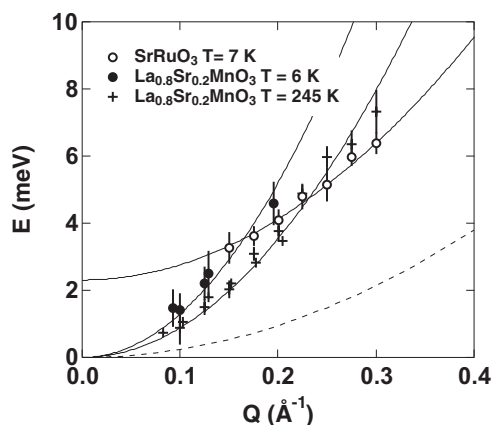


Fig. 10. Spin-wave dispersion curves for $\text{La}_{0.8}\text{Sr}_{0.2}\text{MnO}_3$ and SrRuO_3 determined on the HRC. The solid lines are fitted curves. The dashed line is the upper boundary accessible with a conventional spectrometer.

$\text{Nd}_2\text{Fe}_{14}\text{B}$ is a well-known strong permanent magnet with $T_C = 580$ K. At room temperature, all spins are aligned along the c^* -axis. We measured spin waves in a $\text{Nd}_2\text{Fe}_{14}\text{B}$ polycrystalline sample at 300 K with $E_i = 257$ meV and $\Delta E = 5.7$ meV. The spin wave peak positions were determined in Fig. 11. The observed peak positions were on the dispersion curve along the c^* -axis reported in the previous experiment.

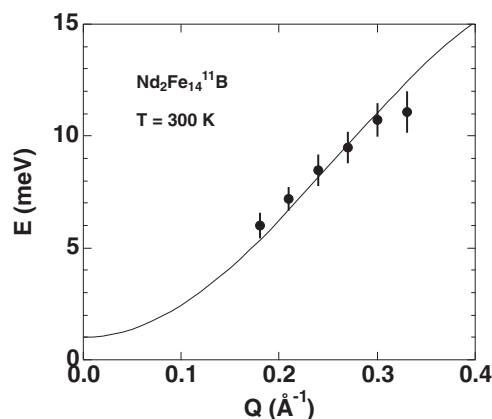


Fig. 11. Spin wave dispersion relation of $\text{Nd}_2\text{Fe}_{14}\text{B}$. The solid line is the dispersion curve along the c -axis determined using a single crystal sample.

Phononic excitations in a liquid D_2O were measured at 300 K with $E_i = 102$ meV and $\Delta E = 2.0$ meV. The observed spectra were well fitted with a damped harmonic oscillator scattering function and the peak positions were determined, as shown in Fig. 12. The observed peak positions down to $Q = 0.02$ \AA^{-1} were well fitted to $E = cQ$ with $c = 21.4 \pm 0.2$ $\text{meV}\text{\AA}$, which is equivalent to $c = 3250 \pm 30$ m/s. The observed sound velocity c was in good agreement with that for the fast sound observed in the previous experiment with $E_i = 80$ meV and $\Delta E = 4.8$ meV down to $Q = 0.035$ \AA^{-1} .

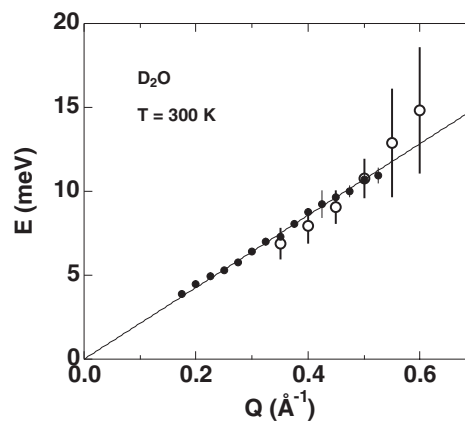


Fig. 12. Dispersion relation for phononic excitations, the fast sound, in D_2O (closed circles). The open circles are previous results. The solid line is a fitted line.

Investigation of Degradation Mechanism of ITER CS Conductor Sample using TAKUMI (T. Hemmi et al.)

ITER was constructed in France under an international collaboration with India, China, EU, Korea, Russia, USA and Japan to prove the viability of nuclear fusion as a power source. To confine and control the plasma, the ITER magnet system consists of a Central Solenoid (CS), 18 Toroidal Field (TF) coils and 6 Poloidal Field (PF) coils. The CS, which is 13.5 m in height and 4.1 m in diameter, generates and controls the plasma current by varying the magnetic field as a maximum of 13 T. JAEA has to responsibly procure all ITER CS conductors. The CS conductor is a cable-in-conduit conductor (CICC) composed of a superconducting cable consisting of 576 Nb₃Sn strands and 288 copper strands, a SS316L central spiral and a JK2LB stainless steel square jacket as shown in Fig 13. After the operation of 60,000 cycles, a current sharing temperature (T_{cs}) of 5.2 K is required at currents of 40 kA under the magnetic fields of 13 T. Several conductor samples were fabricated to evaluate the performance of the CS conductor and validate its design concept. Two CS conductor samples named CSJA01 and CSJA02, consisting of a pair of conductor samples, were tested in the SULTAN test facility in Switzerland. The gradual degradation was observed in the results for both CSJA01 and CSJA02, being the same as that of many TF conductors as shown in Fig. 14.

Up to now, the transverse electromagnetic loading has been considered as a major origin of T_{cs} degradations of Nb₃Sn CICC's due to the local bending at the high loading side (HLS) in the high field zone (HFZ). From the destructive investigation in the HFZ after SULTAN testing, the deflection of strands on the low transverse loading side (LLS) is larger than that for the HLS as shown in Fig.15. Since the bending pith is around 5 mm due to contacting of strands compacted by the electromagnetic transverse loading in the HLS, there is

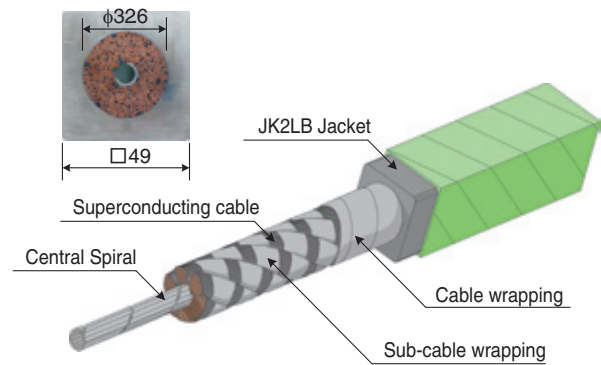


Fig. 13. Schematics of ITER CS conductor.

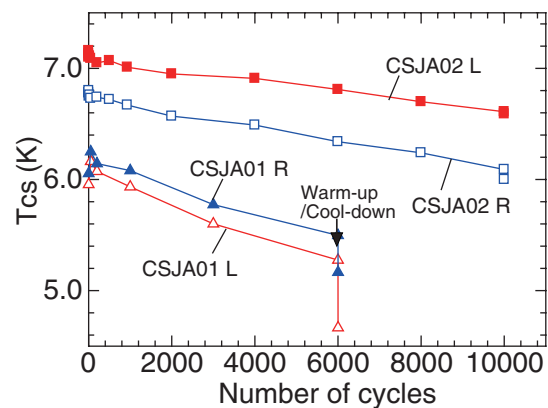


Fig. 14. T_{cs} result of CSJA01 and CSJA02.

a possibility of large bending strain with small deflection of strands in the HLS.

The neutrons, which have a large penetration depth, are a powerful tool to evaluate the internal strain of Nb₃Sn in the CICC. In order to evaluate the internal strain in ITER CS conductor samples non-destructively and quantitatively, a neutron diffraction measurement using the engineering materials diffractometer 'TAKUMI' (BL19) was carried out on the CSJA01 left leg at room temperature.

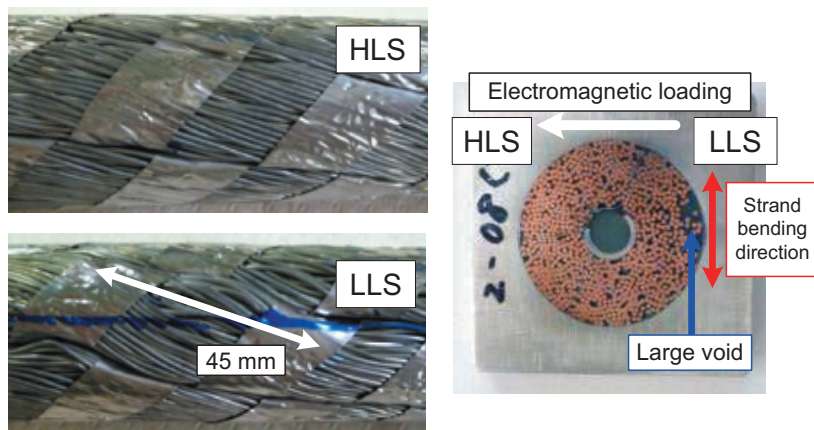


Fig. 15. Visually inspected cable in the HFZ of CSJA01 right leg.

For the neutron diffraction measurement using TAKUMI, a conductor sample of 3.6 m was arranged. The neutron beam was focused using a pair of radial collimators to the gauge volume of $7 \times 2 \times 16 \text{ mm}^3$ in the measured position of the conductor sample. The sample conductor was turned over to measure if the LLS and the HLS have the same path as the neutron beam. Figure 16 shows the diffraction profiles for the axial direction of Nb_3Sn (211) at the LLS and the HLS of the field center and 1150 mm from the field center. The Nb_3Sn filaments were taken from the same strand using a chemical process to compare the diffraction profile of the conductor sample. The diffraction peak shapes and positions at the HLS in the HFZ and the low field zone (LFZ) were similar, and the peaks were located at a lower level than that of Nb_3Sn filaments. This peak shift is due to the difference in the thermal contraction between copper/ Nb_3Sn filament and cable/jacket from the reaction temperature of Nb_3Sn . However, the peak of the LLS in the HFZ shifted to a tensile direction and became broader compared to the other peak. The bending strain with the relaxation of the compression strain in the Nb_3Sn strand remained irreversible after the SULTAN testing.

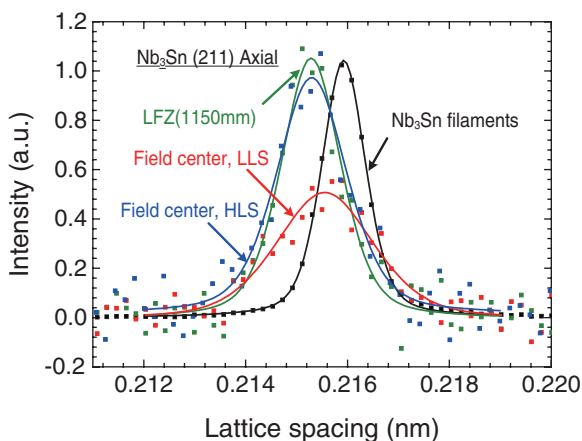


Fig. 16. Differences in diffraction profile.

After the neutron diffraction measurement, a larger bending strain was found at the LLS of the HFZ in the conductor sample. As a degradation mechanism, the strand buckling is seen as follows: 1) The void at the LLS of the HLS is generated by the transverse movement of the strands in the conductor sample. 2) There is an axial compressive force induced by the difference in the thermal contraction from the reaction temperature of Nb_3Sn . 3) The buckling of the Nb_3Sn strand is occurring via the axial compressive force because the supporting and the friction of the jacket and the cable on the strand are varied by the large void.

The shorter twisting pitch (STP) could be considered as a method to improve the conductor performance on the strand buckling. The cable with the STP has withstood the strand buckling since its bending stiffness and rigidity are quite significant. Figure 17 shows photographs of the cables with original twisting pitch and STP. The result of the SULTAN testing of the conductor sample with STP found it to be very effective, and the performance degradation along cyclic testing was almost negligible as shown in Fig. 18.



Fig. 17. Photograph of the cable with original twisting pitch and STP.

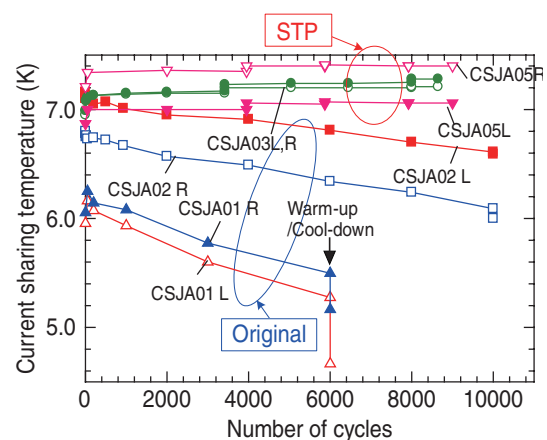


Fig. 18. T_{cs} results of SULTAN testing.

Neutron diffraction measurement on the ITER CS conductor sample was performed to investigate the degradation mechanism of the conductor sample. As a result of the neutron diffraction measurement, large bending at the LLS of the HFZ was found. Therefore, it was concluded that the T_{cs} degraded position of the conductor sample due to the cyclic loading was the LLS of the HFZ. The large bending originated from the strand buckling due to the large void generated by the transverse electromagnetic loading and the thermally induced residual compressive strain. By applying the STP on the cable to control the strand buckling, the problem of the performance degradation along cyclic testing was solved.

Muon Science

At MUSE, we had a steady operation at the D-line in the fiscal year of 2012. At the U-line, we managed to install new axial focusing muon beamline components, to extract intense surface muons dedicated for

D-line operation

Consequently, we managed to operate users' run at the D-line with proton intensity of up to 300 kW. We installed a switch yard, a kicker and septum magnets to allow a single bunched muon beam up to 60 MeV/c towards D1 and D2 areas in the D-line. Everything worked successfully, delivering a single pulse towards

Installation of the U-line

We were funded to install a second muon beamline, the so called U-line, which consists of a large acceptance solenoid made of mineral insulation cables (MIC), a superconducting curved transport solenoid magnet and a superconducting axial focusing magnets system. There, we can collect surface muons with a large acceptance of 400 mSr. Compared to the conventional beamlines such as the D-line, the large acceptance of the front-end solenoid allows us to capture 10 times more intensity pulsed surface muons of 5×10^8 /s, when the proton beam intensity reaches 1 MW. The U-line components of the superconducting curved and axial focusing magnets were already fabricated and their commissioning was performed in October, 2012. Figure 19 (Left) shows a picture of the celebration of the delivery of the superconducting curved transport solenoid magnet. Figure 19 (Right) shows a picture of the superconducting axial focusing magnets associated

ultra slow muon production. Also, we completed the installation of front-end magnets in the vicinity of the muon target during a shut-down period in the summer of 2012 under an intense radiation field.

the D1 area, with negligibly small S/N ratio appeared in the μ SR spectrum. At the D1-area, a dilution refrigerator which had been used at KEK-Tsukuba, was brought to MUSE, fixed and installed, enabling us to perform μ SR measurements as low as 25 mK.

with three sets of ± 400 kV DC separators.

In the commissioning works, we succeeded in extracting the world's highest intensity pulsed muons, 2,500,000 muons per pulse (6.4×10^7 /s at 212 kW, corresponding to 3×10^8 /s at 1 MW) to the U1 experimental area. This intensity achieved at the U-line exceeds the previous intensities, 72,000 muons per pulse (120 kW) and 180,000 muons per pulse (300 kW), which were achieved at the D-line of this facility in 2010, respectively. It means that for the first time globally we achieved the world's strongest pulsed muon intensity. The achieved intensity not only shortens the measurement time to one-twentieth compared with the present measurement, but it also may open a new era to capture novel information that could not be recognized before. According to the simulation, we could extract 2×10^8 /s surface muons (at the 1 MW operation) to the experimental area, with an approximate transport



Fig. 19. (Left) The celebration of the delivery of the superconducting curved transport solenoid magnet. (Right) The superconducting axial focusing magnets associated with three sets of ± 400 kV DC separators.

efficiency of 40%. It demonstrates that the beam line design concept adopting axial focusing extraction for the first time is working very well. Figure 20 shows a lifetime spectrum of the surface muons extracted to the U1 area on Al target, showing 2-bunched structure of the surface muons and electrons. It demonstrated that very intense surface muons as much as $6.4 \times 10^7/s$ @212 kW were extracted to the U1 shielding area, which was 20 times stronger than the D-line.

As a next step, we are planning to stop such intense pulsed muons towards a hot tungsten target for generating intense ultra-slow muon beams in order to realize "ultra-slow muon microscopes". When the production

of an intense ultra-slow muon source is realized, the use of its short-range penetration depth (eg. 1 nm resolution at a penetration of 1 nm, and 10 nm at a penetration of 6 nm in gold) will allow the muon science to expand into a variety of new scientific fields, such as:

- 1) Surface/boundary magnetism utilizing its spin polarization and unique time-window.
- 2) Surface chemistry, utilizing a feature of a light isotope of hydrogen, such as catalysis reactions.
- 3) Precise atomic physics such as QED,
- 4) Ion sources towards possible $\mu^+\mu^-$ collider experiments in high-energy physics.

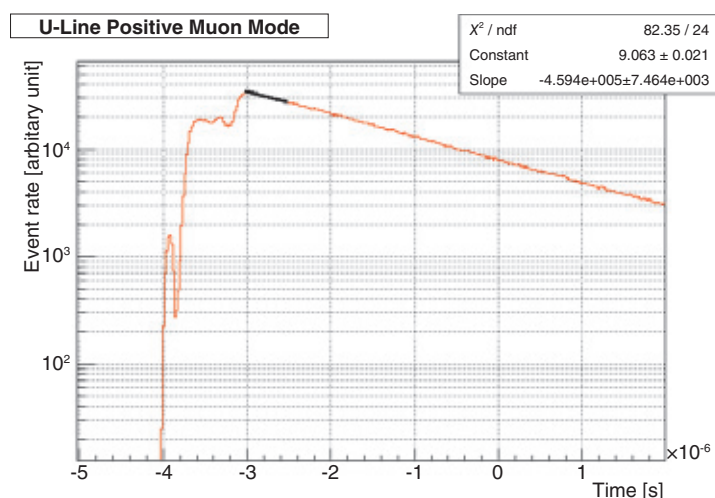


Fig. 20. Lifetime spectrum of the surface muons extracted to the U1 area, showing the 2-bunched structure of the surface muons and electrons. It demonstrates that surface muons as much as $6.4 \times 10^7/s$ @212 kW were extracted to U1 shielding area, corresponding to 20 times stronger than the D-line.

Installation of the front-end magnets for the S-line and H-line in the vicinity of the muon target

During a shutdown period in the summer of 2012, we worked on the installation of front-end magnets for the S-line, which is a surface muon beam line dedicated for the materials science with a modest-acceptance (about 50 mSr), and the H-line at which various problems of the fundamental physics research will be studied, for instance, the precise measurement of the hyperfine splitting of Muonium, implying the existence of new physics laws beyond the Standard Model, or the precise measurement of the anomalous magnetic moment ($g-2$) of muons. Although the radiation level in the vicinity of the muon target was very high to be in the order of Sv/h, we finally managed to install the SQ4,5,6 and HS1, HS2, HS3 and HB1 associated with guide shields and pillow seals between those elements. Figure 21 shows a picture of the installation of the HS1,

HS2, HS3 and HB1 in severe radiation environment in the vicinity of the muon target.



Fig. 21. A picture of the installation of the HS1, HS2, HS3 and HB1 in the vicinity of the muon target.

Neutron Device

Focusing supermirrors on precisely figured elliptical surfaces (D.Yamazaki et al.)

Reflective optics is one of the most useful techniques for focusing a neutron beam with a wide wavelength range since there is no chromatic aberration. We have been developing aspherical supermirror optics by using an ion beam sputtering technique to coat high performance supermirrors and a numerically controlled local wet etching (NC-LWE) technique to figure aspherical mirror substrates. Previously, we fabricated a plano-elliptical supermirror with a clear aperture of size of $90 \times 40 \text{ mm}^2$ by applying these techniques and obtained a focusing gain of 6 and a reflectivity of 0.64-0.7 in the critical-angle region for $m=4$. Increasing the mirror size is essential for increasing the focusing gain. We report fabrication result of an elliptical supermirror with large clear aperture size and the focusing performance of the neutron beam.

We fabricated a 400-mm-long elliptical neutron-focusing supermirror by a combined fabrication process consisting of precision grinding, HF dip etching, NC-LWE figuring, low-pressure polishing and ion beam sputtering deposition. We succeeded in obtaining a figure error of $0.43 \mu\text{m p-v}$ with a surface roughness of less than 0.2 nm rms .

The focusing performance of the fabricated ellip-

tical supermirror was evaluated at BL10 NOBORU. We show a schematic of the setup for measuring the neutron beam profile in Fig. 22. A flat supermirror with $m = 4$ is used to reflect the neutrons into the focusing device to reduce the background and the gamma radiation from the direct beam. The wavelength of the neutron beam was varied from 3.5 to 10 \AA . Two-dimensional images of focused and nonfocused direct neutron beams were measured using an imaging plate (Fujifilm BAS-ND; resolution: $50 \mu\text{m}$). The width of the slit in this experiment was 0.10 mm . The magnification of the optical design was 1. Figure 23 (A) and (B) shows two-dimensional images of focused and nonfocused direct neutron beams, the neutron beam detected using the imaging plate. A neutron beams with a wide wavelength range was uniformly focused on the mirror where it had an effective width of 30 mm . The neutrons detected beyond the mirror were due to the horizontal divergence of the neutron beam. The full width at half maximum (FWHM) of the focused beam was 0.128 mm , and a focusing gain of 52 in terms of the peak intensity was achieved compared with the nonfocused direct beam. At the peak intensity for a neutron beam, a wavelength range is $3.5\text{-}10 \text{ \AA}$.

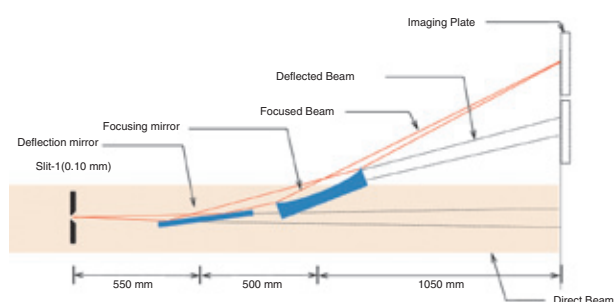


Fig. 22. A schematic of the setup for measuring the neutron focusing profile.

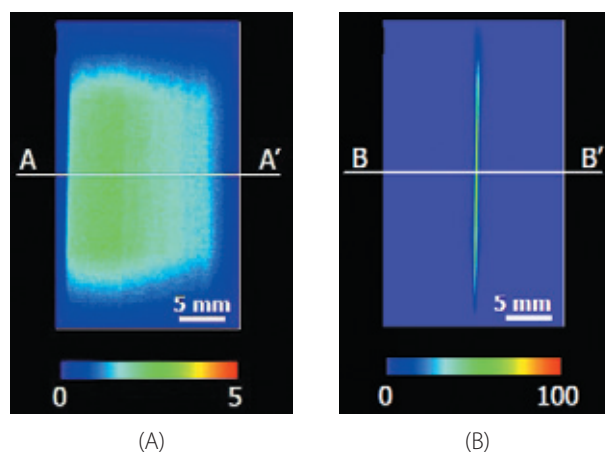
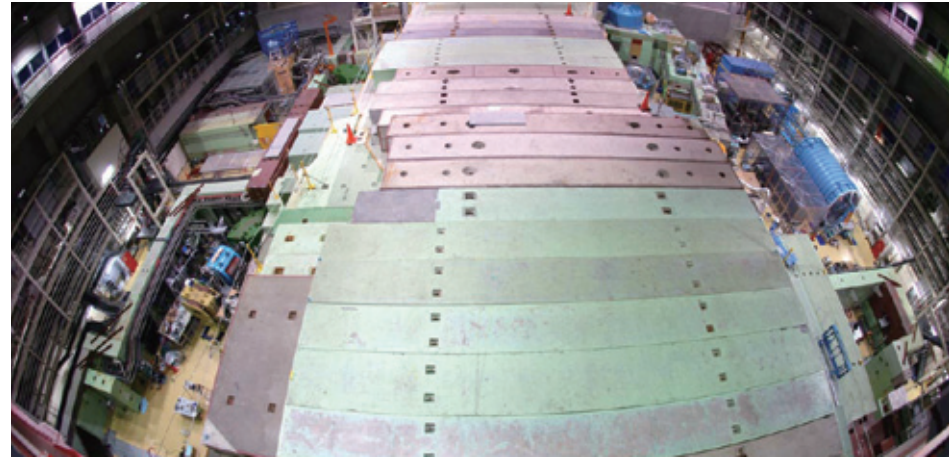
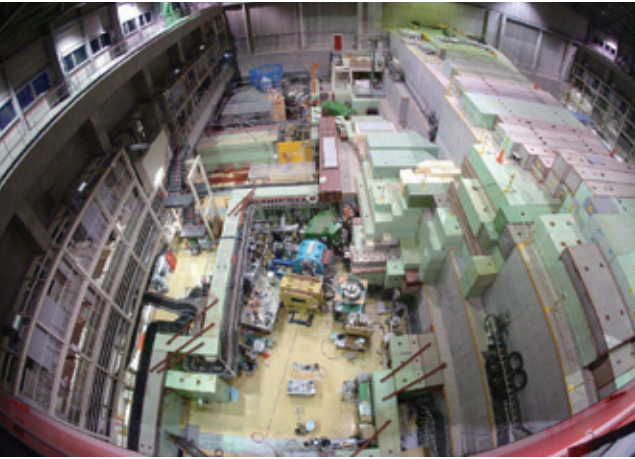
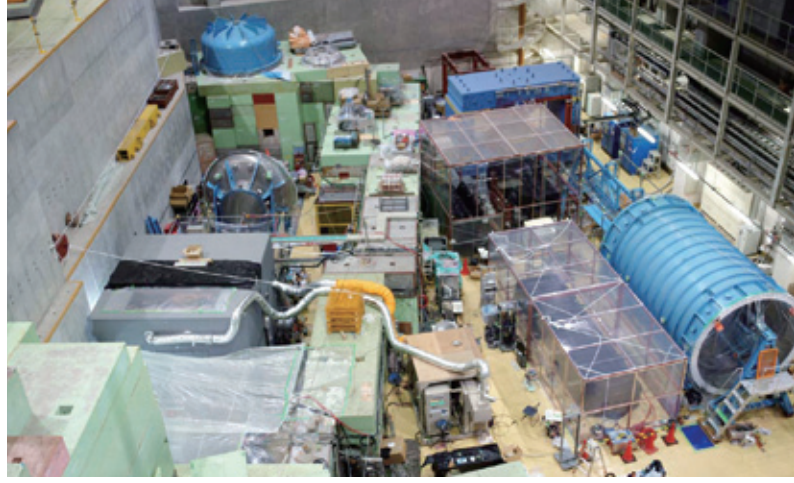
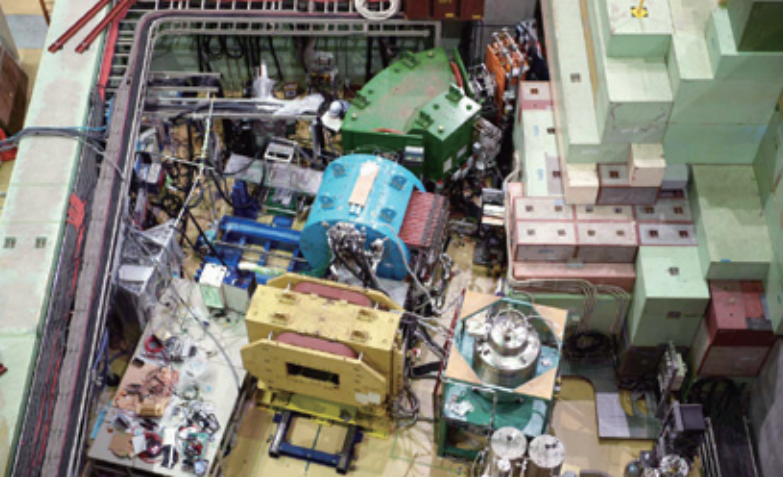


Fig. 23. 2-d images of the focused beam.



Particle and Nuclear Physics

Hadron and Nuclear Physics

Recent research has indicated that strangeness plays a very important role in the behavior of high-density nuclear matter such as the core of a neutron star. At such high-density, the neutron Fermi energy exceeds the strange particle production threshold; therefore, hyperons that contain strange quark(s) and other forms of strangeness may emerge. The recent discovery of a neutron star with two solar masses seems to contradict the naïve picture above. However, certain behaviors of the nuclear matter, such as the density at which strangeness emerges and the states in which strangeness exists, depend on the interactions of strange particles in such high-density nuclear matter. Thus, the knowledge of the interactions and nuclei exhibiting strangeness (hypernuclei) becomes exceedingly important. Strangeness physics is one of the major research subjects at the J-PARC hadron facility. Several experiments related to these topics were carried out in 2012.

Neutron-rich Λ hypernuclei provide valuable information on Λ hyperon interaction and potential in a neutron-rich environment such as neutron-star matter. Among these hypernuclei, ${}^6_{\Lambda}\text{H}$ is of particular interest. In the ${}^6_{\Lambda}\text{H}$ hypernucleus, an unbound ${}^5\text{H}$ may be bound with an additional Λ hyperon due to an attractive Λ -nucleon interaction (glue-like role of Λ) and a coherent ΛN - ΣN coupling effect, which is expected to play a very important role in neutron-rich matter. In the J-PARC E10 experiment, a ${}^6_{\Lambda}\text{H}$ spectrum was measured using SKS spectrometer at the K1.8 beam line through a double charge exchange (π^+, K^+) reaction on ${}^6\text{Li}$. Since a small cross section of ~ 10 nb/sr is expected for this reaction, a high-intensity beam of 12 M/spill should be used, in spite of its poor time structure. In total, 1.65×10^{12} π^+ were irradiated on a 3.5 g/cm² target. Analysis is currently underway. In this experiment, the ${}^{12}\text{C}(\pi^+, K^+){}^{12}_{\Lambda}\text{C}$ spectrum was also measured, for the first time at J-PARC, in order to evaluate spectrometer performance as shown in Fig.1.

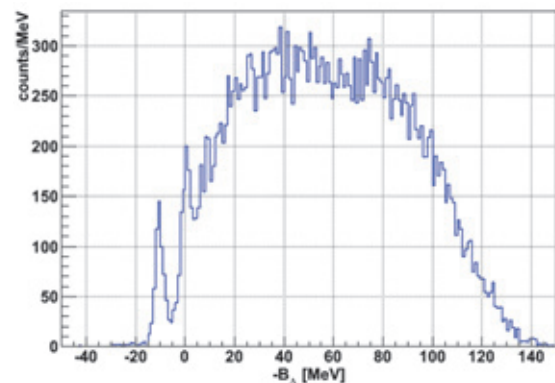


Fig. 1. ${}^{12}\text{C}$ spectrum measured by the (π^+, K^+) reaction on a 3.5 g/cm² carbon target. Missing mass resolution of ~ 3 MeV/c² (FWHM) has been achieved.

Kaon bound nuclei are also objects of interest because of their high-density nuclear matter that exhibits strangeness. Two experiments at J-PARC are aimed at discovering the simplest system of such kind, Kpp . E27 searches for Kpp bound system that may be produced through the $\Lambda(1405)$ doorway in the $d(\pi^+, K^+)$ reaction at 1.7 GeV/c. Two protons are measured simultaneously in order to suppress the huge background arising from the quasi-free production of Λ , Σ , and Y^* . Pilot data were taken at the K1.8 beam line, using liquid deuterium and hydrogen targets, in order to understand the background processes in detail. The feasibility of the tagging method for one- and two-proton(s) was checked. An inclusive spectrum is shown in Fig.2. Another experiment, E15 at the K1.8BR beam line, aims to search for Kpp in both the production and decay channels. The Kpp is produced via the ${}^3\text{He}(K, n)$ reaction and its decay, $Kpp \rightarrow \Lambda p \rightarrow \pi pp$, is detected by the Cylindrical Detector System surrounding the liquid ${}^3\text{He}$ target. The collection of data began in March 2013.

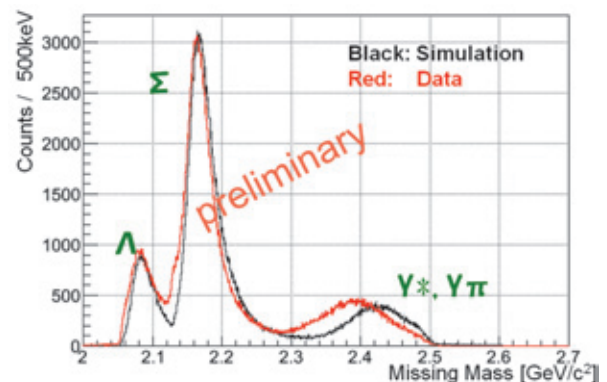


Fig. 2. Inclusive spectrum of $d(\pi^+, K^+)$ at 1.7 GeV/c. The red curve shows the data while the black one shows the simulation spectrum of the known background processes.

Kaon Physics

The quantum transition of a heavy particle into lighter particles is called “decay” in particle physics. The decay of a particle proceeds via several paths or “decay modes.” Once experimentally determined, the branching fraction for a decay mode is compared to the theoretical predictions. Any discrepancy between the experimental results and the theoretical predictions is a new piece of evidence for physics beyond the Standard Model (SM).

The decay of a long-lived neutral kaon (K_L) into a neutral pi meson (π^0) and pair of neutrinos, represented as $K_L \rightarrow \pi^0 \nu \bar{\nu}$ is known in particle physics as a rare and precious decay mode. New sources of symmetry breaking that can explain the matter-antimatter asymmetry in the universe may be revealed by examining this decay mode. SM predicts that this decay mode occurs once in forty billion K_L decays. For experimentalists, detecting this decay mode is a challenge because only two photons from π^0 decay are observable.

The J-PARC E14 KOTO experiment was proposed

in 2006 to study the $K_L \rightarrow \pi^0 \nu \bar{\nu}$ decay. In the Hadron Experimental Hall, a new neutral beam line was built for KOTO in 2009 and 2716 undoped CsI crystals were stacked in 2010 for the KOTO calorimeter. The crystals and photo-tubes were previously used in the KTeV experiment at Fermilab, USA. After the earthquake in March 2011, the beam line components were realigned, and the KOTO calorimeter was examined and confirmed to be undamaged. The construction of the detector resumed. In 2012, we installed charged-particle veto counters (Fig. 3) to identify the electromagnetic showers in the calorimeter as photons, photon veto counters to detect extra photons from K_L decays, and neutron collar counters to measure the neutrons in the beam halo. The vacuum vessel of the KOTO detector was closed in December 2012, and the vacuum system was installed in early January 2013 (Fig. 4). After engineering runs and commissioning of the detector, the first physics run will be performed by the summer of 2013.

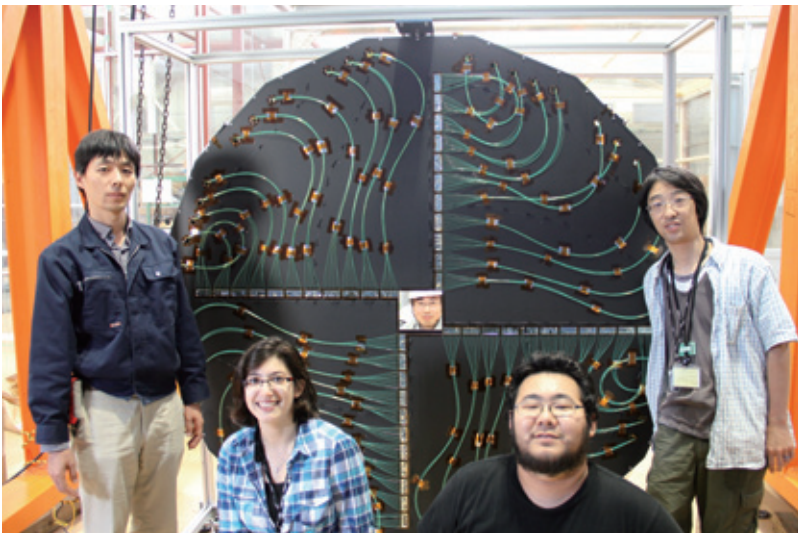


Fig. 3. Charged-particle veto counters developed and constructed by the KOTO collaborators from Kyoto University, Japan, with the help of summer students from the University of Michigan, USA.

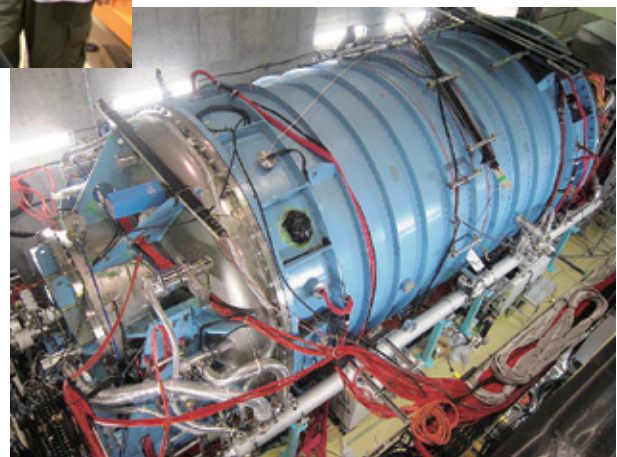


Fig. 4. The KOTO detector in January 2013 after installation of the vacuum system.

Muon Physics

Coherent Muon to Electron Transition (COMET) is an experiment to search for the muon-to-electron (μ -e) conversion in muonic atoms, which also violates the lepton-flavor conservation, using an intense pulsed muon beam generated at the Japan Proton Accelerator Research Complex (J-PARC). Together with the $\mu \rightarrow e\gamma$ search, the μ -e conversion mode is sensitive to more physics cases. Thus, awareness of the search has been expected long after the previous experiment was completed. In 2012, we started constructing an experimental facility to achieve the experimental conditions on time. An accelerator study was required to determine the correct beam for the experiment. The experiment

group plans to start data acquisition to confirm the MEG result and exceed it at an early date.

The group has also continued the R&D studies of the muon anomalous magnetic moment ($g-2$) and electric dipole moment (EDM) measurements. We have been developing the muon source and acceleration, injection and storage of a high-precision magnet, and a high-rate silicon tracker system. The muonium production is extensively studied at the J-PARC Materials and Life Science Experimental Facility (MLF), and will soon be extended to test the muon acceleration. In addition, the development of a tracking detector will be continued with its first prototype currently in preparation.

Neutrino Experimental Facility

Neutrinos are subatomic particles with no electric charge, and have the smallest mass of all known particles. Neutrinos come in three types, or “flavors”: electron, muon, and tau. As they travel, neutrinos can transform, or “oscillate”, from one flavor to another. This is called “neutrino oscillation”, a consequence of the fact that neutrinos have mass and thus mix with each other. Each of the neutrino flavor states appears as a superposition of different mass states, and the difference in their extremely small masses causes a periodic change in flavors during flight.

The Tokai-to-Kamioka (T2K) experiment is a second-generation long-baseline neutrino oscillation experiment. The primary goal of the T2K experiment is the search for the muon neutrino (ν_μ) to electron neutrino (ν_e) oscillation. Its probability is described

with the mixing angle between the first and third generations, θ_{13} , which is last unknown neutrino mixing angle. This θ_{13} is the key quantity to explore CP violation of leptons, which is one of the biggest questions of particle physics.

To achieve this objective, T2K utilizes high-intensity muon neutrino beams with 99.5% purity. The muon neutrino beams produced at the neutrino experimental facility in J-PARC are directed toward the Super-Kamiokande detector (SK), which is located 295 km west of J-PARC. SK is one of the world’s largest underground neutrino detectors, which contains 50,000 tons of purified water as the target for the neutrino beam. The rare interaction between neutrinos and nuclei in the water can be detected by the $\sim 11,000$ photo-sensors fixed on the entire inner surface. The appearance of elec-

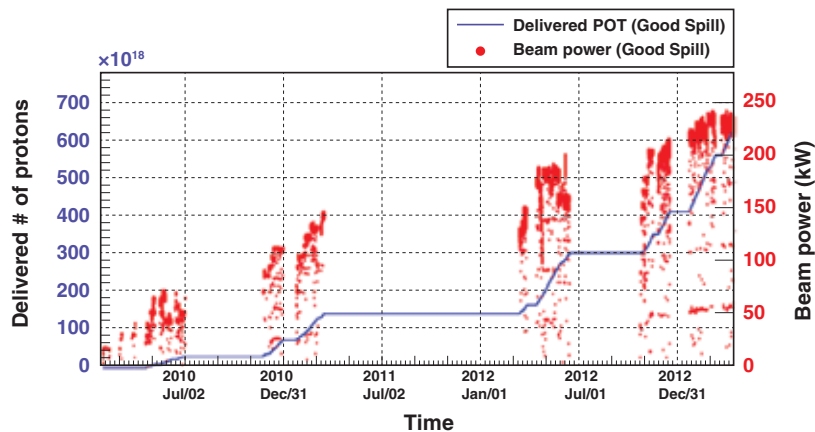


Fig. 5. History of the data taking of T2K from January, 2010. The red dots (see right axis) show the beam intensity, and the blue line (left axis) shows the integrated POT.

trons in the water, charged counterparts of the electron neutrinos, is a clear sign of the ν_μ to ν_e oscillation.

The T2K physics experiment started in January 2010, and continues to accumulate the data by increasing the neutrino beam power for about 4 years. (Figure. 5) In JFY 2012, T2K had released two new results based on the data which was accumulated until June 2012. The first evidence having a 3.2σ significance for ν_μ to ν_e oscillations was obtained by T2K. Eleven ν_e candidates were detected using SK when it was exposed to ν_μ beams generated from 3.01×10^{20} protons on target (POT), while the expected number of counts from the background was only 3.22 ± 0.43 . This results was published in Physical Review. T2K has been awarded a prestigious prize by La Recherche, a French science magazine. This prize is called “Le Prix La Recherche” and has 12 categories including biology, chemistry, mathematics and medicine. T2K received the physics prize for finding the first indications of ν_μ to ν_e oscillations. T2K also precisely measured the disappearance of muon neutrinos precisely and obtained the world’s best estimation of the neutrino oscillation parameters. (Figure. 6)

T2K continued to accumulate beam data in order to obtain a firm ($>5 \sigma$ significance) establishment of the electron-neutrino appearance until May 2013.

The T2K collaboration presented the new results on ν_μ to ν_e oscillation with the improved analysis method based on the data taken by April 2013 at international conferences in the summer of 2013 such as the European Physical Society meeting (EPS-HEP 2013) in July. Based on the data corresponding to 6.39×10^{20} POT, which is the doubled statistics from the previous year, T2K observes 28 ν_e candidates while the expected number of background is 4.64 ± 0.53 . (Figure. 7) The probability of background fluctuation to yield 28 or more events (p-value) is 9.9×10^{-14} corresponding to a 7.5σ level of significance. The obtained results for θ_{13} value is $\sin^2 2\theta_{13} = 0.150 (+0.039 -0.040)$ assuming no CP violation in neutrino oscillations and normal hierarchy of neutrino mass states. T2K has proofed the existence of ν_μ to ν_e oscillation firmly, and achieve its first goal of discovering ν_μ to ν_e oscillation for the first time in the world.

The neutrino beam operation will be resumed after the maintenance of the electromagnetic horns that are the key component of the neutrino beam-line. T2K will search the CP violation in neutrinos by doing the precise measurement of the neutrino oscillation and comparing the neutrino oscillation of neutrino and anti-neutrino.

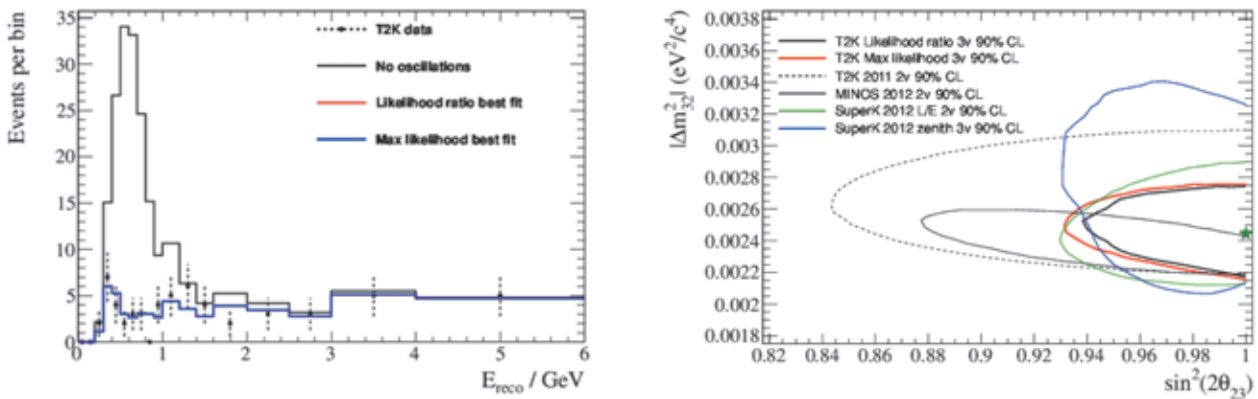


Fig. 6. (Left) The reconstructed energy spectrum of the muon neutrinos that are generated from J-PARC and observed in Super-Kamiokande. The black histogram shows the extrapolation from the neutrino beam flux measured in Tokai. The dot shows the observed events in SK. The clear deficit due to the neutrino oscillation is appeared, and the distribution is well much with the prediction by the neutrino oscillation (Blue line and Red lines). (Right) The allowed region of the neutrino oscillation parameters obtained by the muon neutrino disappearance by T2K (solid black line and solid red line) with the results by other experiments. T2K gives the most precise results in JFY2012.

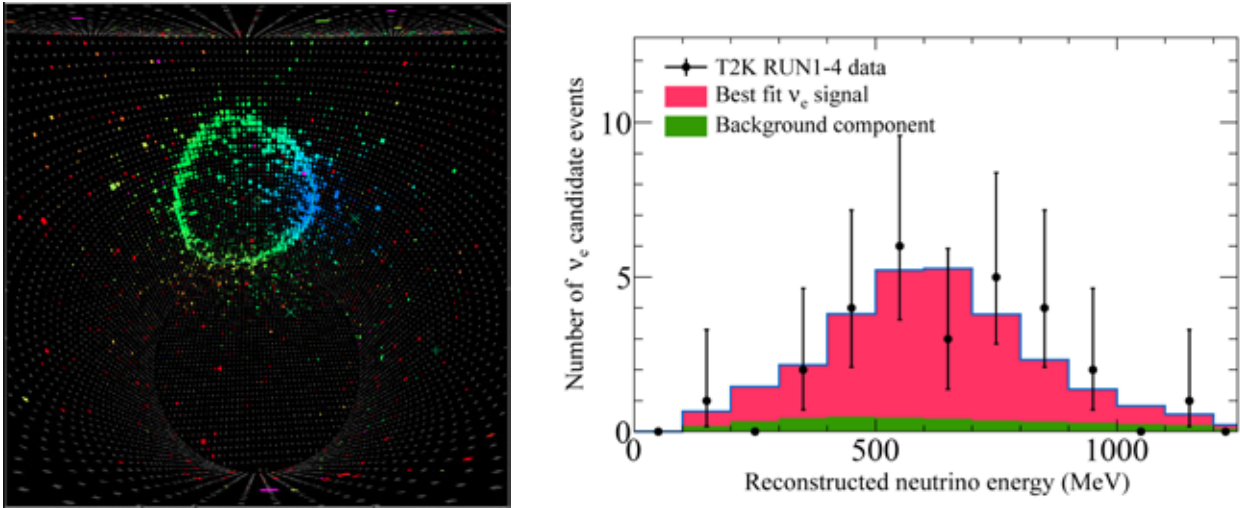


Fig. 7. (Left) The event display of the electron neutrino candidate. (Right) Reconstructed neutrino energy spectrum of the events, which passed all electron neutrino event selection criteria (closed circles), overlaid with the theoretical expectation (histograms). A total 28 events was observed, which is well reproduced by assuming electron neutrino appearance signal (red histogram) plus expected background events.



Cryogenics Section

Overview

The Cryogenics Section supports scientific activities in applied superconductivity and cryogenic engineering, carried out at J-PARC. It also supplies cryogen of liquid helium and liquid nitrogen. The support work includes the operation of the superconducting magnet system for the neutrino beamline, and support of the

construction and operation of a superconducting solenoid magnet system for the new muon beamline at the Materials and Life Science Experimental Facility (MLF). It also actively conducts R&D works to back future projects in J-PARC.

Superconducting Magnet System for the T2K Beamline

The Cryogenics Section operates the superconducting magnet system for the T2K neutrino beam line. The operation record for FY 2012 is summarized in Table 1. The superconducting magnet system was operated con-

tinuously from Sep. 2013 until May 2013 as scheduled, except for a short shutdown during the New Year holiday. The system had no incidents during that period and contributed to the successful results of the T2K beam line.

Table 1. Operation history of the superconducting magnet system for the J-PARC neutrino beamline.

	2012						2013					
	Jul	Aug	Sep	Oct	Nov	Dec	Jan	Feb	Mar	Apr	May	Jun
Operation			Beam Operation				Beam Operation					
Incidents			No incidents									

Superconducting Kaon Spectrometer (SKS)

The Cryogenics Section also supports the Superconducting Kaon Spectrometer (SKS) operation at the J-PARC Hadron Hall. Because the SKS magnet suffered damage from the Great East Japan Earthquake, repair was planned. The plan included replacement of the magnet stand with a new one, correction of the gaps between the iron yoke plates and attaching a gap prevention mechanism. The moving method of the magnet was also changed from an air floating system into a rail and wheel system. The construction of the rails was first performed from April to May, 2013, as shown in Figure 1.



Fig. 1. The Superconducting Kaon Spectrometer (SKS) magnet and the newly constructed rails (right).

The Superconducting Magnet System for the Muon Beam Line at MLF

The Cryogenics Section supports the construction of the intense ultra-slow muon beam line (U-line) in the Muon Science MLF. One of the major contributions of the Cryogenics Section in FY2012 was the commissioning of the superconducting curved solenoid and the superconducting focusing solenoids (Figure 2). The superconducting magnets were installed at the beam line in the summer of 2012 and commissioning to extract muon beam in the beam line was successfully performed in the winter of the same year.



Fig. 2. Picture of the superconducting focusing solenoids with positron separators for the ultra-slow muon beam line at MLF.

Cryogen Supply and Technical Support

The Cryogenics Section provides liquid helium cryogen for physics experiments in J-PARC. The liquid helium is supplied to the users in collaboration with the Accelerator Division using the helium liquefier owned by the Accelerator Division. The used helium is recovered by the helium gas recovery facility, which is provided and operated by the Cryogenics Section. Figure

3 summarizes the liquid helium supply in FY 2012. The major users of liquid helium were the SKS and the liquid hydrogen target in the Hadron Hall. The helium gas recovery fraction was better than 90%. Liquid nitrogen was also supplied to the users for their convenience and its amount during the period from July 2012 to May 2013 is summarized in Figure 4.

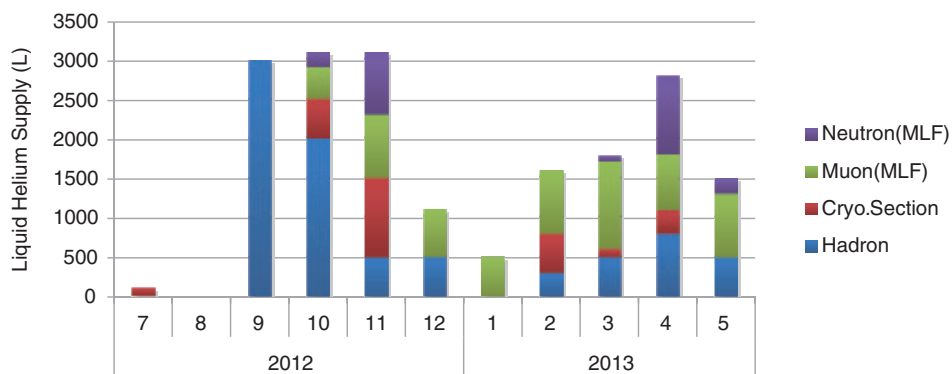


Fig. 3. Liquid helium supply at J-PARC from July 2012 to May 2013.

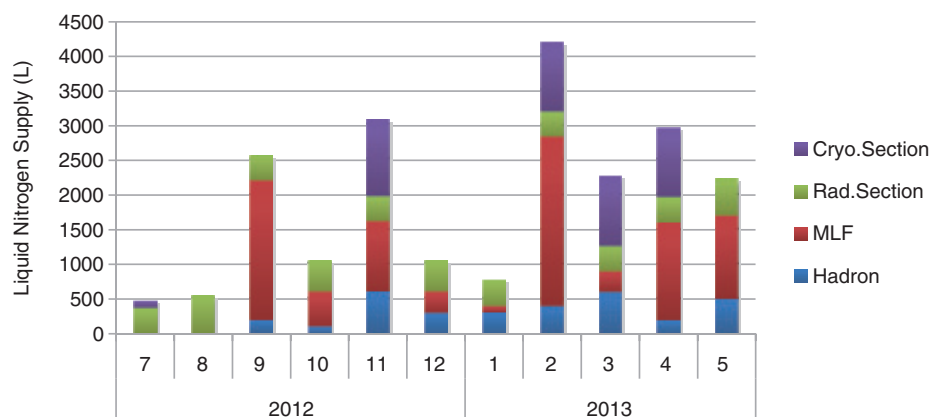


Fig. 4. Liquid nitrogen supply at J-PARC from July 2012 to May 2013.

R&D for the J-PARC Project: COMET

A new experiment, COherent Muon to Electron Transition (COMET), has been proposed to search for mu-e conversion processes using the high intensity proton beam from the Main Ring. The Cryogenics Section has been involved in the COMET experiment to develop the superconducting magnet system. The project requires a large aperture solenoid that covers a pion production target to capture pions with large acceptance. A major issue for the R&D is the irradiation of neutrons to the solenoid. The resistivity degradation by neutron irradiation in aluminum and copper (stabilizer materials in the superconducting cable) has been investigated at the Kyoto University Research Reactor Institute, and the test was continued in FY2012. In addition, instrumentation of an R&D coil with aluminum stabilized cable was fabricated as shown in Figure 5 and shipped to the Fermi National Accelerator Laboratory

to measure its basic performance. The COMET project was partially approved in 2013 and procurement to construct the superconducting magnets has been started.



Fig. 5. Instrumentation work on the R&D coil of the capture solenoid for COMET.

R&D for the Future J-PARC Project: New Muon g-2/EDM and Muonium HFS

The g-2/EDM project using H-line of MUSE, which is the muon beam line in MLF, was proposed by a group of IPNS in 2009. The experiment aims for the precise measurement of the anomalous magnetic moment and the electric dipole moment of muons. In this experiment, a superconducting solenoid with high field homogeneity better than 1 ppm locally is a key component to store muons during the measurement of their precession frequency. Design study of the magnet is in progress in collaboration with IPNS and the Cryogenics Science Center. Magnetizations of the electrical devices for the detector were measured, showing that an optical module strongly disturbs the field homogeneity.

A muonium hyperfine structure (MuHFS) measurement using the same beam line as the g-2/EDM project has been also proposed by a group of IMSS. In this experiment, the energy state transition in muonium will be observed under a static magnetic field with local homogeneity of 1 ppm. A superconducting magnet for

a MRI system has been purchased and prepared for the experiment (Figure 6). A magnetic shield room to isolate the magnet from magnetic disturbances has been designed.



Fig. 6. Superconducting magnet for the MuHFS experiment in MLF.



Information System

J-PARC Network (JLAN) Upgrade

Since 2002 the J-PARC network infrastructure, called JLAN, has been operated independently from KEK LAN and JAEA LAN in terms of logical structure and operational policy. The Information System Section designs, manages and operates the network system and also performs the research and development activities of the Authentication System and the Data Base System for J-PARC. Each System is aiming to be both secure and easy-to-use ICT (Information Communication Technology) infrastructure for the J-PARC users and staffs.

In July 2012, the JLAN was upgraded to cope with

the increasing demands for network bandwidth. The older network system provided a bandwidth of 100 Mbps for terminal ports, 1 Gbps for the Internet and 2 Gbps for the Tokai-Tsukuba connection. The newly upgraded system provides bandwidth of 1 Gbps for terminal ports, 10 Gbps for the Internet and 8 Gbps for the Tokai-Tsukuba connection respectively. In addition to increased network capacity, the upgrade has made JLAN more robust by introducing redundant switch configuration and connections. Figure 1 shows the logical configuration of the network before and after the upgrade.

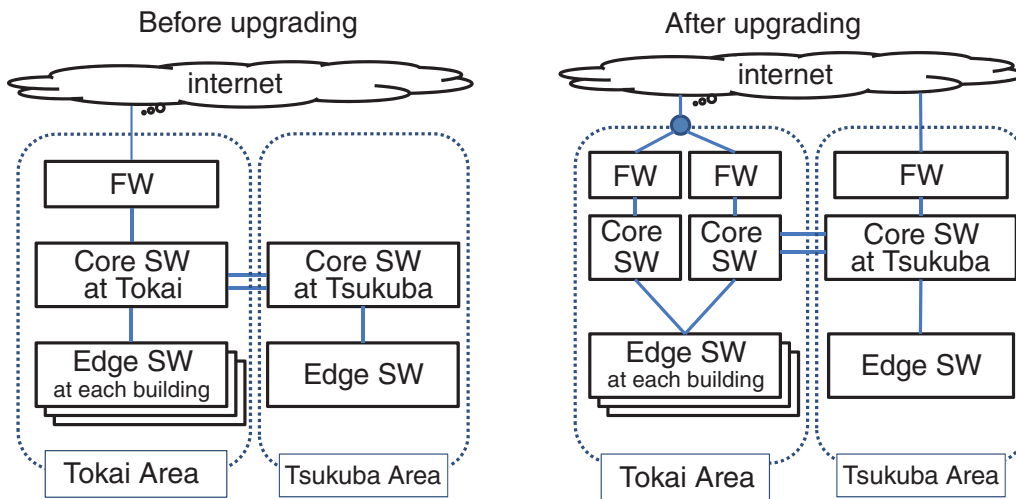
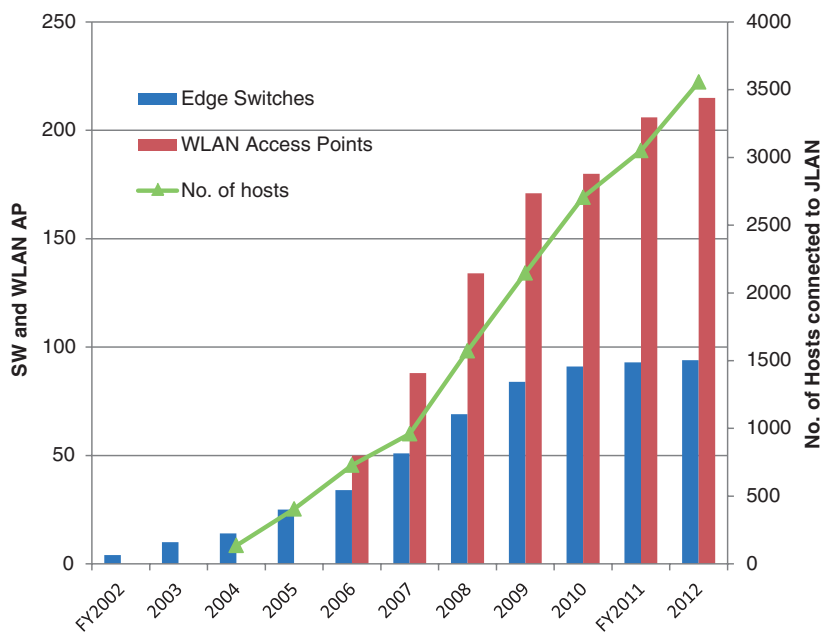


Fig. 1. After the JLAN upgrade, the firewall system and core switch, connections between core and edge switches and gateway to the internet were made redundant.

Statistics of Network Utilization

In 2012, the total number of hosts on JLAN exceeded 3500 and the number has increased by 117% from the last year. The growth curve of edge switches, wireless LAN access points, and hosts connected to JLAN are shown in Fig. 2. JLAN has also played an important role in connecting the Tokai area, where the main J-PARC facilities were built, and the Tsukuba area, where the major computer resources for data analysis are located.

Figure 3 shows the statistics of annual data transfer between the two sites. The bandwidth capacity for the connection is currently 1 Gbit/s x 8 = 8 Gbit/s and the usage level has been approaching half of it, especially during the period when the Hadron facility was running. Figure 4 also shows the network utilization of the internet. The bandwidth capacity for the internet is 10 Gbit/sec, which allows enough extra activity.



No. of Hosts, edge SW and wireless AP on JLAN

Fig. 2. Increase of hosts, edge switches and wireless access points on JLAN.

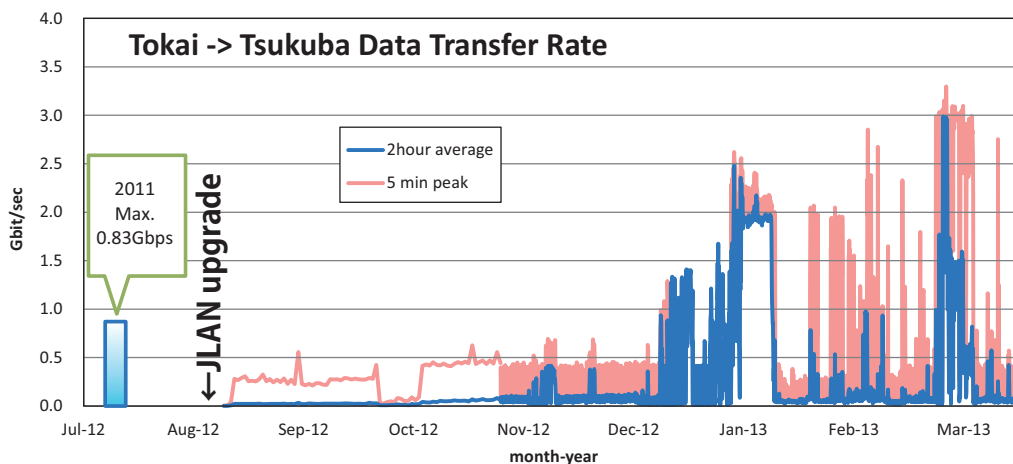


Fig. 3. Tokai - Tsukuba Data transfer rate.

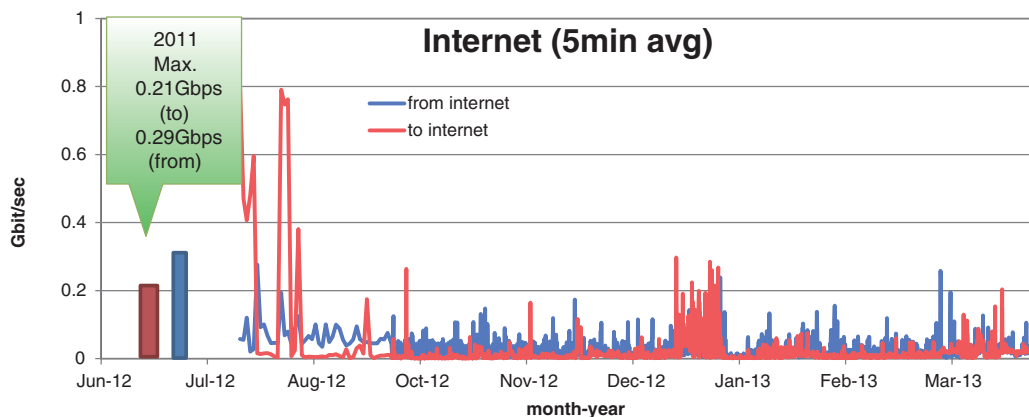


Fig. 4. Data transfer rate between JLAN and the Internet.

Statistics of Computer Resources Utilization

Though J-PARC does not have its own computing facility for physics analysis, since 2009 the KEK central computer system at KEK Tsukuba site has been mainly used for the purpose. For J-PARC the resources of 1600 SPECint06 computing power, 150 TBytes RAID disks and 2 PBytes tape libraries were assigned. In April 2012, the KEK central computer system was upgraded and computer resources of 25,000 SPECint06 computing power, 1.2 PBytes disks and 5 PBytes tapes were newly assigned for J-PARC.

In the Neutrino (T2K experiment) and Hadron experiments, the data taken in the J-PARC experimental hall will be temporarily saved at the Tokai site and then

promptly transferred to, stored and analyzed at the system in Tsukuba. The storage of the system will also be utilized as a permanent data archive for the Neutrino, Hadron and MLF experiments. Figures 5, 6 and 7 show the utilization statistics of the computer resources in 2012. The main Hadron users who used the system constantly were those who continue their experiment (Koto Exp. Group) in series from the former KEK 12 GeV Proton synchrotron to J-PARC. The Neutrino experiment group sometimes used the CPU power, but not so much. On the other hand, they stored the experiment's data steadily both to the disks and tapes on the system.

Assigned resources to J-PARC	New system	Old system	ratio
CPU (SPECint06)	25,000	1,600	× 16
Disk (TB)	1,200	150	× 8
Tape (PB)	5	2	× 2.5

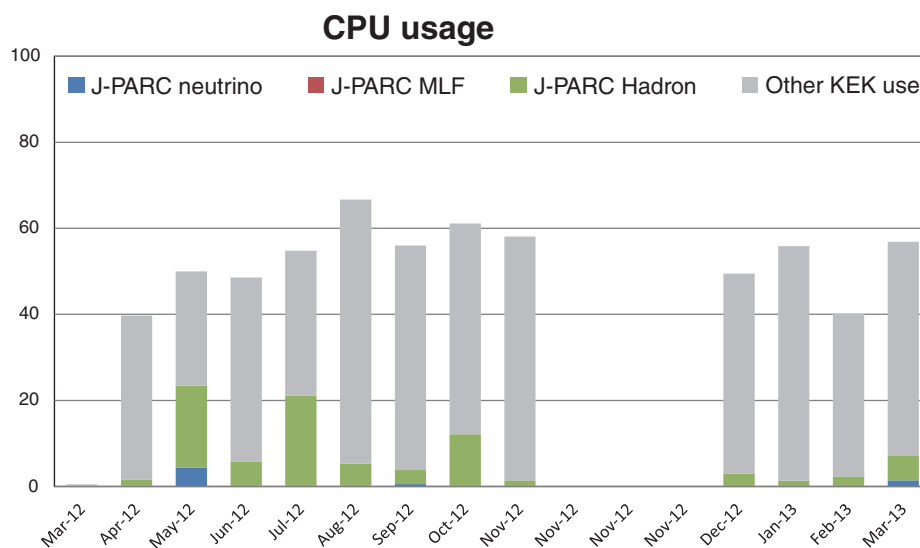


Fig. 5. CPU utilization on the KEK central computer system by the J-PARC groups.

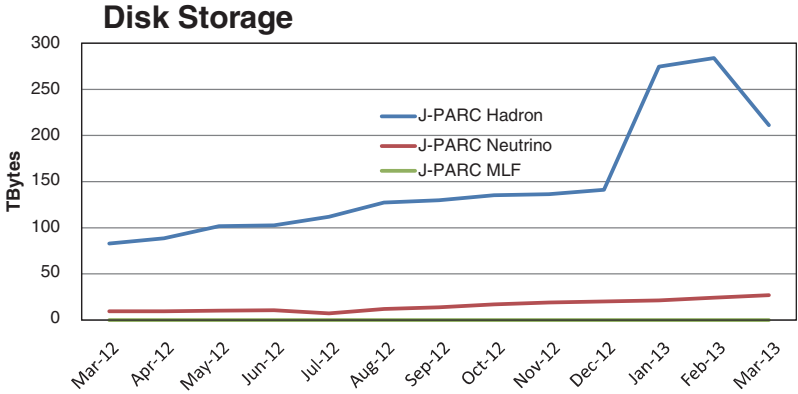


Fig. 6. Disk utilization on the KEK central computer system by the J-PARC groups.

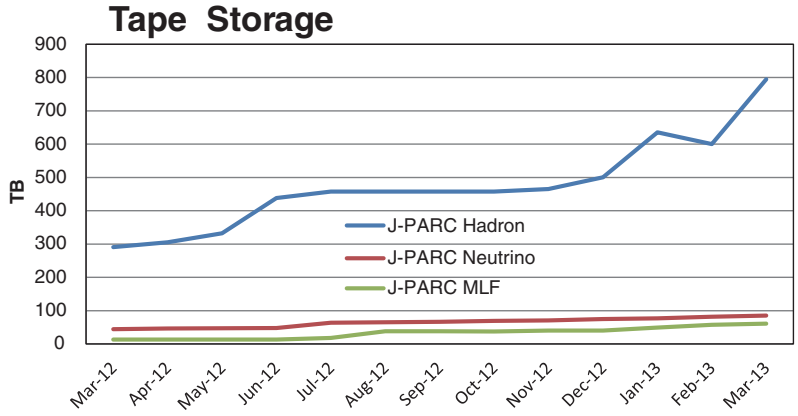


Fig. 7. Tape utilization on the KEK central computer system by the J-PARC groups.



Transmutation Studies

Activities

MEGAPIE

Several meetings on MEGAPIE (MEGAwatt Pilot Experiment) were held at Paul Sherrer Institute (PSI), Switzerland in April 2013. The meetings dealt with the status of the MEGAPIE target Post Irradiation Examination (PIE) and the sample shipping, the PIE plan of each institute. Another discussion topic was the scheduling of PIE and the condition of each of the tests.

As of PIE, the scientists reported the results of analysis of the Lead-Bismuth Eutectic Alloy (LBE) taken from the irradiated target. The γ -spectra measurement revealed that elements with low solubility in LBE or sensitive to oxidation (rare earth elements) are enriched at LBE/steel and LBE/cover gas interfaces. The α -spectra measurement showed that Polonium is homogeneously

distributed in LBE.

With regard to the sample shipping, it was reported that the cutting of the samples, followed by sample cleaning, finished by the end of February and in late March the sample transport has already started. After the meetings, in May 2013, samples from the Japan Atomic Energy Agency (JAEA) were shipped and successfully transported to WASTEF in JAEA-Tokai.

In the meetings, the PIE plan of each institute including JAEA was presented and considered. The scheduling and the test conditions were also discussed. Deadline of the PIE report was decided as TRM (Technical Review Meeting) to be held in October 2014. Test conditions for tensile test were determined for the present.

SPALLATION TARGET DESIGN for the Transmutation Experimental Facility

JAEA studies an accelerator-driven system (ADS) for transmutation of long-lived radioactive nuclides. ADS is a tank-type subcritical reactor with thermal power of 800 MW_{th}, which uses LBE as a target material and a coolant, driven by a 30 MW superconducting proton LINAC. The construction of the Transmutation Experimental Facility (TEF) was planned in order to perform basic and elemental R&D for ADS within the framework of the J-PARC project. TEF consists of a 250kW spallation target facility and a 500W critical assembly facility, designed to perform elemental study for the LBE spallation target and fundamental research for the subcritical core of ADS. An important issue in the development of TEF is the estimation of the thermal-fluid properties of the flowing LBE in the high power spallation target, which is illustrated in Figure 1. LBE has the tendency to cause corrosion/erosion to the structural materials. And the beam window of ADS, which separates the proton accelerator and the LBE subcritical core vessel, is exposed to the high temperature environment induced by the incidence of proton beams. Therefore, the feasibility of the beam window is the most important issue during the construction of TEF. A test to determine the feasibility of the designed beam window for the TEF target using numerical analysis with a 3D model was performed. The analysis took into consideration (1) the current density and shape of the incident beam, (2) the thermal-fluid behaviour of LBE around the beam window as a function of the flow rate and the inlet temperature, (3) the material and the thickness of the beam

window, (4) the structural strength of the beam win-

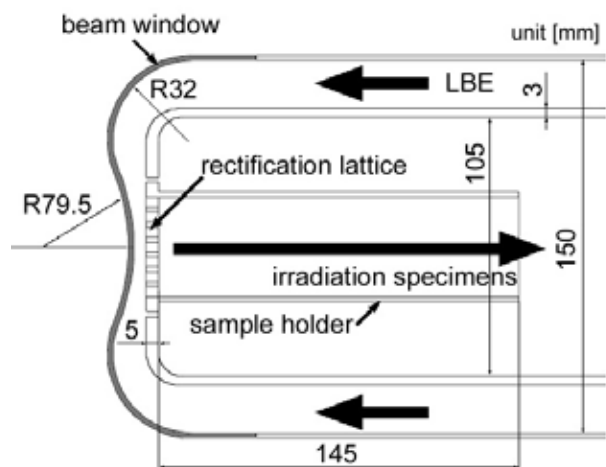


Fig. 1. Prototype design of the spallation target head for TEF.

In the reference case, the peak current density and the profile of the proton beam were set to 20 $\mu\text{A}/\text{cm}^2$ and a Gaussian shape, respectively. The material for the beam window was 2-mm thick SUS316 stainless steel. The flow rate of LBE and the temperature at the inlet position were assumed to be 1 liter/sec and 350 $^{\circ}\text{C}$. These parameters were fixed based on the rated operation condition of 800MW ADS. In this reference case, the maximum velocity of LBE was formed at the center of the beam window with a value of about 1.2 m/sec. At the same position, a maximum temperature of 477 $^{\circ}\text{C}$ at the beam window is observed, as shown in figure 2. By increasing the flow rate of LBE by up to 4

litter/sec, the maximum temperature of the beam window was reduced to around 420 °C. In the reference case, the maximum shear stress was 194 MPa, which was observed at the center on the outside surface of the beam window. The analyzed stress in the reference case was lower than the tolerance level of the material's stress strength at this operation temperature, hence the feasibility of the designed beam window was confirmed by the reference case of the TEF spallation target operation.

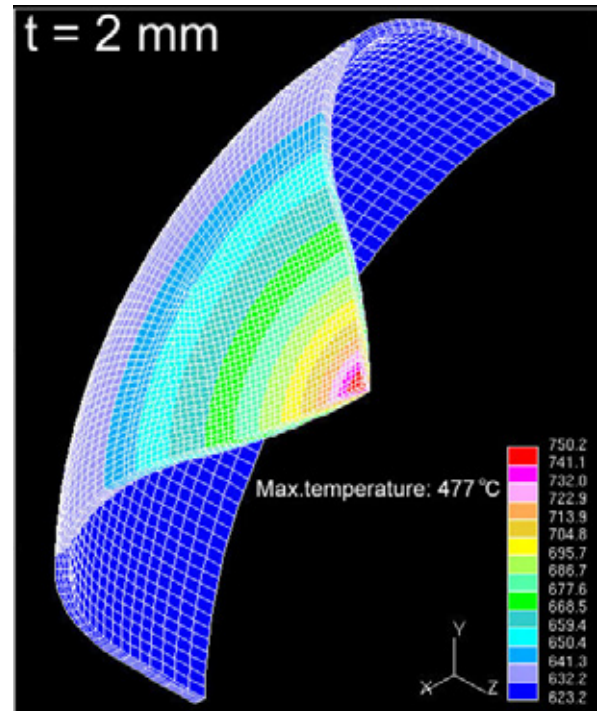


Fig. 2. Temperature profile at the reference condition.



Safety

Radiation Safety

J-PARC is managed under the Law Concerning Prevention from Radiation Hazards Due to Radio-Isotopes, etc. in the Japanese legal system. A license for its use must be issued by the Ministry of Education, Culture, Sports, Science and Technology (MEXT), and the related safety inspection must be conducted by the Nuclear Safety Technology Center (NUSTEC). Table 1 shows lists of existing licenses at the end of Japanese fiscal year (JFY) 2011 and license applications for JFY 2012.

The 13th Radiation Safety Committee of J-PARC met on June 18, 2012 and discussed the alternative application of the J-PARC facilities. The main topics were 1) the power-up for all of the facilities (except the Hadron Experimental Facility (HD)), 2) the new secondary beam line (muon) in the Materials and Life Science experimental Facility (MLF). The intended power-up level at this time is 300 kW for user operation in MLF. And the Neutrino Experimental Facility (NU) aims to reach 450 kW operation.

The 14th Radiation Safety Committee of J-PARC met on December 19, 2012 and discussed the alternative application of the J-PARC facilities. The main topic was the installation of the beam line in the LINAC facility to test the first-stage accelerator (Radio Frequency Quadrupole: RFQ), which is designed to allow a larger beam power and will replace the current RFQ in the accelerator tunnel.

Figure 1 shows the increase of the number of radiation workers since 2005. In JFY 2012, 3133 individuals were registered as radiation workers in J-PARC. Table 2 shows the distribution of annual radiation doses by type of workers. The radiation exposure of the workers has been monitored individually with glass dosimeters and solid state nuclear track detectors. Almost all the records for individual exposure were undetectable, while 96 persons (3.1% of the workers) were recorded to have received less than 5.0 mSv.

Table 1. License at the end of fiscal year 2011 and application items for license in fiscal year 2012.

	Licenses at the end of fiscal year 2011	License applications for fiscal year 2012
MLF	Power : 3 GeV/320 kW Secondary beam lines (neutron) : 18 Secondary beam lines (muon) : 1	Power : 3 GeV/350 kW Secondary beam lines (muon) : 1
HD	Power : 30 GeV/50 kW Secondary beam lines (meson) : 4	
Neutrino facilities	Power : 30 GeV/300 kW	Power : 30 GeV/450 kW

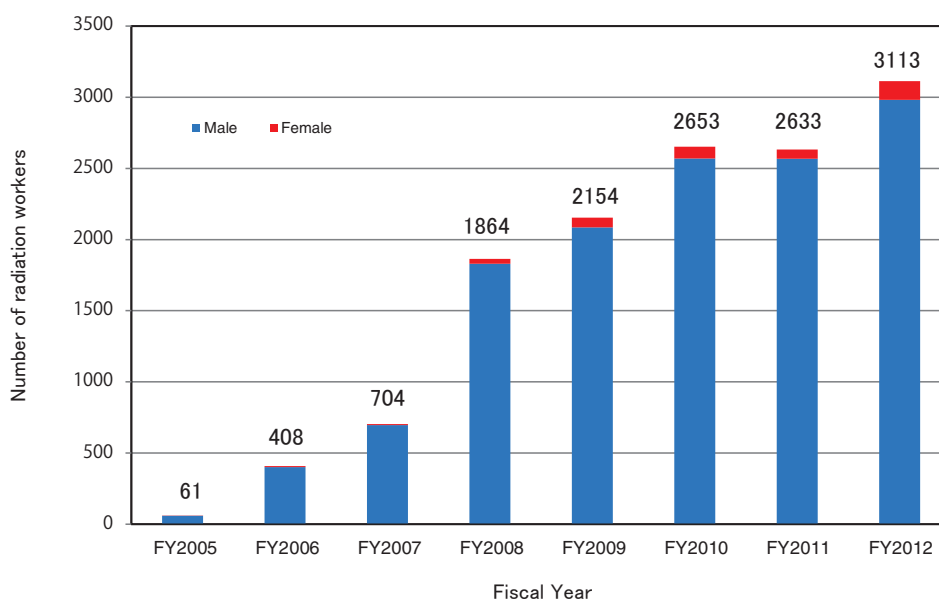


Fig. 1. Transition of the number of radiation workers.

Table 2. Distribution of annual doses by the type of worker in fiscal year 2012.

	Dose range (mSv)					Total worker	Collective dose (person-mSv)	Average dose (μ Sv)
	Undetectable	0.1 - 0.5	>0.5 - 1.0	>1.0 - 5.0	>5.0+			
In-house staff	556	28	8	0	0	592	10.9	18.2
User	964	0	0	0	0	964	0	0
Contractor	1497	48	10	2	0	1557	16.6	10.6
Total *	3017	76	18	2	0	3113	27.5	8.8



Users Office

The J-PARC Project was approaching the end of its Phase 1, when the J-PARC Center Users Office (UO) was created on April, 2007, as part of the Users Affairs Section. Around that time, there were no so-called J-PARC users and the number of J-PARC visitors was far smaller than today. However, preparing a system for receiving J-PARC users was one of the challenges the section was facing. UO was located in a corner of a room of the Administration Division, which consisted of two sections, one of which was the Users Affairs Section.

Since it was estimated that the number of users would increase, UO moved on December, 2007, to the Ibaraki Quantum Beam Research Center (IQBRC) building located about "300 m" from the main gate of the J-PARC. The new UO office was large enough to deal with the numerous users expected to come. In addition to the large office, there was another advantage. Since it was located outside the J-PARC site, the users could firstly come to it to complete the necessary procedures for conducting experiments and receive J-PARC User ID Cards, which were required to pass through the main gate of the J-PARC. Here at IQBRC the UO team members have been committing themselves to their tasks.

The primary function of UO in the Japanese fiscal year (JFY) 2012 was to provide support to the J-PARC users. The support covered a wide range: user registration, procedures for conducting experiments, daily life information, etc. The team members who had direct contact with the users were crucial to fulfilling the tasks. However, there were other indispensable team members. System engineers maintained or developed four main web-based systems: proposal submission system, proposal review system, user support system and experimental report management system. Some team members took care of management and maintenance of the Tokai Dormitory, which was a main accommodation for the J-PARC users, built and maintained user database, renewed the contract of renting the UO office rooms in IQBRC, etc.

From the perspective of the time and human resources devoted, we should describe first the achievements conducted by the team members who had direct contact with the users. However, in this Annual Report 2012, the development and improvement conducted in JFY 2012 are firstly described to highlight them, followed by other achievements.

J-PARC safety instructions were executed at UO or facilities where users were scheduled to conduct their experiments. The instruction consisted of general safe-

ty instruction, specialized safety instruction for each facility and J-PARC radiation safety instruction. UO and other departments in charge considered the possibility of adopting online safety instruction. As a result it was decided that general safety instruction and specialized safety instruction for each facility could be executed online. And the online general safety instruction application was embedded in the user support system.

UO constructed bicycle parking lot with roof which could accommodate about 40 bikes.

UO and International Affairs Department of Japan Atomic Energy Agency (JAEA) built up a database of samples and chemicals foreign users were scheduled to bring into J-PARC. To observe Foreign Exchange and Foreign Trade Control Law, it was helpful in deciding the necessary procedures before shipping them.

Other achievements were as follows:

1. User registration and pre-visit procedures:

(1) confirmed eligibility of user registrations and approved them through the user support system; (2) arranged the Tokai Dormitory bookings in the case the automatic booking system did not function; (3) booked other accommodations when the Tokai Dormitory was fully booked; (4) checked applications for individual dosimeters; (5) arranged safety instructions; (6) issued temporary Shuttle Bus Passes; (7) checked eligibility of Foreign National Visit Proposals; (8) issued letters of guarantee for visa application; (9) applied for certificates of eligibility for visa application; (10) calculated the amount of travel expenses of inter-university research users whom KEK had accepted.

2. Procedures upon arrival:

(1) issued J-PARC User ID Cards; (2) executed safety instructions; (3) handed users individual dosimeters; (4) issued car driving permission passes; (5) issued J-PARC card keys to enter the J-PARC facilities during off-hours; (6) lent out bikes and handy phones for internal calls at J-PARC.

3. Post-visit Procedures:

(1) checked MLF machine time completion forms or MLF experimental reports submitted by users and forwarded them to persons who had responsibilities for approving them.

4. User Statistics:

(1) collected fundamental user statistics; (2) produced other user statistics when required.

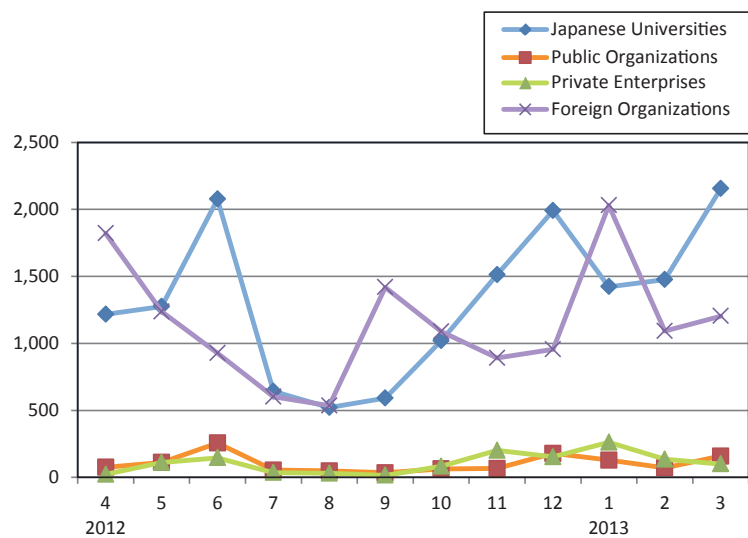
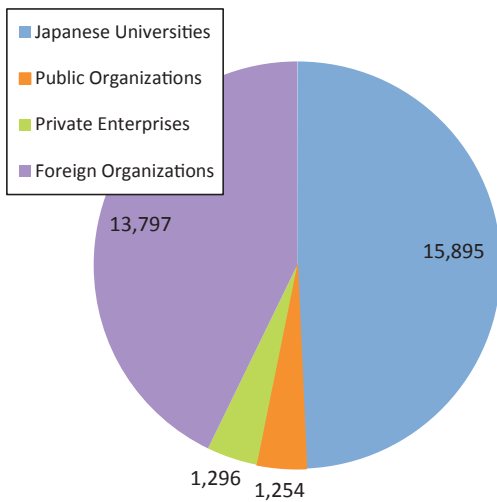
5. Others:

(1) closed the Tokai dormitory's books every day; (2) took sick or injured users to hospitals; (3) booked taxis or airport limousines; (4) posted announcements about user support system shutdown, blackout, etc.

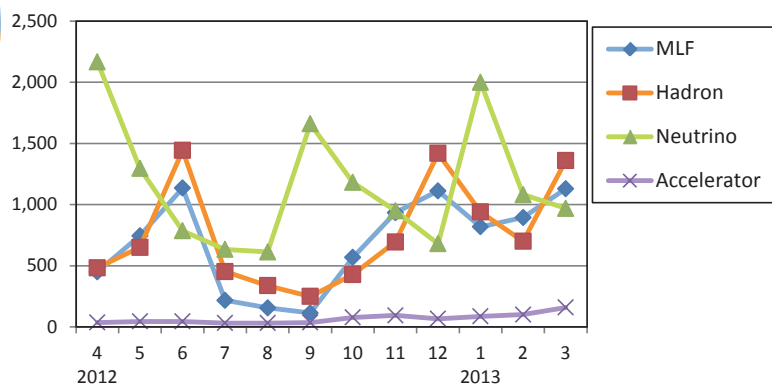
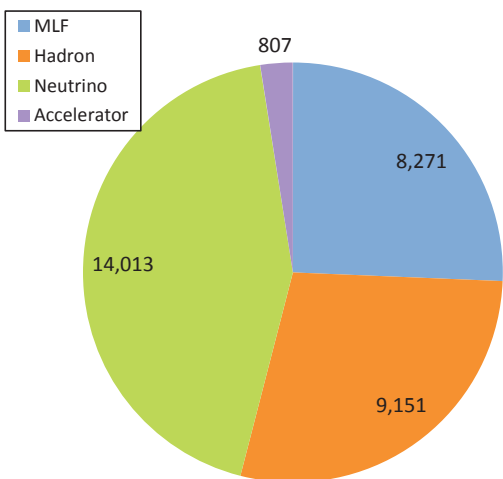
The final item covered here is the number of the users. The numbers of annual users in a JFY counted by

person-days are chronologically 27,555 in JFY 2009, 29,030 in JFY 2010, 15,539 in JFY 2011 and 32,242 in JFY 2012. The cause of the plummet in JFY 2011 was the Great East Japan Earthquake, which occurred on March 11, 2011. However, as J-PARC recovered from the damage, the users came back. And in January, J-PARC received more users than those in the same month of the previous year.

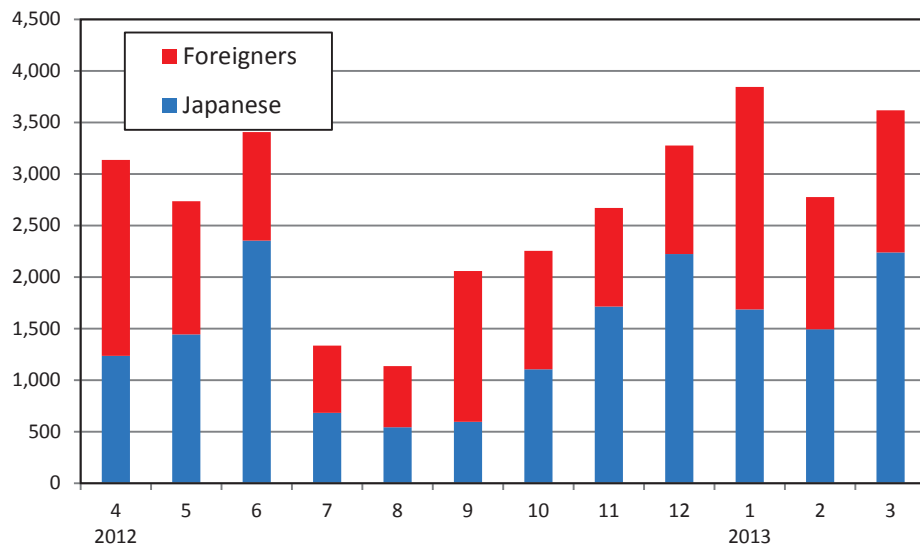
(1) Users in 2012 (according to organizations, person-days)



(2) Users in 2012 (according to facilities, person-days)



(3) Users in 2012 (Japanese · Foreigners, person-days)



User Program

Overview of MLF Use

(1) Basic policy of MLF use

The Materials and Life Science Experimental Facility (MLF) is available to Japanese and overseas users for both academic research and industrial applications. The following peer review systems are introduced for fair, clear and user-oriented facility management: User Consultative Committee, Neutron/Muon Science Proposal Review Committee, and Neutron/Muon Science Instrument Review Committee. All nonproprietary proposals are reviewed and ranked by the Neutron/Muon Program Review Committee. The J-PARC Center is responsible for the beamtime allocation for approved proposals.

(2) Registered Institution for Facility Use Promotion (RIFUP)

Consistent with its longstanding policy of promoting open access to major publicly-funded research facilities, the Japanese Government in July 2009 designated the accelerators (linac and 3 GeV proton synchrotron) and some beamlines at J-PARC MLF as Public Neutron Beam Facility under the terms of the so-called "Public Use Promotion" legislation. The aim of the legislation is to advance science and technology through the effective promotion and operation of general user access program at designated large-scale research facilities. The legislation requires that the user program on the Public Beamlines be managed and supported by an independent, third-party organization. This organization is known as RIFUP.

Comprehensive Research Organization for Science and Society (CROSS) applied for RIFUP in February 2011 and was allowed by the Minister of the Ministry of Education, Culture, Sports, Science and Technology (MEXT) to operate as RIFUP. Accordingly, CROSS commenced its operation on the 1st of April 2011 at its Tokai office in the Ibaraki Quantum Beam Research Center (IQBRC) adjacent to the J-PARC site.

(3) MLF Instrument Use

There are 23 neutron beam extraction ports for the pulsed spallation neutron source and 4 muon extraction channels for the muon target at MLF.

Not only can JAEA or KEK, the parent organizations of J-PARC, construct instruments for conducting experiments using the neutron and the muon beams, but third parties can do it too. However, the manufacturers of the instruments at MLF are obliged to manage and maintain their beamline instruments.

Beamtime provided to J-PARC users is classified into three categories: one managed by J-PARC Center, one managed by a third-party, and one managed by CROSS-Tokai. The third-party must supply to the J-PARC Center a little portion of its full beamtime in exchange for having exclusive rights to use the beamline instruments.

Therefore, the J-PARC user program is carried out using all the beamtime for the instruments owned by JAEA or KEK and part of the beamtime for those owned by the third parties. Proposals for MLF use program are reviewed uniformly and openly.

(4) MLF Access modes

(a) Beamtime managed by J-PARC Center

There are three access modes to obtain outstanding scientific results or to meet the various needs of users: general use, project use and instrument group use. An applicant to general use must be an employee of or affiliated with a legal organization or entity that may be any of the following: a public or private college, university or other institute of higher education, a public or not-for-profit research organization, or a private company. A postdoctoral fellow is also eligible to submit proposals with the permission of his/her manager or supervisor at the home institute/organization to conduct research activities at MFL. Project use is the access mode in which JAEA or KEK conducts its mission-oriented programs such as inclusive scientific research projects or research programs proposed to fulfill plans to achieve midterm goals of JAEA, joint research programs and contract research programs with other institute(s)/organization(s). Experiment proposals requesting beamtime longer than one year may be acceptable for the project use. Only personnel belonging to either JAEA or KEK or a person approved by the director of the J-PARC Center can apply for project use. Instrument group use is the access mode in which the scientists responsible for the instruments maintain them in good condition and/or develop their performances to provide the J-PARC users with the most superior experimental environments.

(b) Beamtime managed by a third party-Ibaraki Prefecture

Ibaraki Prefecture constructed, for industrial application research, Ibaraki Biological Crystal Diffractometer (iBIX) and Ibaraki Materials Design Diffractometer (iMATERIA).

There are three access modes: Industrial Use Open Projects, Prefectural projects and Urgent use. Industrial Use Open Projects are classified into two types of uses: regular-interval use for which projects are accepted in either the first or the second half of the year and occasional use for which projects are accepted as late as about one month prior to the date the desired cycle starts. Prefectural projects are for industry-academic-government collaboration research led by Ibaraki Prefecture or for promoting an advantage of neutron use to a certain industry. Urgent use is for projects more urgent than the regular ones.

(c) Beamtime managed by CROSS-Tokai

CROSS-Tokai manages and supports the user program on the six neutron Public Beamlines (BL01, BL02, BL11, BL15, BL17, BL18). There are six kinds of access modes for these Beamlines.

1) General Use

General Use access works in exactly the same way for the Public Beamlines as it does for all other MLF instruments. This is the appropriate access mode for most researchers wishing to use the neutron Public Beamlines at J-PARC MLF.

To encourage and provide access to the widest possible range of users, General Use is, in principle, open to all local and international researchers who wish to exploit the neutron beams and instruments in their research programs. Proposals are welcomed from researchers with academic, government or private research affiliations.

2) Elements Strategic Use

The government project to generate materials which serve as alternatives to rare materials such as rare earth or rare elements started in 2012. There are four categories in the project: magnet materials, catalytic or battery materials, electronic materials and construction materials. Elements Strategic Use is aimed at promoting that project.

3) Trial Use

Trial Use is aimed at assisting novice users of neutron-based experimental techniques to gain experience and expertise that will allow them to become independent General Use applicants in the future. It may also be used for first-time users of pulsed neutrons to determine the experimental feasibility.

The Trial Use framework offers a wide range of services to potential new users, including support and guidance provided by a CROSS-Tokai Science Coordinator.

4) Director's Discretion

A proportion of the total available beamtime is reserved for allocation at the discretion of the Director of CROSS-Tokai. This time may be allocated to urgent proposals that warrant expedited access or used for approved outreach or education activities of CROSS-Tokai.

5) CROSS-Tokai Research

In this access mode, members of the Neutron R&D Division of CROSS-Tokai can apply for beamtime to carry out research aimed at developing and advancing research activities on the Public Beamlines. Proposals with strong scientific objectives that expand the range of facility usage will be assessed and ranked together with General Use proposals.

6) Facility Use

To ensure that instruments with the highest possible performance and capability are available to users, this access mode allows members of the beamline group to carry out work associated with the maintenance, development and testing of the instruments. This access mode also facilitates the use of beamlines for approved research projects of the beamline owner organization (JAEA).

(5) Call for General Use Proposals to access the neutron and muon beamlines

J-PARC Center and CROSS-Tokai announced the Call for General Use Proposals to access the neutron and muon beamlines in the 2012A and 2012B operations periods.

Call for proposals for the first half of 2012 (2012A term):
Nov. 17 - Dec. 7, 2011

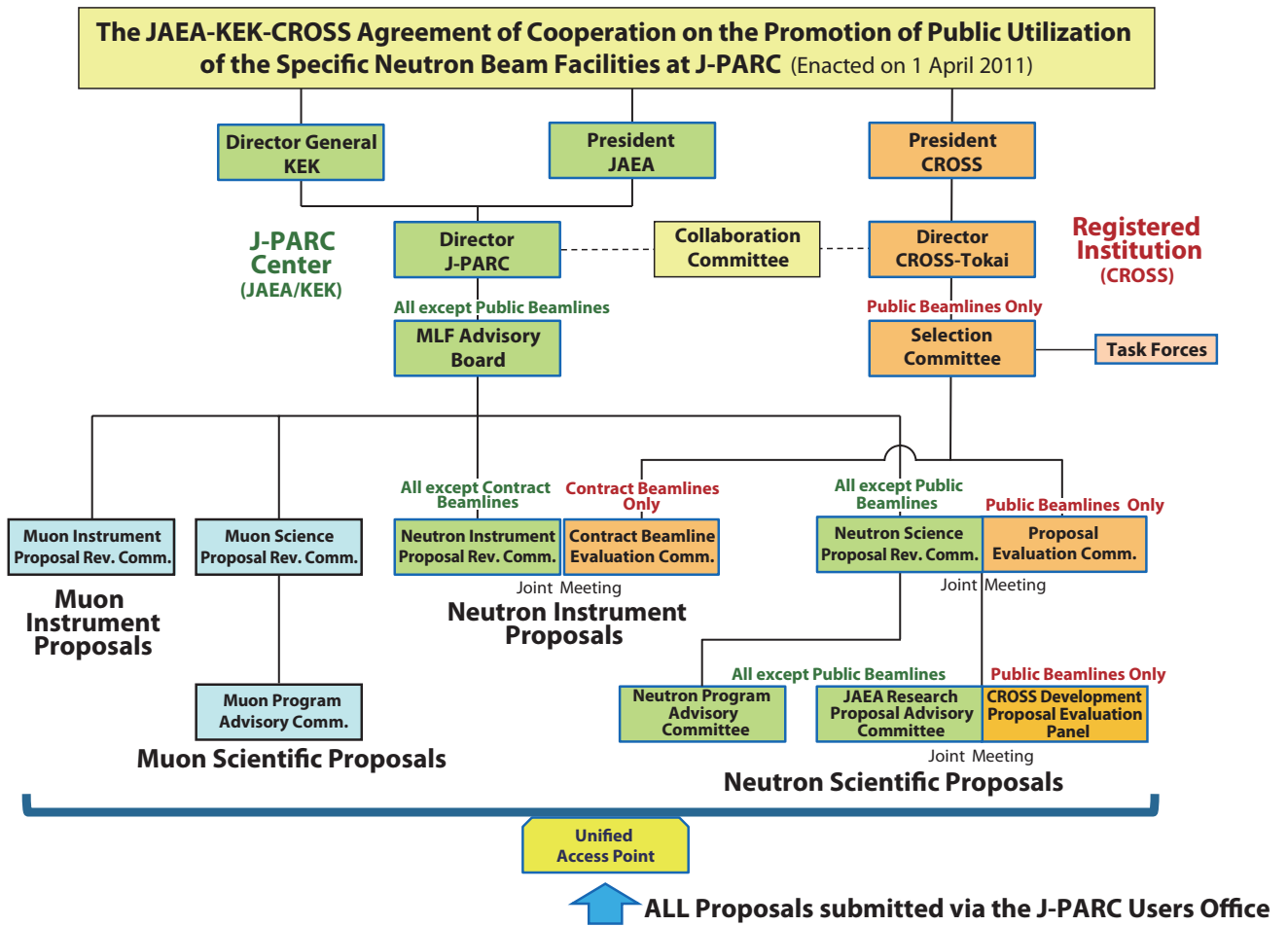
The review results were announced on March 30, 2012.
Call for proposals for the second half of 2012 (2012B term): May 17 - June 7, 2012

The review results were announced on Sep. 21, 2012.

(6) Basic Concept of Nonproprietary Use

Research results obtained through J-PARC use should widely be shared by people all over the world, which enable us to step into the unknown world effectively and efficiently. Based on this idea, no beamtime fee is charged as long as the research results are published for public viewing.

Proposal Review System for MLF



MLF Proposal Summary - FY2012

Table 1. Breakdown of Proposal Numbers for the 2012A & 2012B Rounds.

Beam-line	Instrument	2012A						2012B							
		Submitted			Approved			Submitted			Approved				
		GU	PU/S	IU	GU	PU/S	IU	GU	PU/S	IU	GU	PU/S	IU		
BL01	4D-Space Access Neutron Spectrometer - 4SEASONS	9	2	2	9	2	2	15	2	2	8	2	2		
BL02	Biomolecular Dynamics Spectrometer - DNA	3	3	2	2	3	2	8(2#)	3	2	7(1#)	3	2		
BL03	Ibaraki Biological Crystal Diffractometer - iBIX	(100-β) [‡]		1	0	0	1	0	0	1	0	0	1	0	0
		(β) [†]		1	11	0	1	11	0	2	11	0	2	11	0
BL04	Accurate Neutron-Nucleus Reaction Measurement Instrument - ANNRI	2	1	1	2	1	1	7	1	1	7	1	1		
BL05	Neutron Optics and Physics - NOP	2	1	0	2	1	0	1	1	0	1	1	0		
BL08	Super High Resolution Powder Diffractometer - S-HRPD	9	1	0	6	1	0	16	1	0	10	1	0		
BL10	Neutron Beamline for Observation and Research Use - NOBORU	8	4	1	8	4	1	14	4	1	11	4	1		
BL11	High-Pressure Neutron Diffractometer - PLANET	0	0	1	0	0	1	0	0	1	0	0	1		
BL12	High Resolution Chopper Spectrometer - HRC	5	1	0	1	1	0	4	1	0	4	1	0		
BL14	Cold-neutron Disk-chopper Spectrometer - AMATERAS	16	2	1	11	2	1	16	2	1	11	2	1		
BL15	Small and Wide Angle Neutron Scattering Instrument - TAIKAN	16	6	1	16	6	1	35(5 [‡] , 2 ⁺)	6	1	19(5 [‡] , 2 ⁺)	6	1		
BL16	High-Performance Neutron Reflectometer with a horizontal Sample Geometry - SOFIA	7	1	0	7	1	0	17	1	0	17	1	0		
BL17	Polarized Neutron Reflectometer - SHARAKU	8	3	2	5	3	2	18(3 [‡])	3	2	9(3 [‡])	3	2		
BL18	Extreme Environment Single Crystal Neutron Diffractometer - SENJU	4	2	3	4	2	3	11(1 [‡])	2	3	5(1 [‡])	2	3		
BL19	Engineering Diffractometer - TAKUMI	18	4	1	15	4	1	26	4	1	21	4	1		
BL20	Ibaraki Materials Design Diffractometer - iMATERIA	(100-β) [‡]		15	0	0	11	0	0	15	0	0	9	0	0
		(β) [†]		28	12	0	27	12	0	23	12	0	23	12	0
BL21	High Intensity Total Diffractometer - NOVA	6	1	0	6	1	0	21	1	0	15	1	0		
D1	Muon D1	7	1	1	5	1	1	16	1	1	13	1	1		
D2	Muon D2	14	0	1	12	0	1	9	0	1	8	0	1		
U	Muon U	0	1	0	0	1	0	0	1	0	0	1	0		
Subtotal		179	57	17	151	57	17	275	57	17	161	57	17		
Total		253			225			349			235				

GU : General Use **PU** : Project Use or Ibaraki Pref. Project Use **IU** : Instrument Group Use
S : S-type Proposals **†** : Ibaraki Pref. Exclusive Use Beamtime (β = 80% in FY2012)
‡ : J-PARC Center General Use Beamtime ((100-β = 20% in FY2012)
: Proposal Numbers under Trial Use Access System in GU
+ : Proposal numbers under Element Strategy in GU

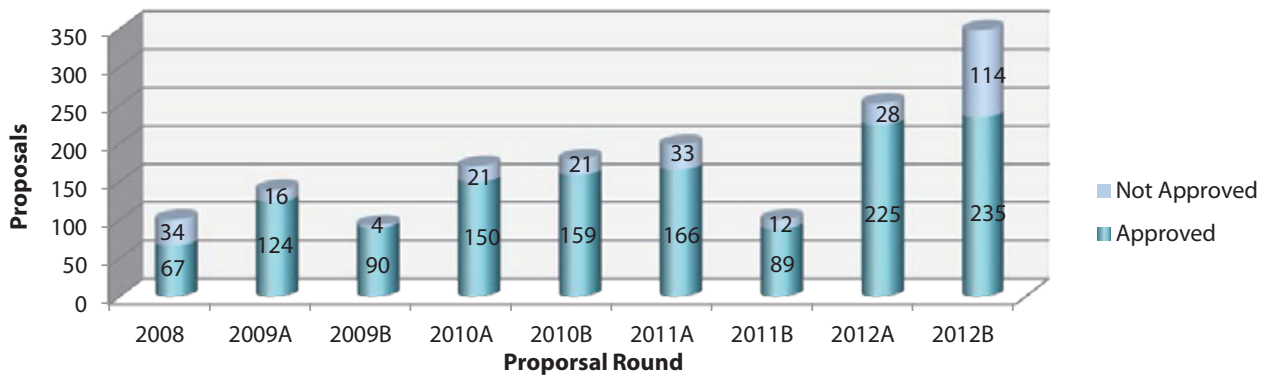


Figure 1. MLF Proposal Numbers over Time.

Table 2. Principal Investigator Affiliations in FY2012.

Universities (Japan)	JAEA	Companies (Japan)	KEK	Foreign Organizations	Research Institutes (Japan)
212	141	101	34	46	68

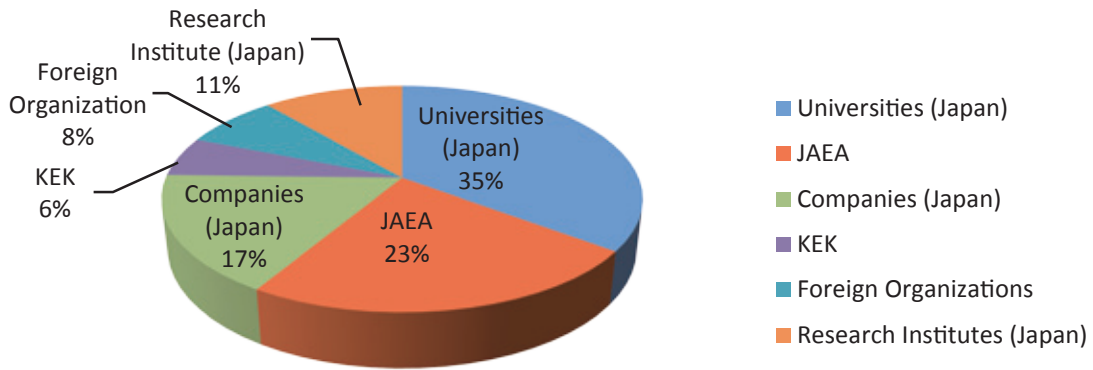


Figure 2. Origin of Proposals in FY2012.

Table 3. Proposals by Sub-committee/Expert Panel – FY2012.

Sub-committee Expert Panel	P1	P2	P3	P4	P5	P6	P7	P8	P9	P10	Q1	Q2
No. of Proposals	96	29	44	14	77	15	56	25	11	2	14	32

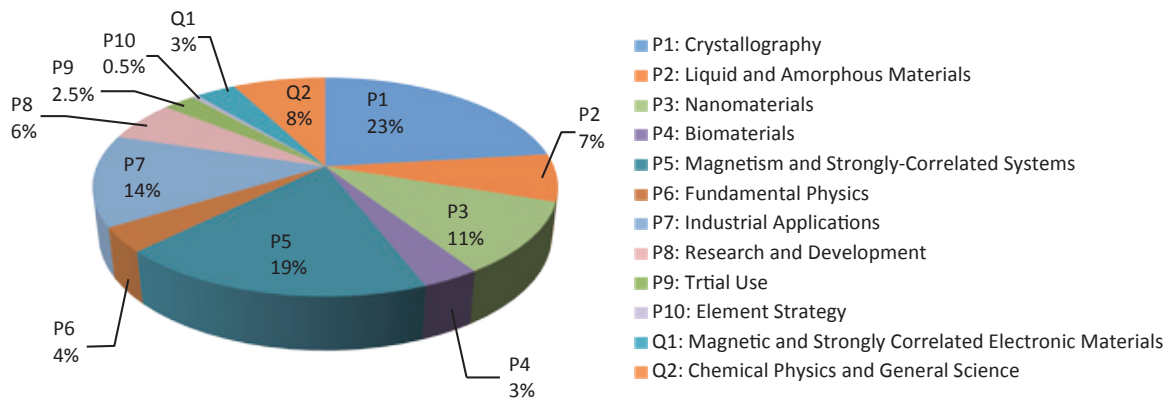
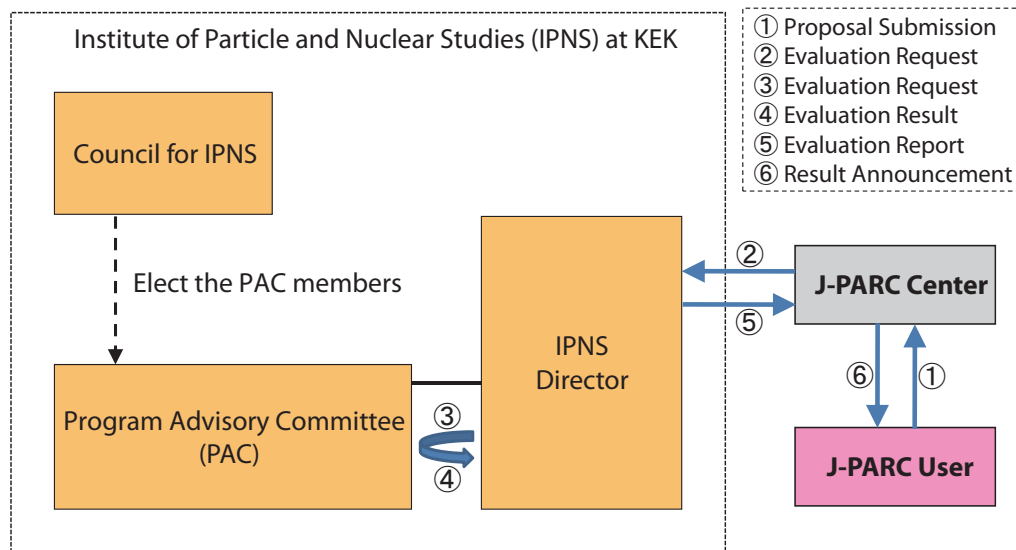


Figure 3. Submitted Proposals by Sub-committee/Expert Panel – FY2012.

Proposal Review System for Nuclear and Particle Physics Experiments at the J-PARC "50 GeV" Proton Synchrotron



The 15th Program Advisory Committee (PAC) meeting was held on July 13 - 15, 2012.
The 16th PAC meeting was held on January 9 - 11, 2013.

Approval Summary of the Nuclear and Particle Physics Experiments after the 16th PAC Meeting (January 9, 2013)

	(Co-) pokespersons	Affiliation	Title of the experiment	Approval status (PAC recommendation)	Slow line priority		Beamline
					Day1	Day1 Priority	
E03	K. Tanida	SNU	Measurement of X rays from Ξ^- Atom	Stage 2			K1.8
P04	J.C. Peng; S. Sawada	U.of Illinois at Urbana-Champaign; KEK	Measurement of High-Mass Dimuon Production at the 50-GeV Proton Synchrotron	Deferred			Primary
E05	T. Nagae	Kyoto U	Spectroscopic Study of Ξ -Hypernucleus, $^{12}_{\Xi}\text{Be}$, via the $^{12}\text{C}(K^-, K^+)$ Reaction	Stage 2	Day1	1	K1.8
E06	J. Imazato	KEK	Measurement of T-violating Transverse Muon Polarization in $K^+ \rightarrow \pi^0 \mu^+ \nu$ Decays	Stage 1			K1.1BR
E07	K. Imai, K. Nakazawa, H. Tamura	JAEA, Gifu U, Tohoku U	Systematic Study of Double Strangeness System with an Emulsion-counter Hybrid Method	Stage 2			K1.8
E08	A. Krutenkova	ITEP	Pion double charge exchange on oxygen at J-PARC	Stage 1			K1.8
E10	A. Sakaguchi, T. Fukuda	Osaka U Osaka EC U	Production of Neutron-Rich Lambda-Hypernuclei with the Double Charge-Exchange Reaction (Revised from Initial P10)	Stage 2			K1.8
E11	T. Kobayashi	KEK	Tokai-to-Kamioka (T2K) Long Baseline Neutrino Oscillation Experimental Proposal	Stage 2			neutrino
E13	T. Tamura	Tohoku U	Gamma-ray spectroscopy of light hypernuclei	Stage 2	Day1	2	K1.8
E14	T. Yamanaka	Osaka U	Proposal for $K_L \rightarrow \pi^0 \nu \bar{\nu}$ Experiment at J-PARC	Stage 2			KL
E15	M. Iwasaki, T. Nagae	RIKEN, Kyoto U	A Search for deeply-bound kaonic nuclear states by in-flight $^3\text{He}(K, n)$ reaction	Stage 2	Day1		K1.8BR
E16	S. Yokkaichi	RIKEN	Electron pair spectrometer at the J-PARC 50-GeV PS to explore the chiral symmetry in QCD	Stage 1			High p
E17	R. Hayano, H. Outa	U Tokyo, RIKEN	Precision spectroscopy of Kaonic ^3He 3d- \rightarrow 2p X-rays	Stage 2	Day1		K1.8BR
E18	H. Bhang, H. Outa, H. Park	SNU, RIKEN, KRISS	Coincidence Measurement of the Weak Decay of $^{12}_{\Lambda}\text{C}$ and the three-body weak interaction process	Stage 2			K1.8
E19	M. Naruki	KEK	High-resolution Search for Θ^+ Pentaquark in $\pi p \rightarrow K X$ Reactions	Stage 2	Day1		K1.8

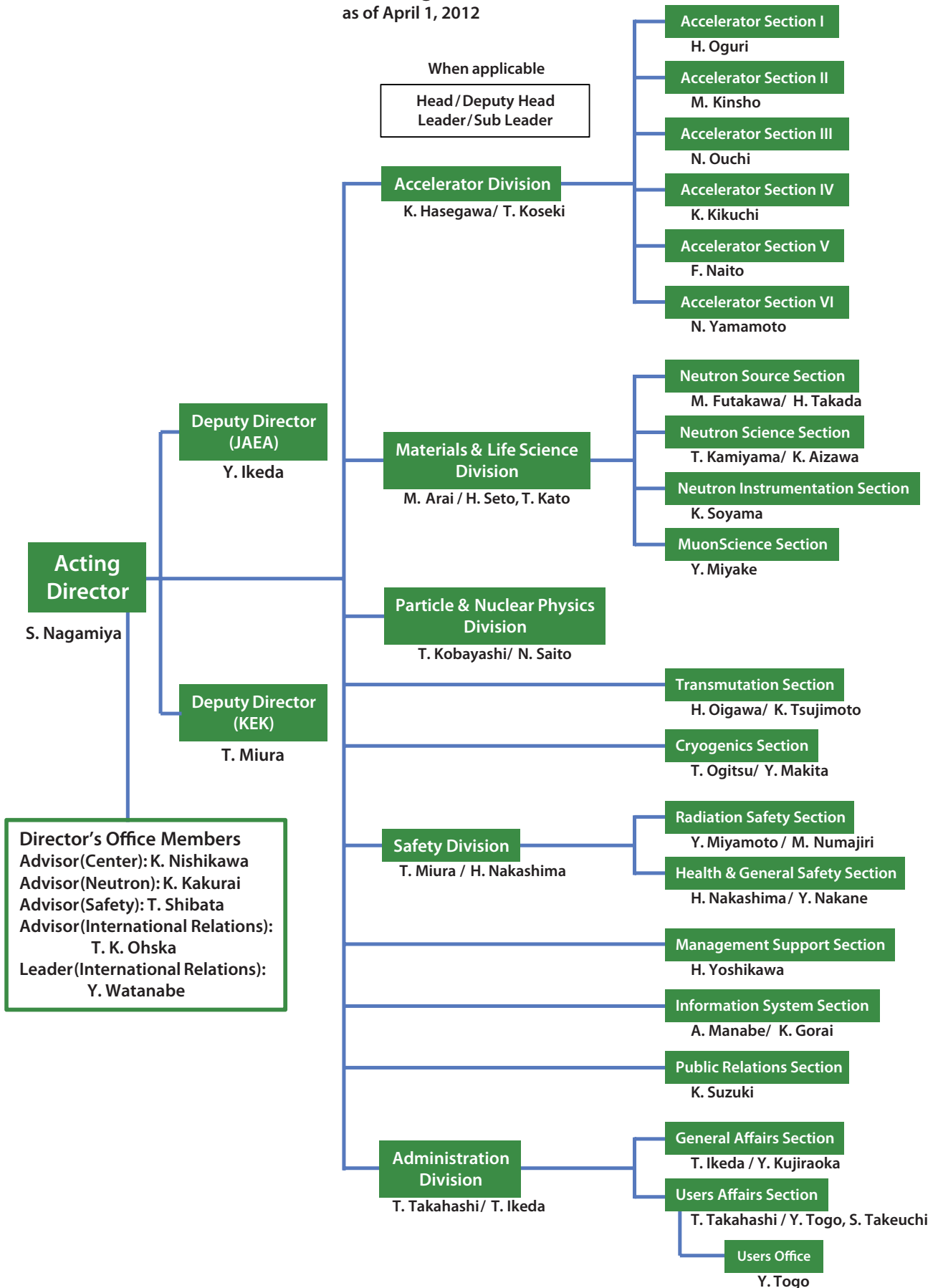
	(Co-) pokespersons	Affiliation	Title of the experiment	Approval status (PAC recommendation)	Slow line priority		Beamline
					Day1	Day1 Priority	
E21	Y. Kuno	Osaka U	An Experimental Search for $\mu - e$ Conversion at a Sensitivity of 10^{-16} with a Slow-Extracted Bunched Beam	Stage 1			New beamline
E22	S. Ajimura, A. Sakaguchi	Osaka U	Exclusive Study on the Lambda-N Weak Interaction in A=4 Lambda-Hypernuclei (Revised from Initial P10)	Stage 1			K1.8
T25	S. Mihara	KEK	Extinction Measurement of J-PARC Proton Beam at K1.8BR	Test Experiment	will be coordinated by JPNC		K1.8BR
P26	K. Ozawa	KEK	Search for ω -meson nuclear bound states in the $\pi^+ + ^AZ \rightarrow n + ^{(A-1)}\omega(Z-1)$ reaction, and for ω mass modification in the in-medium $\omega \rightarrow \pi^0 \gamma$ decay.	Stage 1			K1.8
E27	T. Nagae	Kyoto U	Search for a nuclear Kbar bound state K^+pp in the $d(\pi^+, K^+)$ reaction	Stage 2			K1.8
P29	H. Ohnisi	RIKEN	Search for ϕ -meson nuclear bound states in the $pbar + AZ \rightarrow \phi + (A-1)\phi(Z-1)$ reaction	Stage 1			K1.1
E31	M. Noumi	Osaka U	Spectroscopic study of hyperon resonances below KN threshold via the (K, n) reaction on Deuteron	Stage 2			K1.8BR
T32	A. Rubbia	ETH, Zurich	Towards a Long Baseline Neutrino and Nucleon Decay Experiment with a next-generation 100 kton Liquid Argon TPC detector at Okinoshima and an intensity upgraded J-PARC Neutrino beam	Test Experiment	schedule and beam time will be coordinated by JPNC		K1.1BR
P33	H.M. SHIMIZU	Nagoya U	Measurement of Neutron Electric Dipole Moment	Deferred			Linac
P34	N. Saito, M. Iwasaki	KEK, RIKEN	An Experimental Proposal on a New Measurement of the Muon Anomalous Magnetic Moment g-2 and Electric Dipole Moment at J-PARC	Stage 1			MLF
E36	M. Kohl, S. Shimizu	Ohio U, Osaka	Measurement of $\Gamma(K^+ \rightarrow e^+ \nu) / \Gamma(K^+ \rightarrow \mu^+ \nu)$ and Search for heavy sterile neutrinos using the TREK detector system	Stage 1			K1.1BR
P40	K. Miwa	Tohoku U	Measurement of the cross sections of Σp scatterings	Stage 1			K1.8
P41	M. Aoki	Osaka U	An Experimental Search for $\mu - e$ Conversion in Nuclear Field at a Sensitivity of 10^{-14} with Pulsed Proton Beam from RCS	Deferred			MLF
E42	J.K. Ahn	Pusan National U	Search for H-Dibaryon with a Large Acceptance Hyperon Spectrometer	Stage 1			K1.8
P45	K.H. Hicks, H. Sako	Ohio U, JAEA	3-Body Hadronic Reactions for New Aspects of Baryon Spectroscopy	Stage 1			K1.8
T46	K. Ozawa	KEK	EDIT2013 beam test program	Test Experiment	(will be performed before next summer)		K1.1BR
T47	Y. Aramaki	RIKEN	Test of Lead-glass EMC and GEM Tracker for the J-PARC E16 Experiment	Test Experiment	(completed)		K1.1BR
T48	A. Toyoda	KEK	Test of Aerogel Cherenkov counter for the J-PARC E36 experiment	Test Experiment	(completed)		K1.1BR
T49	T. Maruyama	KEK	Test for 250L Liquid Argon TPC	Test Experiment	(will be performed before next summer)		K1.1BR
P50	H. Noumi	Osaka U	Charmed Baryon Spectroscopy via the (π, D^{*-}) reaction	Deferred			High p



Organization and Committees

Organization Structure

J-PARC Center Organization Chart
as of April 1, 2012



Members of the Committees Organized for J-PARC

(as of March, 2013)

1) Steering Committee

Yujiro Ikeda	J-PARC Center, Japan
Kazuhisa Kakurai	Japan Atomic Energy Agency, Japan
Satoru Kondo	Japan Atomic Energy Agency, Japan
Hideki Namba	Japan Atomic Energy Agency, Japan
Masaharu Nomura	High Energy Accelerator Research Organization, Japan
Katsunobu Oide	High Energy Accelerator Research Organization, Japan
Takayuki Sumiyoshi	High Energy Accelerator Research Organization, Japan
Yasuhide Tajima	Japan Atomic Energy Agency, Japan
Kazuyoshi Yamada	High Energy Accelerator Research Organization, Japan
Masanori Yamauchi	High Energy Accelerator Research Organization, Japan
Hideaki Yokomizo	Japan Atomic Energy Agency, Japan

2) International Advisory Committee

Hamid Ait Abderrahim	Belgian Nuclear Research Center, Belgium
Hiroshi Amitsuka	Hokkaido University, Japan
Kelly Beierschmitt	Oak Ridge National Laboratory, USA
Sergio Bertolucci	CERN, Switzerland
Shinian Fu	Institute of High Energy Physics, Chinese Academy of Science, China
Hidetoshi Fukuyama	Tokyo University of Science, Japan
Donald Geesaman	Argonne National Laboratory, USA
Andrew Harrison	Institut Laue-Langevin, France
Hugh Montgomery	Thomas Jefferson National Accelerator Facility, USA
Jean-Michel Poutissou	TRIUMF, Canada (chair)
Thomas Roser	Brookhaven National Laboratory, USA
Hoerst Stoecker	GSI, Germany
Andrew Taylor	Science and Technology Facilities Council, UK
Robert Tschirhart	Fermi National Accelerator Laboratory, USA
Hajimu Yamana	Research Reactor Institute, Kyoto University, Japan

3) User Consultative Committee for J-PARC

Masatoshi Arai	Japan Atomic Energy Agency, Japan
Yasuhiko Fujii	CROSS, Japan
Makoto Hayashi	Ibaraki Prefecture, Japan
Tomohiko Iwasaki	Tohoku University, Japan
Toshiji Kanaya	Kyoto University, Japan
Yoshiyuki Kawakami	Eisai Co., Ltd., Japan
Yoshiaki Kiyanagi	Hokkaido University, Japan
Takashi Kobayashi	High Energy Accelerator Research Organization, Japan
Yoji Koike	Tohoku University, Japan
Sachio Komamiya	University of Tokyo, Japan
Yasuhiro Miyake	High Energy Accelerator Research Organization, Japan
Junichirou Mizuki	Kwansei Gakuin University, Japan
Tomofumi Nagae	Kyoto University, Japan
Takashi Nakano	Osaka University, Japan
Tsuyoshi Nakaya	Kyoto University, Japan
Nobuyuki Osakabe	Central Research Laboratory, Hitachi, Ltd., Japan
Taku Sato	Tohoku University, Japan
Shinya Sawada	High Energy Accelerator Research Organization, Japan
Masaaki Sugiyama	Kyoto University, Japan
Jun Sugiyama	Toyota Central R&D Labs., Inc., Japan
Hirokazu Tamura	Tohoku University, Japan
Kazuhiro Tanaka	High Energy Accelerator Research Organization, Japan
Eiko Torikai	Yamanashi University, Japan
Taku Yamanaka	Osaka University, Japan
Satoru Yamashita	University of Tokyo, Japan

4) Accelerator Technical Advisory Committee

Alberto Facco	National Institute of Nuclear Physics, Italy
David Findlay	Rutherford Appleton Laboratory, UK
Ronald Garoby	CERN, Switzerland
Subrata Nath	Los Alamos National Laboratory
Akira Noda	Kyoto University, Japan
Michael Plum	Oak Ridge National Laboratory, USA
Thomas Roser	Brookhaven National Laboratory, USA (chair)
Jie Wei	Michigan State University, USA
Robert Zwaska	Fermi National Accelerator Laboratory, USA

5) Neutron Advisory Committee

Kurt Clausen	Paul Scherrer Institut, Switzerland
Phillip Ferguson	Oak Ridge National Laboratory, USA
Toshiji Kanaya	Kyoto University, Japan
Mahn Won Kim	KAIST, Korea
Yoshiaki Kiyonagi	Hokkaido University, Japan
Dan Neumann	National Institute of Standards and Technology, USA (chair)
Robert Robinson	Australian Nuclear Science and Technology Organization, Australia
Uschi Steigenberger	ISIS, UK
Werner Wagner	Paul Scherrer Institute, Switzerland

6) Muon Science Advisory Committee

Hiroshi Amitsuka	Hokkaido University, Japan
Toshiyuki Azuma	RIKEN, Japan
Klauss Jungmann	University of Groningen, Netherland
Elvezio Morenzoni	Paul Scherrer Institute, Switzerland (chair)
Yasuo Nozue	Osaka University, Japan
Francis Pratt	ISIS, UK
Jeff E. Sonier	Simon Fraser University, Canada
Jun Sugiyama	Toyota Central R&D Labs., Inc., Japan

7) Radiation Safety Committee

Yoshihiro Asano	RIKEN, Japan
Shuichi Ban	High Energy Accelerator Research Organization, Japan
Yukihide Kamiya	High Energy Accelerator Research Organization, Japan
Satoru Kondo	Japan Atomic Energy Agency, Japan
Takeshi Murakami	National Institute of Radiological Science, Japan
Tetsuo Noro	Kyushu University, Japan
Shinichi Sasaki	High Energy Accelerator Research Organization, Japan
Seiichi Shibata	Kyoto University, Japan (chair)
Yoshitomo Uwamino	RIKEN, Japan
Takenori Yamaguchi	Japan Atomic Energy Agency, Japan
Yoshihiro Yamaguchi	Japan Atomic Energy Agency, Japan

8) MLF Advisory Board

Jun Akimitsu	Aoyama Gakuin University, Japan
Masatoshi Arai	Japan Atomic Energy Agency, Japan
Koichiro Asahi	Tokyo Institute of Technology, Japan
Yasuhiko Fujii	CROSS, Japan
Masatoshi Futakawa	Japan Atomic Energy Agency, Japan
Makoto Hayashi	Ibaraki Prefecture, Japan
Shinichi Ito	High Energy Accelerator Research Organization, Japan
Masahiko Iwasaki	RIKEN, Japan
Ryosuke Kadono	High Energy Accelerator Research Organization, Japan
Takashi Kamiyama	High Energy Accelerator Research Organization, Japan
Toshiji Kanaya	Kyoto University, Japan
Mikio Kataoka	Nara Institute of Science and Technology, Japan
Takashi Kato	Japan Atomic Energy Agency, Japan
Yukinobu Kawakita	Japan Atomic Energy Agency, Japan
Kazuya Aizawa	Japan Atomic Energy Agency, Japan
Yoji Koike	Tohoku University, Japan
Yasuhiro Miyake	High Energy Accelerator Research Organization, Japan
Toshiya Ohtomo	High Energy Accelerator Research Organization, Japan
Taku Sato	Tohoku University, Japan
Hideki Seto	High Energy Accelerator Research Organization, Japan
Mitsuhiro Shibayama	University of Tokyo, Japan
Masaaki Sugiyama	Kyoto University, Japan
Jun Sugiyama	Toyota Central R&D Labs., Inc., Japan
Wataru Utusmi	Japan Atomic Energy Agency, Japan
Toshio Yamaguchi	Fukuoka University, Japan

9) Program Advisory Committee (PAC) for Nuclear and Particle Physics Experiments at the J-PARC 50GeV Proton Synchrotron

Edward Blucher	University of Chicago, USA
Thomas Browder	University of Hawaii, USA
Akinobu Dote	High Energy Accelerator Research Organization, Japan
Junji Haba	High Energy Accelerator Research Organization, Japan
Kenichi Imai	Japan Atomic Energy Agency, Japan
Kunio Inoue	Tohoku University, Japan
Gino Isidori	Frascati National Laboratories, Italy
Tadafumi Kishimoto	Osaka University, Japan
Konrad Kleinknecht	Mainz University, Germany
William C. Louis	Los Alamos National Laboratory, USA
Tomofumi Nagae	Kyoto University, Japan
Matthias Gross Perdekamp	University of Illinois, USA
Hiroyoshi Sakurai	University of Tokyo, Japan
Hajime Shimizu	Tohoku University, Japan
Wolfram Weise	Technische Universität München, Germany

Main Parameters

Present main parameters of Accelerator

Linac	
Accelerated. Particles	Negative hydrogen
Energy	181 MeV
Peak Current	15 mA
Pulse Width	0.5 ms
Repetition Rate	25 Hz
Freq. of RFX, DTL, and SDDL	324 MHz
RCS	
Circumference	348.333 m
Injection Energy	181 MeV
Extraction Energy	3 GeV
Repetition Rate	25 Hz
RF Frequency	0.938 MHz → 1.67 MHz
Harmonic Number	2
Number of RF cavities	11
Number of Bending Magnet	24
Main Ring	
Circumference	1567.5 m
Injection Energy	3 GeV
Extraction Energy	30 GeV
Repetition Rate	~0.3 Hz
RF Frequency	1.67 MHz → 1.72 MHz
Harmonic Number	9
Number of RF cavities	6
Number of Bending Magnet	96

Key parameters of Materials and Life Science Experimental Facility

Injection Energy	3 GeV
Repetition Rate	25 Hz
Neutron Source	
Target Material	Mercury
Number of Moderators	3
Moderator Material	Supercritical hydrogen
Moderator Temperature/Pressure	20 K / 1.5 MPa
Number of Neutron Beam Ports	23
Muon Production Target	
Target Material	Graphite
Number of Muon Beam Extraction Ports	4
Neutron Instruments*	
Open for User Program (General Use)	11
Under Commissioning/Construction	5/3
Muon Instruments*	
Open for User Program (General Use)	2

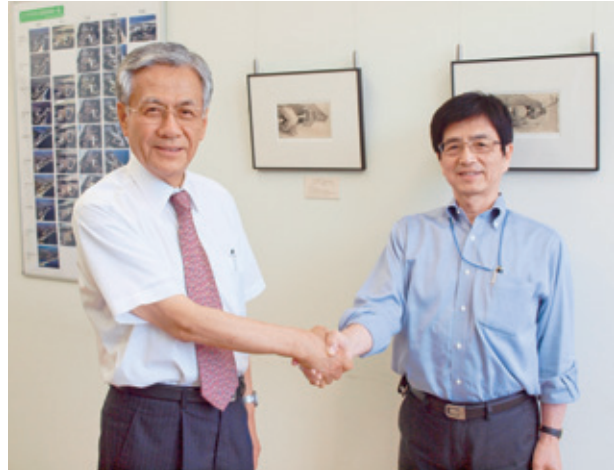
(* as of March, 2013)

Events

Events

New J-PARC Director Takes Over - Shoji Nagamiya Passes the Baton to Yujiro Ikeda (July 1)

After 6 years at the helm of the J-PARC project, Dr. Shoji Nagamiya formally retired in the end of June 2012. In the process he handed the mantle of the J-PARC Center Director to Dr. Yujiro Ikeda, who was selected after an extensive search. The new management team led by Dr Ikeda took over the reins at J-PARC on July 1, keen to take up the challenge of leading J-PARC into the future.



The former Director, Dr. Nagamiya (left) and the new Director, Dr. Ikeda (right)

J-PARC Open House (July 29)

The first J-PARC open house after the earthquake in 2011 was held on July 29, 2012, and attracted 2,100 visitors. The visitors had the chance to observe the three experimental facilities and the tunnel of the 50-GeV synchrotron accelerator, where can be accessed during only summer shutdown of J-PARC. The visitors intently listened to researchers' explanations about the instruments used or the scientific studies performed at each facility (and in the demonstration areas, many kids, who would be future scientists of J-PARC, were enjoying simple experiments using liquid nitrogen and electromagnets, etc.)



Materials and Life Science Experimental Facility (MLF)



Electromagnets in the tunnel of the 50-GeV synchrotron

Ceremony to Mark the Completion of a New Neutron Diffraction Device, SPICA (September 4)

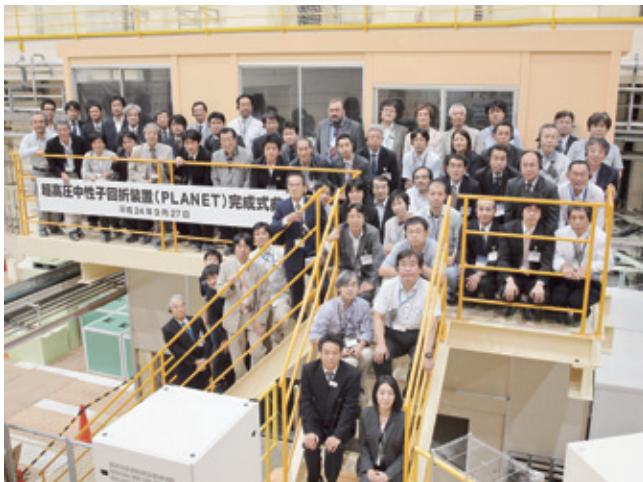
The Special Environment Neutron Powder Diffractometer (SPICA) for analyzing the internal atomic structure and behavior in batteries was installed on BL 09 at MLF and a celebration party was held by KEK, NEDO and Kyoto University.

It has the highest time and space resolutions and is expected to be a great tool to develop batteries by understanding the processes that take place inside of a battery. Furthermore, it is expected to contribute to the development of a new generation of batteries.



The ribbon-cutting ceremony at MLF

Ceremony to Mark the Completion of a New Neutron Diffraction Device, PLANET (September 27)



Ceremony attendees

The ceremony to celebrate the completion of the new neutron powder diffractometer, PLANET, at MLF was held on September 27. It was attended by many of the people involved in this joint project of JAEA, Ehime University and The University of Tokyo. PLANET, which has been installed on BL11, is specifically designed to study the physical properties of materials under extremely high temperature and pressure conditions (up to 2000°C and 20 GPa) such as those found in the earth mantle. Because neutron scattering is particularly useful in studying the distribution of water in a material, PLANET is expected to be a powerful tool for understanding the geochemical cycle of water in the earth mantle.

The 4th J-PARC MLF Symposium and the FY2011 Ibaraki-Beamline Progress Meeting (October 10-11)

The Symposium and the Meeting were held jointly at the National Museum of Emerging Science and Innovation (KAGAKU MIRAIKAN) in Tokyo, Japan, on October 10-11. Approximately 200 participants attended. For two days, the results of experiments at MLF and the updated status of each beamline, including the development of new equipment, were reported. In the last session, they also discussed the future plans to improve the experimental environment and user accessibility. These meetings were hosted by J-PARC, Ibaraki Prefecture, JAEA, KEK, IMSS and CROSS.



The joint meeting at KAGAKU MIRAIKAN in Tokyo

1st J-PARC Colloquium (November 20)



The 1st J-PARC Colloquium was held at the Ibaraki Quantum Beam Research Center on November 20, 2012. The invited speaker was Dr. Guido Tonelli (Professor, University of Pisa, Italy), previously the leader of CERN's CMS (Compact Muon Solenoid) Experiment team. He gave an extremely interesting talk on the background of the discovery of the Higgs boson, the only elementary particle predicted by the Standard Model of particle physics, which had yet to be found; the new scientific progress due to the discovery of the Higgs boson, such as the elucidation of the origin of mass and the mystery of the creation of the universe; and the expectations for new physics going beyond the Standard Model.

Invited speaker, Dr. Guido Tonelli, professor at the University of Pisa

1st MLF School (December 18-21)

MLF at J-PARC conducts state-of-the-art experiments in materials and life science using world-class pulsed neutron and muon instruments. In order to educate the next generation of researchers and improve the quality of science, we recently held the 1st MLF School for inexperienced graduate students and young researchers with an interest in experiments using neutron and muon beams. Twenty-four people participated as students.



Participants and instructors



SAT Technology Showcase 2013 (January 22)

The 12th SAT Technology Showcase 2013 was held at Tsukuba International Congress Center by the Science Academy of Tsukuba (SAT) on January 22, 2013. In the exhibition, researchers and engineers interacted and presented their current research results, ideas, and techniques. There were 86 poster presentations. J-PARC displayed brochures, posters, DVDs, and exhibit panels at its display booth.

The J-PARC booth at the science exhibition

International School for Strangeness Nuclear Physics 2013 (February 14-20)

From February 14 through 20, the Second International School for Strangeness Nuclear Physics (SNP School 2013) was held at the J-PARC site and Tohoku University, with the participation of 40 students and young researchers from Japan and 30 from foreign countries. The first half (Feb. 14-16) was held at the J-PARC site. First, lectures were held at the Ibaraki Quantum Beam Research Center (IQBRC), and then the participants toured J-PARC on the afternoon of the 15th. They visited MLF, Central Control Room, Neutrino Experimental Facility and Hadron

Experimental Facility. Researchers active at each facility provided detailed explanations, and the participants had many questions. As an assignment, all participants were asked to prepare beforehand posters about their own research topics. On the afternoon of the 16th, there were presentations and a poster session by young researchers, and a lively discussion on the benefits of attending the school. On the 17th, everyone moved to Tohoku University, where the second half of the school (Feb. 18-20) was held.



Listening to a lecture at IQBRC

Workshop on “Multi-purpose Use of the J-PARC Accelerator-Driven Transmutation Experimental Facility” (March 18)

J-PARC plans to build the Accelerator-Driven System (ADS) Experimental Facility as the second phase of the J-PARC project. On March 18, 2013, the workshop was launched by Yujiro Ikeda (Director, J-PARC Center), who explained the main purpose of the gathering. He was followed by people affiliated with ADS, who reported on the purpose and nature of their research, and provided an overview of the facility. An experimental facility for multi-purpose use is being considered; it will enable branched use of the proton beam from the accelerator injected into nuclear spallation targets relating to ADS, and the use of neutron beams from the nuclear spallation targets. Four types of projected uses of this facility were presented by users. At the end of the workshop, these presenters held a lively discussion on the topic “The Need for Multi-purpose Use of Quantum Beams” and

the participants discussed the best approaches for implementing the multi-purpose use of facilities.



The workshop in Tokyo

Visitors (2012)



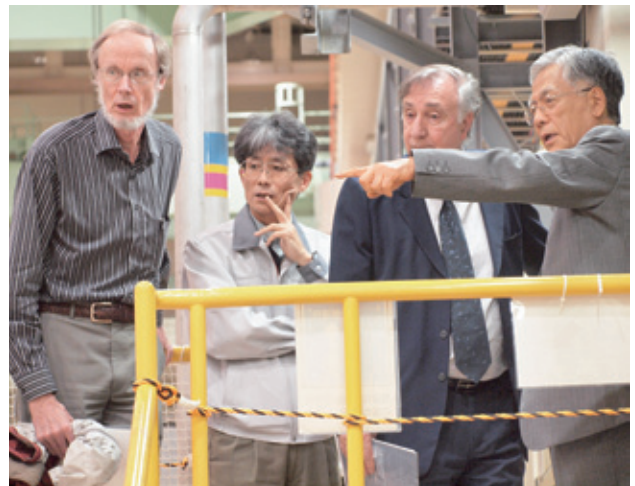
Susan J. Seestrom, Chair of the United States Nuclear Science Advisory Committee (Los Alamos National Laboratory) (August 16)



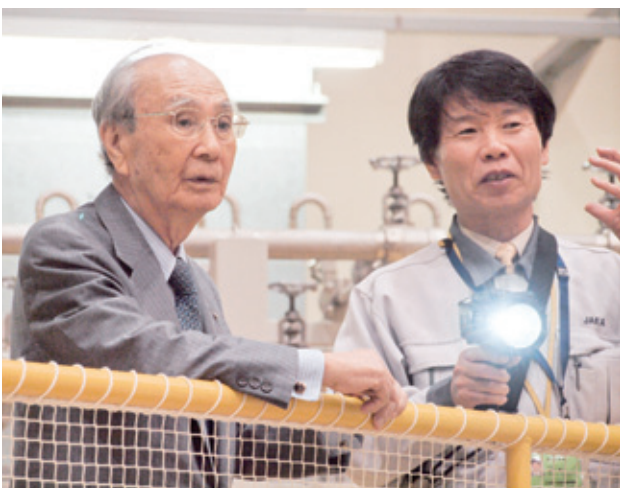
Shunichi Mizuoka, Assistant to the Prime Minister of Japan (September 20)



Tetsuhisa Shirakawa, President of Japan Synchrotron Radiation Research Institute (JASRI) (October 26)



Sydney Gales, Former director of Grand Accélérateur National d'Ions Lourds (GANIL) (October 26)



Shigeru Goto, Nuclear Systems Association (Former member of the House of Representatives)



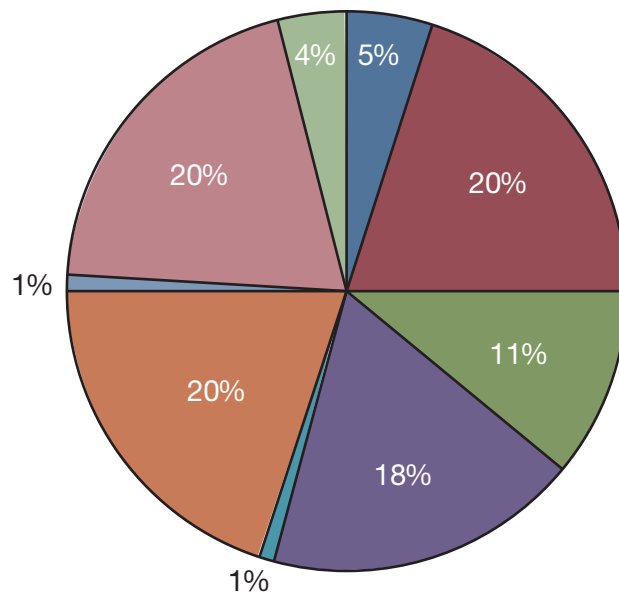
Dochai Chung, Science and Technology Policy Institute (STEPI) (January 25)



John Womersley, CEO of Science and Technology Facilities Council (STFC)
Peter Fletcher, Head of the International Office of STFC (February 24)

There were 3,816 visitors to J-PARC for the period from April 2012 to the end of March 2013.

In 2011 the number of the visitors decreased due to the Great East Japan Earthquake (March 11, 2011). However, in fiscal year 2012, 3,816 people visited J-PARC, which was an increase of over 1,000 visitors compared to fiscal year 2011.



Publications

Publications in Periodical Journals

- A-001
Su, Y.H. et al.
Deformation-induced grain coalescence in an electrodeposited pure iron sheet studied by in situ neutron diffraction and electron backscatter diffraction
Acta Materialia, Vol 60, 3393 (2012)
- A-002
Mizuguchi, M. et al.
Quaternary structure, aggregation and cytotoxicity of transthyretin
Amyloid, Vol 19, Suppl 1, 5 (2012)
- A-003
Oigawa, H.
Reduction of burden for waste disposal by accelerator-driven transmutation technology; Preparing for unforeseeable future by nuclear fuel cycle for back-end
ATOMOS, Vol 54, 315 (2012)
- A-004
Ninomiya, K. et al.
Development of Nondestructive and Quantitative Elemental Analysis Method Using Calibration Curve between Muonic X-ray Intensity and Elemental Composition in Bronze
Bulletin of the Chemical Society of Japan, Vol 85, 228 (2012)
- A-005
Ueda, Y. et al.
Ferromagnetic Metal-Insulator Transition: Peierls Mechanism for Spinless Fermions (Current Topics)
BUTSURI, Vol 67, 571 (2012)
- A-006
Lee, S.C. et al.
Charge-order driven proton arrangement in a hydrogen-bonded charge-transfer complex based on a pyridyl-substituted TTF derivative
Chemical Communications, Vol 48, 8673 (2012)
- A-007
Han, J. et al.
Experimental visualization of lithium conduction pathways in garnet-type $\text{Li}_7\text{La}_3\text{Zr}_2\text{O}_{12}$
Chemical Communications, Vol 48, 9840 (2012)
- A-008
Iiyama, T. et al.
Structure Determination of Hydrogen-bonding Network of Water in Hydrophobic Nanospace by Neutron and X-ray Diffractions
Chemistry Letters, Vol 41, 1267 (2012)
- A-009
Yashima, M. et al.
Role of Ga^{3+} and Cu^{2+} in the High Interstitial Oxide-Ion Diffusivity of Pr_2NiO_4 -Based Oxides: Design Concept of Interstitial Ion Conductors through the Higher-Valence d^{10} Dopant and Jahn-Teller Effect
Chemistry of Materials, Vol 24, 4100 (2012)
- A-010
Takeda, M. et al.
Current Status of a New Polarized Neutron Reflectometer at the Intense Pulsed Neutron Source of the Materials and Life Science Experimental Facility (MLF) of J-PARC
Chinese J. Phys., Vol 50, 161 (2012)
- A-011
Jin, X. et al.
Tensile strain dependence of critical current of RHQ-Nb3Al wires
Cryogenics, Vol 52, 805 (2012)
- A-012
Shikama, T. et al.
Magnetism and Pressure-Induced Superconductivity of Checkerboard-Type Charge-Ordered Molecular Conductor β -(meso-DMBEDT-TTF) $_2$ X (X = PF_6 and AsF_6)
Crystals, Vol 2, 1502 (2012)
- A-013
Ohshima, Y. et al.
High-Temperature-Operating Dielectrics of Perovskite Oxides
ECS Transactions, Vol 45, 195 (2012)
- A-014
Idemoto, Y. et al.
Investigation on Crystal and Electronic Structures of $0.5\text{Li}_2\text{MnO}_3$ - $0.5\text{LiMn}_x\text{Ni}_x\text{Co}_{(1-2x)}\text{O}_2$ ($x = 1/3, 5/12$) Samples Heat-Treated under Vacuum Reducing
Electrochemistry, Vol 80, 791 (2012)
- A-015
Ikeda, K. et al.
The Materials and Life Science Experimental Facility of J-PARC / J-PARC の物質・生命科学実験施設
Engineering Materials (Kogyo Zairyo), Vol 60, 28 (2012)
- A-016
Kajimoto, R. et al.
Development of a High-efficient Inelastic Neutron Scattering Method with Multiple Incident Energies on a Chopper Spectrometer
Hamon, Vol 22, 145 (2012)
- A-017
Sato, H.
Quantitative Imaging of Crystalline Structural Information by Pulsed Neutron Transmission
Hamon, Vol 22, 156 (2012)
- A-018
Arai, M.
Recovery from the Earthquake at MLF
Hamon, Vol 22, 216 (2012)
- A-019
Futakawa, M.
Seismic Damages at MLF Neutron Source
Hamon, Vol 22, 228 (2012)
- A-020
Arimoto, Y. et al.
Development of Longitudinal-Gradient Magnet for Time Focusing of Ultra-Cold Neutron With Anisotropic Inter-Pole
IEEE Trans. Appl. Supercond., Vol 22, 4500704 (2012)
- A-021
Takahashi, K. et al.
Prebending effect on three-dimensional strain in $\text{CuNb}/(\text{Nb}, \text{Ti})_3\text{Sn}$ wires under a tensile load
IEEE Trans. Appl. Supercond., Vol 22, 6000204 (2012)
- A-022
Takeda, M.
Structural analysis of interfaces in thin films using neutron reflectometry
J of JIEP, Vol 15, 492 (2012)
- A-023
Kadono, R. et al.
Quasi-One-Dimensional Spin Dynamics in LiV_2O_4 : One-to-Three-Dimensional Crossover as a Possible Origin of Heavy Fermion State
J Phys Soc Jpn, Vol 81, 014709 (2012)
- A-024
Kawasaki, T. et al.
Structure of Morpholinium Tribromoplumbate $\text{C}_4\text{H}_8\text{ONH}_2\text{PbBr}_3$ Studied Using Single-Crystal Neutron Diffraction
J Phys Soc Jpn, Vol 81, 094602 (2012)
- A-025
Iwase, K. et al.
In situ lattice strain mapping during tensile loading using the neutron transmission and diffraction methods
J. Appl. Cryst., Vol 45, 113 (2012)
- A-026
Oishi-Tomiyasu, R. et al.
Application of matrix decomposition algorithms for singular matrices to the Pawley method in Z-Rietveld
J. Appl. Cryst., Vol 45, 299 (2012)
- A-027
Iwase, H. et al.
Optimization of the thickness of a $\text{ZnS}^{60}\text{LiF}$ scintillator for a high-resolution detector

- installed on a focusing small-angle neutron scattering spectrometer (SANS-U)
J. Appl. Cryst., Vol 45, 507 (2012)
- A-028
Takahashi, K. et al.
Axial and lateral lattice strain states under a tensile load in as-reacted and prebent CuNb/Nb₃Sn wires using neutron diffraction
J. Appl. Phys., Vol 111, 043908 (2012)
- A-029
Tomita, M. et al.
Non-destructive magneto-strain analysis of YB₂Cu₃O₇, superconducting magnets using neutron diffraction in the time-of-flight mode
J. Appl. Phys., Vol 112, 063923 (2012)
- A-030
Kasugai, Y. et al.
Fitting Method for Spectrum Deduction in High-Energy Neutron Field Induced by GeV-Protons Using Experimental Reaction-Rate Data
J. ASTM Int., Vol 9, 675 (2012)
- A-031
Nakamura, T. et al.
A wavelength-shifting-fibre-based scintillator neutron detector implemented with the median point calculation method
J. Instrum., Vol 7, C02003 (2012)
- A-032
Toh, K. et al.
Improved micro-pixel detector element for neutron measurement under high pressure
J. Instrum., Vol 7, C01025 (2012)
- A-033
Kitamura, N. et al.
Particle morphology, electrical conductivity, crystal and electronic structures of hydrothermally synthesized (Ce,Sr)PO₄
J. Mater. Sci., Vol 47, 6220 (2012)
- A-034
Naoe, T. et al.
Quantification of fatigue crack propagation of an austenitic stainless steel in mercury embrittlement
J. Nucl. Mater., Vol 431, 133 (2012)
- A-035
Kawai, M. et al.
Development of advanced materials for spallation neutron sources and radiation damage simulation based on multi-scale models
J. Nucl. Mater., Vol 431, 16 (2012)
- A-036
Teshigawara, M. et al.
Development of invar joint for hydrogen transfer line in JSNS
J. Nucl. Mater., Vol 431, 212 (2012)
- A-037
Ooi, M. et al.
Development status of low activation ternary Au-In-Cd alloy decoupler for a MW class spallation neutron source: 1st Production of Au-In-Cd alloy
J. Nucl. Mater., Vol 431, 218 (2012)
- A-038
Kimura, A. et al.
Neutron-capture cross-sections of ²⁴⁴Cm and ²⁴⁶Cm measured with an array of large germanium detectors in the ANNRI at J-PARC/MLF
J. Nucl. Sci. Technol., Vol 49, 708 (2012)
- A-039
Hemmi, K. et al.
Cr- and Mo-Doping Effects on Structural and Orbital Order Phase Transition in Spinel-Type MnV₂O₄
J. Phys. Soc. Jpn., Vol 81, SB030 (2012)
- A-040
Kaneko, K. et al.
Neutron Scattering Study on High-Quality Single Crystals of Non-Centrosymmetric Heavy-Fermion Superconductor CePt₃Si
J. Phys. Soc. Jpn., Vol 81, SB006 (2012)
- A-041
Takemori, A. et al.
Correlation between T_c and Transport Properties in PrFeP_{1-x}As_xO_{0.9}F_{0.1}
J. Phys. Soc. Jpn., Vol 81, SB043 (2012)
- A-042
Ohishi, K. et al.
Magnetic Penetration Depth in the FeAs-Based Superconductor KFe₂As₂
J. Phys. Soc. Jpn., Vol 81, SB046 (2012)
- A-043
Ito, T.U. et al.
Microscopic Evidence for Long-Range Magnetic Ordering in the Γ₈ Ground Quartet Systems SmTr₂Al₂₀ (Tr: Ti, V, Cr)
J. Phys. Soc. Jpn., Vol 81, SB050 (2012)
- A-044
Kiyonagi, R. et al.
Structural and Magnetic Phase Determination of (1-x) BiFeO₃-xBaTiO₃ Solid Solution
J. Phys. Soc. Jpn., Vol 81, 4603 (2012)
- A-045
Itoh, S. et al.
Anomalous Spin Diffusion on Two-Dimensional Percolating Network in Dilute Antiferromagnet Rb₂Mn_{0.4}Mg_{0.4}F₄
J. Phys. Soc. Jpn., Vol 81, 4704 (2012)
- A-046
Itoh, S. et al.
Quantum Renormalization Effect in One-Dimensional Heisenberg Antiferromagnets
J. Phys. Soc. Jpn., Vol 81, 4706 (2012)
- A-047
Nakao, A. et al.
Observation of Structural Change in the Novel Ferromagnetic Metal-Insulator Transition of K₂Cr₈O₁₆
J. Phys. Soc. Jpn., Vol 81, 4710 (2012)
- A-048
Kawamoto, T. et al.
T_c of 11 K Identified for the Third Polymorph of the (BEDT-TTF)₂Ag(CF₃)₄(TCE) Organic Superconductor
J. Phys. Soc. Jpn., Vol 81, 023705 (2012)
- A-049
Mito, T. et al.
Mechanism of Field Induced Fermi Liquid State in Yb-Based Heavy-Fermion Compound: X-ray Absorption Spectroscopy and Nuclear Magnetic Resonance Studies of YbCo₂Zn₂₀
J. Phys. Soc. Jpn., Vol 81, 033706 (2012)
- A-050
Onodera, Y. et al.
Structural Evidence for High Ionic Conductivity of Li₇P₃S₁₁ Metastable Crystal
J. Phys. Soc. Jpn., Vol 81, 044802 (2012)
- A-051
Nakajima, S. et al.
Microscopic Phase Separation in Triangular-Lattice Quantum Spin Magnet κ-(BEDT-TTF)₂Cu₂(CN)₃ Probed by Muon Spin Relaxation
J. Phys. Soc. Jpn., Vol 81, 063706 (2012)
- A-052
Iida, K. et al.
Two-dimensional incommensurate magnetic fluctuations in Sr₂(Ru_{0.99}Ti_{0.01})O₄
J. Phys. Soc. Jpn., Vol 81, 124710 (2012)
- A-053
Kinsho, M.
Status of J-PARC after the Great East Japan Earthquake
J. Vac. Soc. Jpn., Vol 55, 1 (2012)
- A-054
Kamiya, J. et al.
Magnetic field shielding by vacuum chambers of magnetic material for beam loss reduction
J. Vac. Soc. Jpn., Vol 55, 100 (2012)
- A-055
Kamiya, J. et al.
Development of an in-situ bake-out method for outgassing reduction of kicker ferrite cores
J. Vac. Soc. Jpn., Vol 55, 156 (2012)
- A-056
Jin, X. et al.

- Observation of A15 phase transformation in RHQ-Nb₃Al wire by neutron diffraction at high-temperature
Journal of Alloys and Compounds, Vol 535, 124 (2012)
- A-057
Nyuta, K. et al.
Zwitterionic heterogemini surfactants containing ammonium and carboxylate headgroups 2: Aggregation behavior studied by SANS, DLS, and cryo-TEM
Journal of Colloid and Interface Science, Vol 370, 80 (2012)
- A-058
Yokoyama, T. et al.
Hydrogen-bond network and pH sensitivity in transthyretin: Neutron crystal structure of human transthyretin
Journal of Structural Biology, Vol 177, 283 (2012)
- A-059
Ikeda, K. et al.
Structural Analysis of Hydrogen Storage Materials by High Intensity Neutron Total Diffractometer NOVA/ 高強度中性子全散乱装置 NOVA による水素貯蔵材料の構造解析
Journal of the Hydrogen Energy Systems Society of Japan/ 水素エネルギーシステム Vol 37, 328 (2012)
- A-060
Takeda, M. et al.
Small-Angle Neutron Scattering Measurements of the Averaged Internal Structures in Neodymium-Iron-Boron (Nd-Fe-B) Sintered Magnets
Journal of the Japan Institute of Metals and Materials, Vol 76, 165 (2012)
- A-061
Idemoto, Y. et al.
Dependencies of Piezoelectric and Ferroelectric Properties and Crystal Structure on Synthesis and Sintering Processes in BaTiO₃ Prepared by Hydrothermal and Solid-state Methods
Journal of the Japan Society of Powder and Powder Metallurgy, Vol 59, 101 (2012)
- A-062
Kusano, T. et al.
Structural and Rheological Studies on Growth of Salt-Free Wormlike Micelles Formed by Star-Type Trimeric Surfactants
Langmuir, Vol 28, 16798 (2012)
- A-063
Yoshimura, T. et al.
Star-Shaped Trimeric Quaternary Ammonium Bromide Surfactants: Adsorption and Aggregation Properties
Langmuir, Vol 28, 9322 (2012)
- A-064
Su, C. et al.
Nucleosome-like Structure from Dendrimer-Induced DNA Compaction
Macromolecules, Vol 45, 5208 (2012)
- A-065
Iwase, H. et al.
Hierarchical Structure Analysis of Graft-Type Polymer Electrolyte Membranes Consisting of Cross-Linked Polytetrafluoroethylene by Small-Angle Scattering in a Wide-Q Range
Macromolecules, Vol 45, 9121 (2012)
- A-066
Hoshino, N. et al.
Three-way switching in a cyanide-bridged [CoFe] chain
Nat Chem, Vol 4, 921 (2012)
- A-067
Isono, T. et al.
Hydrogen bond-promoted metallic state in a purely organic single-component conductor under pressure
Nat Commun, Vol 4, 1344 (2013)
- A-068
Fujiwara, T. et al.
Study on Ce:LiCAF scintillator for 3He alternative detector
Neutron News, Vol 23, 31 (2012)
- A-069
Itoh, S. et al.
Fermi chopper developed at KEK
Nucl. Instrum. Meth. A, Vol 661, 58 (2012)
- A-070
Itoh, S. et al.
T0 chopper developed at KEK
Nucl. Instrum. Meth. A, Vol 661, 86 (2012)
- A-071
Nomura, M. et al.
A convenient way to find an electrical insulation break of MA cores in J-PARC synchrotrons
Nucl. Instrum. Meth. A, Vol 668, 83 (2012)
- A-072
Itoh, S. et al.
Large area window on vacuum chamber surface for neutron scattering instruments
Nucl. Instrum. Meth. A, Vol 670, 1 (2012)
- A-073
Ohshita, H. et al.
Stability of neutron beam monitor for High Intensity Total Diffractometer at J-PARC
Nucl. Instrum. Meth. A, Vol 672, 75 (2012)
- A-074
Tomiyasu, K. et al.
Modified cross-correlation for efficient white-beam inelastic neutron scattering spectroscopy
Nucl. Instrum. Meth. A, Vol 677, 89 (2012)
- A-075
Hayashi, N. et al.
Beam position monitor system of J-PARC RCS
Nucl. Instrum. Meth. A, Vol 677, 94 (2012)
- A-076
Ohoyama, K. et al.
Development of a non-adiabatic two-coil spin flipper for a polarised thermal neutron diffractometer with a 3He spin filter
Nucl. Instrum. Meth. A, Vol 680, 75 (2012)
- A-077
Nakamura, T. et al.
A large-area two-dimensional scintillator detector with a wavelength-shifting fibre readout for a time-of-flight single-crystal neutron diffractometer
Nucl. Instrum. Meth. A, Vol 686, 64 (2012)
- A-078
Arimoto, Y. et al.
Demonstration of focusing by a neutron accelerator
Phys. Rev. A, Vol 86, 023843 (2012)
- A-079
Murai, N. et al.
Effect of out-of-plane disorder on superconducting gap anisotropy in Bi_{2+x}Sr_{2-x}CaCu₂O_{8+δ} as seen via Raman spectroscopy
Phys. Rev. B, Vol 85, 020507 (2012)
- A-080
Sugiyama, J. et al.
Diffusive behavior in LiMPO₄ with M=Fe, Co, Ni probed by muon-spin relaxation
Phys. Rev. B, Vol 85, 054111 (2012)
- A-081
Hirata, Y. et al.
Correlation between the interlayer Josephson coupling strength and an enhanced superconducting transition temperature of multilayer cuprate superconductors
Phys. Rev. B, Vol 85, 054501 (2012)
- A-082
Nambu, Y. et al.
Block magnetism coupled with local distortion in the iron-based spin-ladder compound BaFe₂Se₃
Phys. Rev. B, Vol 85, 064413 (2012)
- A-083
Burkovsky, R.G. et al.
Diffuse scattering anisotropy and inhomogeneous lattice deformations in the lead magnoniobate relaxor PMN above the Burns temperature
Phys. Rev. B, Vol 85, 094108 (2012)
- A-084
Ishii, K. et al.

- Electronic excitations around the substituted atom in $\text{La}_2\text{Cu}_{1-y}\text{Ni}_y\text{O}_4$ as seen via resonant inelastic x-ray scattering
Phys. Rev. B, Vol 85, 104509 (2012)
- A-085
Onishi, N. et al.
Magnetic ground state of the frustrated honeycomb lattice antiferromagnet $\text{Bi}_3\text{Mn}_4\text{O}_{12}(\text{NO}_3)$
Phys. Rev. B, Vol 85, 184412 (2012)
- A-086
Higemoto, W. et al.
Multipole and superconducting state in $\text{PrIr}_2\text{Zn}_{20}$ probed by muon spin relaxation
Phys. Rev. B, Vol 85, 235152 (2012)
- A-087
Iida, K. et al.
Determination of spin Hamiltonian in the Ni_4 magnetic molecule
Phys. Rev. B, Vol 86, 064422 (2012)
- A-088
Jarrige, I. et al.
Resonant inelastic x-ray scattering study of charge excitations in superconducting and nonsuperconducting PrFeAsO_{1-y}
Phys. Rev. B, Vol 86, 115104 (2012)
- A-089
Kawasaki, Y. et al.
 μSR investigation of magnetically ordered states in the A-site ordered perovskite manganites RBaMn_2O_6 (R=Y and La)
Phys. Rev. B, Vol 86, 125141 (2012)
- A-090
Matsuura, M. et al.
Ni-substitution effects on the spin dynamics and superconductivity in $\text{La}_{1.85}\text{S}_{0.15}\text{CuO}_4$
Phys. Rev. B, Vol 86, 134529 (2012)
- A-091
Jeong, J. et al.
Spin Wave Measurements over the Full Brillouin Zone of Multiferroic BiFeO_3
Phys. Rev. Lett., Vol 108, 077202 (2012)
- A-092
Machida, A. et al.
Formation of NaCl-type monodeuteride LaD by the disproportionation reaction of LaD_2
Phys. Rev. Lett., Vol 108, 205501 (2012)
- A-093
Iida, K. et al.
Coexisting Order and Disorder Hidden in a Quasi-Two-Dimensional Frustrated Magnet
Phys. Rev. Lett., Vol 108, 217207 (2012)
- A-094
Shirotori, K. et al.
Search for the Θ^+ Pentaquark via the $\pi^+\text{p} \rightarrow \text{K}^+\text{X}$ Reaction at 1.92 GeV/c
Phys. Rev. Lett., Vol 109, 132002 (2012)
- A-095
Nakano, T. et al.
Direct Observation by Neutron Diffraction of Antiferromagnetic Ordering in s Electrons Confined in Regular Nanospace of Sodalite
Phys. Rev. Lett., Vol 109, 167208 (2012)
- A-096
Raymond, S. et al.
Evidence for Three Fluctuation Channels in the Spin Resonance of the Unconventional Superconductor CeCoIn_5
Phys. Rev. Lett., Vol 109, 237210 (2012)
- A-097
Ao, H. et al.
First high-power model of the annular-ring coupled structure for use in the Japan Proton Accelerator Research Complex linac
Phys. Rev. ST Accel. Beams, Vol 15, 011001 (2012)
- A-098
Hotchi, H. et al.
Beam loss reduction by injection painting in the 3-GeV rapid cycling synchrotron of the Japan Proton Accelerator Research Complex
Phys. Rev. ST Accel. Beams, Vol 15, 040402 (2012)
- A-099
Takeda, M. et al.
Polarized neutron reflectometer SHARAKU (BL17) at J-PARC
SHIKI, Vol 16, (2012)
- A-100
Izumi, A. et al.
Structural analysis of cured phenolic resins using complementary small-angle neutron and X-ray scattering and scanning electron microscopy
Soft Matter, Vol 8, 8438 (2012)
- A-101
Sato, M. et al.
On the superconducting pairing mechanism of Fe-based systems—Is it new or well-known?
Solid State Communications, Vol 152, 688 (2012)
- A-102
Matsuo, Y. et al.
Scaling of superionic transition temperature in $\text{M}_3\text{D}(\text{XO}_4)_2$
Solid State Ionics, Vol 225, 40 (2012)
- A-103
Takahashi, K. et al.
Strain measurements by neutron diffraction on Nb_3Sn cable with stainless steel reinforcement strands
Superconductor Science and Technology, Vol 25, 054001 (2012)
- A-104
Jin, X. et al.
Residual strain dependence on the matrix structure in $\text{RHQ-Nb}_3\text{Al}$ wires by neutron diffraction measurement
Superconductor Science and Technology, Vol 25, 065021 (2012)
- A-105
Morooka, S. et al.
Quantitative Analysis of Tensile Deformation Behavior by In-Situ Neutron Diffraction for Ferrite-Martensite Type Dual-Phase Steels
Tetsu-to-Hagane, Vol 98, 311 (2012)
- A-106
Kameda, Y.
Neutron diffractometer in J-PARC
The Japan Association of Solution Chemistry News Letter, Vol 65, 1 (2012)
- A-107
Yamazaki, T. et al.
Analysis of buried heterointerfacial hydrogen in highly lattice-mismatched epitaxy on silicon
Thin Solid Films, Vol 520, 3300 (2012)
- A-108
Saito, Y. et al.
Material and surface processing in J-PARC vacuum system
Vacuum, Vol 86, 817 (2012)
- A-109
Ogiwara, N. et al.
A Pirani gauge in a high-intensity proton accelerator
Vacuum, Vol 86, 908 (2012)

Conference Reports and Books

- C-001
Shiotsu, M. et al.
Transient heat transfer from a horizontal flat plate in a pool of liquid hydrogen
AIP Conf. Proc., Vol 1434, 1059 (2012)
- C-002
Shirai, Y. et al.
DNB heat flux in forced flow of subcooled liquid hydrogen under pressures
AIP Conf. Proc., Vol 1434, 1067 (2012)
- C-003
Tatsumoto, H. et al.
Design of a compact type cryogenic accumulator to mitigate a pressure fluctuation caused by a sudden KW-order heat load
AIP Conf. Proc., Vol 1434, 368 (2012)
- C-004
Tatsumoto, H. et al.
Dynamic behavior of the cryogenic hydrogen system using only a heater control
AIP Conf. Proc., Vol 1434, 391 (2012)
- C-005
Tatsumoto, H. et al.
Forced convection heat transfer of subcooled liquid hydrogen in horizontal tubes
AIP Conf. Proc., Vol 1434, 747 (2012)
- C-006
Takashi, I. et al.
A compact SEOP ^3He neutron spin filter with AFP NMR
J. Phys.; Conf. ser., Vol 340, 012006 (2012)
- C-007
Kiyonagi, Y. et al.
A new imaging method using pulsed neutron sources for visualizing structural and dynamical information
J. Phys.; Conf. ser., Vol 340, 012010 (2012)
- C-008
Nagano, M. et al.
High-precision figured thin supermirror substrates for multiple neutron focusing device
J. Phys.; Conf. ser., Vol 340, 012016 (2012)
- C-009
Nagano, M. et al.
One-dimensional neutron focusing with large beam divergence by 400mm-long elliptical supermirror
J. Phys.; Conf. ser., Vol 340, 012034 (2012)
- C-010
Sakai, K. et al.
Development of polarized Xe gas target for neutron experiment at J-PARC
J. Phys.; Conf. ser., Vol 340, 012037 (2012)
- C-011
Tamura, I. et al.
Current status of a time-of-flight single crystal neutron diffractometer SENJU at J-PARC
J. Phys.; Conf. ser., Vol 340, 012040 (2012)
- C-012
Onodera, Y. et al.
Reverse Monte Carlo modeling of $\text{Li}_2\text{S-P}_2\text{S}_5$ superionic conductors
J. Phys.; Conf. ser., Vol 340, 012058 (2012)
- C-013
Hase, M. et al.
Neutron scattering studies of the spin-5/2 antiferromagnetic linear trimer substance $\text{SrMn}_3\text{P}_4\text{O}_{14}$
J. Phys.; Conf. ser., Vol 340, 012066 (2012)
- C-014
Shamoto, S. et al.
Dynamical Spin Susceptibility Studied by Inelastic Neutron Scattering on $\text{LaFeAsO}_{1-x}\text{F}_x$
J. Phys.; Conf. ser., Vol 340, 012075 (2012)
- C-015
Shimakura, H. et al.
Quasi-elastic neutron scattering of dense molecular liquid selenium bromide
J. Phys.; Conf. ser., Vol 340, 012080 (2012)
- C-016
Kambe, S. et al.
Correlation between the superconducting pairing symmetry and magnetic anisotropy in f-electron unconventional superconductors
J. Phys.; Conf. ser., Vol 344, 012003 (2012)
- C-017
Okuchi, T. et al.
Neutron powder diffraction of small-volume samples at high pressure using compact opposed-anvil cells and focused beam
J. Phys.; Conf. ser., Vol 377, 012013 (2012)
- C-018
Hirayama, T. et al.
Pressure-induced Suppression of the Antiferromagnetic Transition in YbNi_3Al_9 Single Crystal
J. Phys.; Conf. ser., Vol 391, 012020 (2012)
- C-019
Iwasa, K. et al.
Neutron scattering study on magnetic ordering in a partially rare-earth filled skutterudite $\text{PrxFe}_4\text{Sb}_{12}$
J. Phys.; Conf. ser., Vol 391, 012025 (2012)
- C-020
Kaneko, K. et al.
Effect of magnetic field in heavy-fermion compound $\text{YbCo}_2\text{Zn}_{20}$
J. Phys.; Conf. ser., Vol 391, 012026 (2012)
- C-021
Matsubayashi, K. et al.
Low temperature properties of a low carrier heavy fermion YbPtSb
J. Phys.; Conf. ser., Vol 391, 012040 (2012)
- C-022
Yano, S. et al.
Magnetic excitations in MnP
J. Phys.; Conf. ser., Vol 391, 012113 (2012)
- C-023
Kobayashi, Y. et al.
NMR Studies on Iron Pnictide Superconductors of $\text{LaFeAsO}_{0.89}\text{F}_{0.11}$ and Ca-Fe-Pt-As
J. Phys.; Conf. ser., Vol 400, 022056 (2012)
- C-024
Kazuki, O. et al.
Flux-line lattice state in FeAs-based superconductor KFe_2As_2
J. Phys.; Conf. ser., Vol 400, 022087 (2012)
- C-025
Sato, M. et al.
Impurity effects on the superconducting transition temperatures of Fe pnictides and superconducting symmetry of the order parameter
J. Phys.; Conf. ser., Vol 400, 022104 (2012)
- C-026
Sato, M. et al.
Study of magnetic excitation spectra of several Fe-pnictide systems
J. Phys.; Conf. ser., Vol 400, 022105 (2012)
- C-027
Itoh, S. et al.
Two-Dimensional Antiferromagnetic Fractons in $\text{Rb}_2\text{Mn}_{0.598}\text{Mg}_{0.402}\text{F}_4$
J. Phys.; Conf. ser., Vol 400, 032030 (2012)
- C-028
Kajimoto, R. et al.
Neutron scattering study of Ag, Mg and Al substitution effects on the magnetic excitations in CuCrO_2
J. Phys.; Conf. ser., Vol 400, 032034 (2012)
- C-029
Okuda, T. et al.
Substitution Effect on the Magnetic State of Delafossite CuCrO_2 Having a Spin-3/2 Antiferromagnetic Triangular Sublattice
J. Phys.; Conf. ser., Vol 400, 032072 (2012)
- C-030
Yokoo, T. et al.

- Magnetic excitations in possible spin-Peierls system TiOBr
J. Phys.; Conf. ser., Vol 400, 032123 (2012)
- C-031
Sugiyama, J. et al.
Lithium Diffusion in Lithium-Transition-Metal Oxides Detected by μ +SR
Physics Procedia, Vol 30, 105 (2012)
- C-032
Adiperdana, B. et al.
Muon Sites Estimation in La_2CuO_4 and A New Vanadium Cluster Compound, $\text{V}_4\text{S}_9\text{Br}_4$, using Electronic and Nuclear Dipole Field Calculations
Physics Procedia, Vol 30, 109 (2012)
- C-033
Chow, K.H. et al.
 μ SR Investigation of the Hollandite Vanadate $\text{K}_2\text{V}_8\text{O}_{16}$
Physics Procedia, Vol 30, 117 (2012)
- C-034
Higemoto, W. et al.
 μ SR Studies on Caged Compound $\text{PrIr}_2\text{Zn}_{20}$
Physics Procedia, Vol 30, 125 (2012)
- C-035
Sugiyama, J. et al.
Magnetic and Diffusive Nature of LiFePO_4
Physics Procedia, Vol 30, 190 (2012)
- C-036
Wikberg, J.M. et al.
Magnetic Order and Frustrated Dynamics in $\text{Li}(\text{Ni}_{0.8}\text{Co}_{0.1}\text{Mn}_{0.1})\text{O}_2$: A Study by μ +SR and SQUID Magnetometry
Physics Procedia, Vol 30, 202 (2012)
- C-037
Shimomura, K. et al.
Photo Detachment of Negatively Charged Muonium in GaAs by Laser Irradiation
Physics Procedia, Vol 30, 224 (2012)
- C-038
Yokoyama, K. et al.
Detection of Conduction Electron Spin Polarization in n-GaAs by Negative Muonium
Physics Procedia, Vol 30, 231 (2012)
- C-039
Sugiyama, J. et al.
Successive Magnetic Transitions in RECoAsO
Physics Procedia, Vol 30, 262 (2012)
- C-040
Higemoto, W. et al.
Muon Beam Slicer at J-PARC MUSE
Physics Procedia, Vol 30, 30 (2012)
- C-041
Ikeda, Y. et al.
Status of the Superomega Muon Beam Line at J-PARC
Physics Procedia, Vol 30, 34 (2012)
- C-042
Miyake, Y. et al.
J-PARC Muon Facility, MUSE
Physics Procedia, Vol 30, 46 (2012)
- C-043
Strasser, P. et al.
New Muon Kicker System for the Decay Muon Beamline at J-PARC
Physics Procedia, Vol 30, 65 (2012)
- C-044
Makimura, S. et al.
Development of a Muon Rotating Target for J-PARC/MUSE
Physics Procedia, Vol 32, 795 (2012)
- C-045
Futakawa, M.
Present status of JSNS and R&D for high power operation in JPARC
Proc of ICANS-XX, Vol 111, (2012)
- C-046
Sakai, K. et al.
Influence of Great East Japan Earthquake on Neutron Target Station in J-PARC
Proc of ICANS-XX, Vol 113, (2012)
- C-047
Meigo, S. et al.
Development of Beam Flattening System Using Non-Linear Beam Optics at J-PARC
Proc of ICANS-XX, Vol 207, (2012)
- C-048
Haga, K. et al.
Development of the high power mercury target and the bubbler installation
Proc of ICANS-XX, Vol 307, (2012)
- C-049
Meigo, S. et al.
Beam Commissioning at J-PARC/JSNS and MUSE
Proc of ICANS-XX, Vol 314, (2012)
- C-050
Riemer, B.W. et al.
Demonstration of Small Gas Bubbles for Mitigation of Cavitation Damage and Pressure Waves in Short-pulse Mercury Spallation Targets
Proc of ICANS-XX, Vol 320, (2012)
- C-051
Teshigawara, M. et al.
R&D on 2nd moderator fabrication for JSNS
Proc of ICANS-XX, Vol 326, (2012)
- C-052
Kinoshita, H. et al.
Development of cut out machine for PIE test pieces from mercury target vessel in J-PARC
Proc of ICANS-XX, Vol 334, (2012)
- C-053
Wakui, T. et al.
First trial for post irradiation examination on the JSNS target
Proc of ICANS-XX, Vol 353, (2012)
- C-054
Ooi, M. et al.
Elemental distribution measurement of the Au-In-Cd alloy by neutron resonance imaging
Proc of ICANS-XX, Vol 439, (2012)
- C-055
Vishik, I.M. et al.
Phase competition in trisected superconducting dome
Proc. of the National Academy of Sciences, Vol 109, 18332 (2012)
- C-056
Meigo, S. et al.
Development of Beam Flattening System Using Non-Linear Beam Optics at J-PARC/JSNS
Proc of 9th Meeting of Particle Accelerator Society of Japan, 75 (2012)
- C-057
Maruta, T. et al.
Simulation study on the longitudinal bunch shape measurement by RF chopper at J-PARC linac
Proc. of 26th Int. Linear Accelerator Conf. (LINAC 2012) 395 (2012)
- C-058
Kamiya, J. et al.
Status of the vacuum system in J-PARC RCS
Proc. of 3rd Int. Particle Accelerator Conf. (IPAC '12) 2522 (2012)
- C-059
Takayanagi, T. et al.
New power supply of the injection bump magnet for upgrading the injection energy in the J-PARC 3-GeV RCS
Proc. of 3rd Int. Particle Accelerator Conf. (IPAC '12) 3626 (2012)
- C-060
Watanabe, M. et al.
Operation and current status of injection, extraction, kicker magnet and the power supply for J-PARC 3 GeV RCS
Proc. of 3rd Int. Particle Accelerator Conf. (IPAC '12) 3629 (2012)
- C-061
Yamamoto, K. et al.
Comparison of the residual doses before and after resumption of user operation in J-PARC RCS
Proc. of 3rd Int. Particle Accelerator Conf. (IPAC '12) 3901 (2012)

- C-062
Kinsho, M.
Status of the J-PARC 3 GeV RCS
Proc. of 3rd Int. Particle Accelerator Conf. (IPAC '12) 3927 (2012)
- C-063
Ogiwara, N. et al.
Reduction of outgassing from the ferrite cores in the kicker magnet of J-PARC RCS
Proc. of 3rd Int. Particle Accelerator Conf. (IPAC '12) 487 (2012)
- C-064
Harada, H. et al.
Upgrade of Ionization Profile Monitor (IPM) in the J-PARC 3-GeV RCS
Proc. of 3rd Int. Particle Accelerator Conf. (IPAC '12) 840 (2012)
- C-065
Hatakeyama, S.
Various methods to measure the betatron tune of the synchrotron
Proc. of 3rd Int. Particle Accelerator Conf. (IPAC '12) 843 (2012)
- C-066
Ikegami, M. et al.
Beam start-up of J-PARC linac after the Tohoku Earthquake
Proc. of 3rd Int. Particle Accelerator Conf. (IPAC '12), 3293 (2012)
- C-067
Hocchi, H. et al.
Beam halo reduction in the J-PARC 3-GeV RCS
Proc. of 3rd Int. Particle Accelerator Conf. (IPAC '12), 3918 (2012)
- C-068
Hayashi, N. et al.
Status of injection energy upgrade for J-PARC RCS
Proc. of 3rd Int. Particle Accelerator Conf. (IPAC '12), 3921 (2012)
- C-069
Saha, P.K. et al.
Effect of the 2011 Great East Japan Earthquake in the injection and extraction of the J-PARC 3-GeV RCS
Proc. of 3rd Int. Particle Accelerator Conf. (IPAC '12), 490 (2012)
- C-070
Maruta, T. et al.
Longitudinal beam diagnosis with RF chopper system
Proc. of 52nd ICFA Advanced Beam Dynamics Workshop on High-Intensity and High-Brightness Hadron Beams (HB 2012), 591 (2012)
- C-071
Shimada, T. et al.
Measurement of inner diameters of MA cores of RF-cavities of J-PARC 3 GeV synchrotron and diameter change over the years
Proc. of 9th Annual Meeting of Particle Accelerator Society of Japan 1143 (2012)
- C-072
Schnase, A. et al.
Iterative Kappa magnet pole shape optimization for MA core annealing
Proc. of 9th Annual Meeting of Particle Accelerator Society of Japan, 1204 (2012)
- C-073
Togashi, T. et al.
Operation maintenance of the thyatron for the power supply of the extraction kicker magnet in the J-PARC 3GeV RCS
Proc. of 9th Annual Meeting of Particle Accelerator Society of Japan, 471 (2012)
- C-074
Watanabe, Y. et al.
Design of a high-precision and wide dynamic range pulsed magnet power supply
Proc. of 9th Annual Meeting of Particle Accelerator Society of Japan, 531 (2012)
- C-075
Tamura, F. et al.
Commissioning of multiharmonic feedforward system for J-PARC MR
Proc. of 9th Annual Meeting of Particle Accelerator Society of Japan, 89 (2012)
- C-076
Tatsumoto, H. et al.
Effect of a Heated Pipe Length on DNB Heat Flux in Forced Flow of Liquid Hydrogen
Proc. of ICEC24-ICMC2012, 157 (2012)
- C-077
Shiotsu, M. et al.
Heat Transfer Characteristic Test of Forced Flow Supercritical Hydrogen for Superconductor Cooling
Proc. of ICEC24-ICMC2012, 165 (2012)
- C-078
Hikawa, K. et al.
Over-Current Characteristics of MgB₂ Wire Cooled by Liquid Hydrogen
Proc. of ICEC24-ICMC2012, 203 (2012)
- C-079
Murakami, K. et al.
Preliminary Test of Hot-Wire Type Flow-Meter for Liquid Hydrogen
Proc. of ICEC24-ICMC2012, 51 (2012)
- C-080
Toh, K.
Development of Gas-Based 2-Dimensional Neutron Detector with Individual Line Readout and Optical Signal Transmission System
Proc. Of the 2012 IEEE Nuclear Science Sympo, 153 (2012)
- C-081
Nakamura, T. et al.
Development of Two-Dimensional Scintillation Detectors for Neutron Spin Echo Spectrometers in J-PARC/MLF
Proc. Of the 2012 IEEE Nuclear Science Sympo, 222 (2012)
- C-082
Sakasai, K. et al.
Storage Characteristics of Mixtures of KCl:Eu²⁺ Phosphors and Polyethylene Powder by Irradiation of Fast Neutrons
Proc. Of the 2012 IEEE Nuclear Science Sympo, 318 (2012)
- C-083
Saha, P.K. et al.
Effect of the 2011 Great East Japan Earthquake in the injection and extraction of the J-PARC 3-GeV RCS
Proc.s of 3rd International Particle Accelerator Conference (IPAC '12) 490 (2012)
- C-084
Meigo, S. et al.
Development of profile monitor system for high intense spallation neutron source
Proc.s of IBIC2012, 227 (2012)
- C-085
Yoshimoto, M. et al.
Development of the beam halo monitor in the J-PARC 3-GeV RCS
Proc.s of IPAC2012, 2122 (2012)
- C-086
Futakawa, M. et al.
Cavitation erosion induced by proton beam bombarding mercury target for high power spallation neutron source
Proc.s of the 8th International Symposium on Cavitation (CAV2012), 822 (2012)
- C-087
Matsumura, H. et al.
Colloid Formation Rates of Radionuclides Produced from Cu Foils in Waterbombarded with 120-GeV Protons
Progress in Nuclear Science and Technology, Vol 3, 127 (2012)
- C-088
Yashima, H. et al.
Spatial Distribution Measurement of Neutrons Produced by 120-GeV Proton Beam in Concrete Shield
Progress in Nuclear Science and Technology, Vol 3, 4 (2012)
- C-089
Arimoto, Y. et al.
Present status of neutron fundamental physics at J-PARC
Progress of Theoretical and Experimental Physics, 02B007, (2012)

C-090

Hotchi, H. et al.

Beam commissioning and operation of the
Japan Proton Accelerator Research Complex
3-GeV rapid cycling synchrotron

*Progress of Theoretical and Experimental
Physics, Vol 2012, 02B003 (2012)*

C-091

Oigawa, H.

Present status and prospect of transmutation
technology for high-level radioactive waste

Radioisotopes, Vol 61, 571 (2012)

C-092

Kadono, R. et al.

MUSE, the goddess of muons, and her future

*Reports on Progress in Physics, Vol 75, 026302
(2012)*

C-093

Morooka, S. et al.

In-Situ Neutron Diffraction Study on Tensile
Deformation Behavior of Steels

*New Methods of Damage and Failure Analysis
of Structural Parts, ed. by Zdeněk Bůžek,
Bohumír Strnadel*

JAEA Reports

- J-001
Nakamura, S. et al.
Neutron capture cross section of palladium-107 in the thermal-neutron energy region
JAEA-Conf 2012-001, Vol 147 (2012)
- J-002
Yamagishi, H. et al.
A Low Noise ASIC for Two Dimensional Neutron Gas Detector with Performance of High Spatial Resolution (Contract Research)
JAEA-research, Vol 2011, 1 (2012)
- J-003
Sugawara, T.
Proceedings of the Int. Symposium on Future of Accelerator-Driven System
JAEA-Review 2012-043, Vol (2012)
- J-004
Division, N.S.S.M.a.L.S.
Technical design report of spallation neutron source facility in J-PARC
JAEA-Technology 2010-030, Vol 2011-035, 536 (2012)
- J-005
Ishikawa, H. et al.
Development of information security and vulnerability risk management system for J-PARC
JAEA-Technology 2011-030, Vol (2012)
- J-006
Sakai, K. et al.
Influence of Great East Japan Earthquake on neutron source station in J-PARC
JAEA-Technology 2011-039, Vol (2012)
- J-007
Teshigawara, M. et al.
Maintenance of used components in spallation neutron source; Moderator's reflector and proton beam window
JAEA-Technology 2012-024, Vol 303 (2012)
- J-008
Nakamura, T.
中性子を光に変えて高位置分解能で検出する -J-PARC の結晶構造解析装置用 2次元シンチレータ中性子検出器を開発 -
未来を拓く原子力 原子力機構の研究開発成果 2012, Vol (2012)

KEK Reports

- K-001
Nagamiya, S. et al.
J-PARC project and its science
Progress in Particle and Nuclear Physics, Vol 67, 580 (2012)
- K-002
Sasaki, K. et al.
Development of a Superconducting Solenoid for Hyperfine Structure Measurement of Muonium at the J-PARC
IEEE Transactions on Applied Superconductivity, Vol 22, 4500904 (2012)
- K-003
Ueno, K. et al.
Conceptual Design of a Radial Vane Silicon Tracker for a New Measurement of the Muon Anomalous Magnetic Moment $g-2$ and Electric Dipole Moment at J-PARC
IEEE Nuclear Science Symposium Conference Record, Vol 2012, 1353 (2012)
- K-004
Ikegami, M. et al.
A Preliminary Consideration on Higher Frequency Option for Muon Drift Tube Linac
KEK_Internal, Vol 2012, 1 (2013)
- K-005
Ikegami, M. et al.
A Preliminary Design Study on Ramped Drift Tube Linac for the Muon $g-2$ Experiment
KEK_Internal, Vol 2012, 1 (2013)
- K-006
Hirose, E. et al.
- Radiation-Resistant Magnets for the Neutrino Beamline at J-PARC
IEEE Transactions on Applied Superconductivity, Vol 22, 4101404 (2012)
- K-007
Charrier, J. et al.
In-Line Control in T2K Proton Beam Line Magnet Safety System
IEEE Transactions on Applied Superconductivity, Vol 22, 4702104 (2012)
- K-008
Abe, K. et al.
Measurements of the T2K neutrino beam properties using the INGRID on-axis near detector
Nuclear Instruments and Methods in Physics Research A, Vol 694, 211 (2012)
- K-009
Kobayashi, T. et al.
Status of T2K experiment
Nuclear Physics B (Proc. Suppl.), Vol 229, 55 (2012)
- K-010
Tanaka, K. et al.
Radiation-Resistant Magnet System for J-PARC Hadron Experimental Hall
IEEE Transactions on Applied Superconductivity, Vol 22, 4100204 (2012)
- K-011
Takahashi, H. et al.
Indirectly Cooled Radiation-Resistant Magnet With Slanting Saddle Shape Coils for
- New Secondary Beam Extraction at J-PARC Hadron Facility
IEEE Transactions on Applied Superconductivity, Vol 22, 4101504 (2012)
- K-012
Shiomi, K. et al.
Measurement of K_{0L} flux at the J-PARC neutral-kaon beam line
Nuclear Instruments and Methods in Physics Research A, Vol 664, 264 (2012)
- K-013
Honda, R. et al.
Development of a tracking detector system with multichannel scintillation fibers and PPD
Nuclear Instruments and Methods in Physics Research A, Vol 695, 206 (2012)
- K-014
Komatsubara, T. et al.
Experiments with K-meson decays
Progress in Particle and Nuclear Physics, Vol 67, 995 (2012)
- K-015
Miwa, K. et al.
Experimental plan of Σ p scatterings at J-PARC
EPJ Web of Conferences, Vol 20, 5001 (2012)
- K-016
Shirakabe, Y. et al.
SIMPLIFIED ANALYTICAL APPROACH TO THE BEAM RIPPLE GENERATION MECHANISM OF THE J-PARC MR SLOW EXTRACTION BEAM

- Proc. Ann. Mtg Part. Accel. Soc. Jpn, Vol 2012, 541 (2012)*
- K-017
Sato, Y. et al.
DEVELOPMENT OF NON-CONTACT BEAM INTENSITY MONITOR BY RESIDUAL GAS IONIZATION
Proc. Ann. Mtg Part. Accel. Soc. Jpn, Vol 2012, 612 (2012)
- K-018
Toyoda, A. et al.
Performance Evaluation of π/K Differential Fitch-type Cherenkov Counter for the J-PARC K1.1BR Beamline
Proc. Ann. Mtg Part. Accel. Soc. Jpn, Vol 2012, 620 (2012)
- K-019
Yamanoi, Y. et al.
Operation status of water-cooling fixed target at J-PARC Hadron Facility
Proc. Ann. Mtg Part. Accel. Soc. Jpn, Vol 2012, 1340 (2012)
- K-020
Igarashi, Y. et al.
Waveform sampler module for J-PARC TREK experiment
IEEE Nuclear Science Symposium Conference Record, Vol 2012, 1376 (2012)
- K-021
Komatsubara, T. et al.
Experiments with K-Meson Decays
KEK_Preprint, Vol 2012, 1 (2013)
- K-022
Takahashi, H. et al.
Radiation-Resistant Equipments for J-PARC Hadron Beam Line
Kasokuki (日本加速器学会誌), Vol 9, 214 (2012)
- K-023
Shirotori, K. et al.
Search for the Θ^+ pentaquark via the $\pi^+p \rightarrow KX$ reaction at 1.92 GeV/c
Phys. Rev. Lett., Vol 109, 132002 (2012)
- K-024
Agari, K. et al.
Primary proton beam line at the J-PARC hadron experimental facility
Prog. Theor. Exp. Phys., Vol 1, 8 (2012)
- K-025
Agari, K. et al.
Secondary charged beam lines at the J-PARC hadron experimental hall
Prog. Theor. Exp. Phys., Vol 1, 9 (2012)
- K-026
Takahashi, T. et al.
Beam and SKS spectrometers at the K1.8 beam line
Prog. Theor. Exp. Phys., Vol 1, 10 (2012)
- K-027
Agari, K. et al.
The K1.8BR spectrometer system at J-PARC
Prog. Theor. Exp. Phys., Vol 1, 11 (2012)
- K-028
Naruki, M.
Hadron physics at J-PARC
Prog. Theor. Exp. Phys., Vol 1, 13 (2012)
- K-029
Tamura, H.
Strangeness nuclear physics experiments at J-PARC
Prog. Theor. Exp. Phys., Vol 1, 12 (2012)
- K-030
Sekiguchi, T.
Neutrino facility and neutrino physics in J-PARC
Prog. Theor. Exp. Phys., Vol 1, 5 (2012)
- K-031
Yamanaka, T. and for the KOTO Collaboration
The J-PARC KOTO experiment
Prog. Theor. Exp. Phys., Vol 1, 6 (2012)
- K-032
Iio, M. et al.
Development of liquid ^3He target for experimental studies of antikaon-nucleon interaction at J-PARC
Nucl. Instr. and Meth. A, Vol 687, 1 (2012)
- K-033
Amaudruz, P.-A. et al.
The T2K fine-grained detectors
Nucl. Instr. and Meth. A, Vol 696, 1 (2012)
- K-034
Aoki, S. et al.
The T2K Side Muon Range Detector (SMRD)
Nucl. Instr. and Meth. A, Vol 698, 135 (2013)
- K-035
Bhadra, S. et al.
Optical transition radiation monitor for the T2K experiment
Nucl. Instr. and Meth. A, Vol 703, 45 (2013)
- K-036
Assylbekov, S. et al.
The T2K ND280 off-axis pi-zero detector
Nucl. Instr. and Meth. A, Vol 686, 48 (2012)
- K-037
Abe, K. et al (T2K Collaboration)
T2K neutrino flux prediction
Phys. Rev. D, Vol 87, 68103 (2013)
- K-038
Ichikawa, A.K.
Design concept of the magnetic horn system for the T2K neutrino beam
Nucl. Instr. and Meth. A, Vol 690, 27 (2012)

J-PARC

JAPAN PROTON ACCELERATOR RESEARCH COMPLEX

High Energy Accelerator Research Organization (KEK)
Japan Atomic Energy Agency (JAEA)



2-4 Shirakata Shirane, Tokai-mura, Naka-gun, Ibaraki 319-1195, Japan

<http://j-parc.jp/>